

**TNL**

# **Monte Carlo Particle Device Simulator User Manual**

**Particle based device simulation Software**

**Tech Next Lab (P) Ltd**

Building No. #417/22/A, Niwaz Ganj,  
Near Napier Road Park, Lucknow - 226 003, (U.P.), India,  
Tel: **(+91) 522 404 1565,**  
Web: [www.technextlab.com](http://www.technextlab.com)

5<sup>th</sup> Oct, 2022

## Notice

The information contained in this document is subject to change without notice.

**Tech Next Lab (P) Ltd is not liable for any kind of warranty related to this material. The limited warranty extends ONLY for warranty of fitness for a purpose of particular requirement.**

**Tech Next Lab (P) Ltd** shall not be held liable for typographical errors contained in the material. The users of this manual will be solely responsible for use of this manual, for incidental or consequential damages in connection with the furnishing, and performance.

The TNL-PD (Particle Device) simulator manual contains proprietary information under the copyright laws. All copyrights are reserved to Tech Next Lab (P) Ltd. Without prior written consent, the photocopy, reproduction, or translation into other language of this manual is prohibited under copyright laws.

**The family of unmatched innovative simulators includes;**

1. **TNL Framework** (*A GUI enabled control frame accommodating the Family of TNL Simulators*)
2. **TNL-EpiGrow Simulator** (*Epitaxial Growth through MBE/CVD/MOCVD reactors processes*)
3. **TNL-FB Simulator** (*Electronic Full Band Structure*),
4. **TNL-EM Simulator** (*Carrier Mobility simulator*)
5. **TNL-TS Simulator** (*THz Spectroscopy with Ultrafast Carrier Dynamics Predictions*)
6. **TNL-PD Simulator** (*2D & 3D Particle based Device Simulator*)
7. **StrViewer** (Structural viewers)
8. **TNLPlot** (Graphical viewers)

All the simulators and visualization tools are proprietary product of **Tech Next Lab (P) Ltd** and under trademarks of **Tech Next Lab (P) Ltd**.

Copyright © 2015 - 2022, **Tech Next Lab (P) Ltd**.

**Additional information is provided at:**

<http://www.technextlab.com>

**Write email to us:**

[info@technextlab.com](mailto:info@technextlab.com)

**TNL**

## Contents

<b>1. Introduction</b>	<b>6</b>
1.1 Need of MC Particle Device Simulator	7
1.2 Nature of electron	9
1.3 MC Particle Device Simulator Overview	10
1.4 Features	11
1.5 Comprehensive details of Models	11
1.6 Integrated Capabilities	12
1.7 Numerical implementation	13
1.7 Benefits can be realized	14
<b>2. Start using MCPDS</b>	<b>15</b>
2.1 Getting Started with Unipolar (NanoMOS)	16
2.2 TNL-PD SIMULATOR window frame	18
2.2.1 Technology tab	18
2.2.1.1 Select Technology	19
2.2.1.2 Workspace Setting	19
2.2.2 Add Region tab	20
2.2.3 Mesh tab	22
2.2.4 Physics tab	24
2.2.5 Biasing	25
2.2.6 Structure tab	27
2.3. Add Region tab in BIPOLAR Simulator	28
2.3.1 Mesh tab	31
2.3.2 Physics Tab	33
2.3.3 Optical Characterization	35
2.3.4 Charge Assignment	37
2.3.5 Parameters	38
2.3.6 Biasing	39
2.3.7 Structure Tab	41
2.4 Run Output Script	42
2.5 Input Script	42
2.6 Menu	42
2.7 Other	43
2.8 Simulation of Examples (Script)	44
<b>3. Physics (Particle Device Simulator)</b>	<b>45</b>
3.1 Electronic Band Structure	47
3.1.1 Energy Bands	48

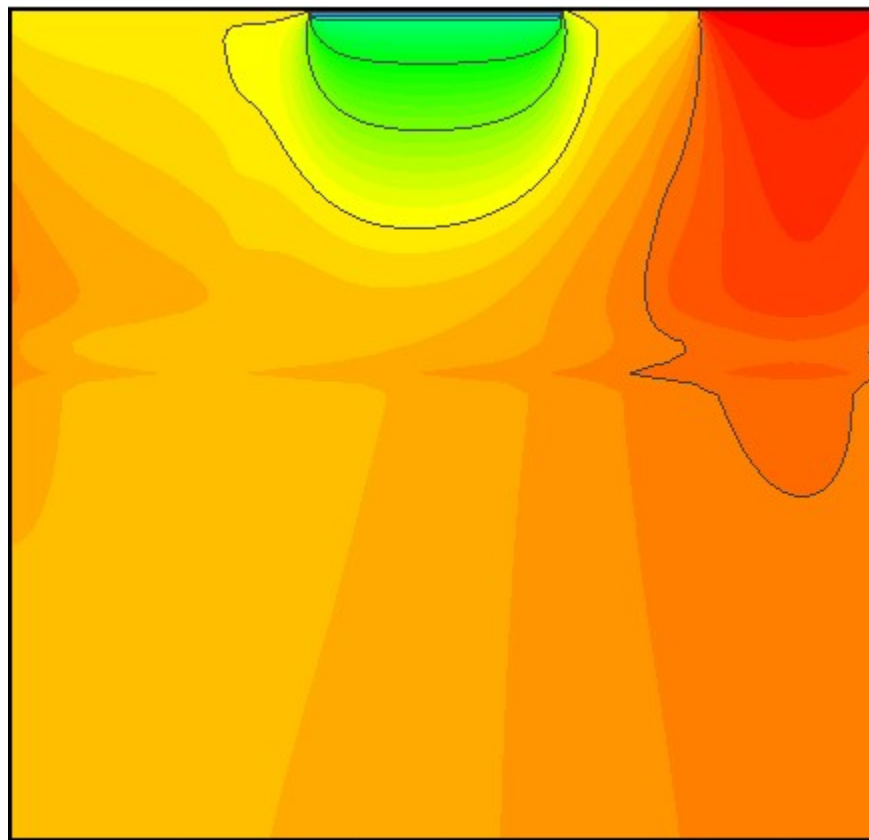
3.1.1.1 Parabolic Band	48
3.1.1.2 Nonparabolic Band	49
3.1.2 Effective Masses	49
3.1.3 Conductivity Effective Mass	49
3.1.4 Density-of-States Effective Mass	50
3.1.5 Nonparabolicity	50
3.2 Carrier Scattering Mechanisms	54
3.2.1 Fermi's Golden Rule	56
3.2.2 Acoustic Deformation Potential Scattering	57
3.2.3 Non-Polar Optical Scattering	58
3.2.4 Polar Optical Phonon Scattering	59
3.2.5 Ionized Impurity Scattering	60
3.2.6 Alloy Scattering	61
3.2.7 Piezoelectric Scattering	62
3.2.8 Dislocation Scattering	63
3.2.9 Carrier-Carrier Scattering	64
3.2.10 Impact Ionization Scattering	65
3.2.11 Interface Roughness Scattering	65
3.3 Ensemble Monte Carlo Device Simulator	69
3.3.1 Carrier Transport Equation	70
3.3.2 Scattering Mechanisms	73
3.3.3 Monte Carlo Technique	75
3.3.3.1 Free Flight Generation	75
3.3.3.2 Choice of Scattering Angles	78
3.3.3.3 Time Step	79
3.3.3.4 Mesh Size	80
3.4 Particle Mesh Coupling	81
3.4.1 Nearest Grid Point (NGP) Technique	82
3.4.2 Nearest Element Center (NEC) Technique	83
3.4.3 Cloud-in-Cell (CIC) Technique	84
3.5 Discretization of Poisson's Equation	86
3.5.1 Uniform Mesh	88
3.5.2 Non-Uniform Meshes	89
3.5.3 Solution of Poisson's Equation in 2D	90
3.6 Boundary Conditions	93
3.6.1 Neumann and Dirichlet boundary conditions	93
3.7 Iterative method	96

3.7.1 The Gauss Seidel Method	98
3.7.2 SOR Method	98
3.8 Electric Field Calculation	99
3.9 Quantum Confinement Effects	100
3.9.1 Density Gradient model	100
3.9.2 The Effective Potential	102
3.9.3 Bohm Quantum Potential	103
3.9.3 Calibrated Bohm Quantum Potential	103
4. <i>BIPOLAR Devices</i>	104
4.1 Introduction	105
4.1.1 MESFET example to start	105
4.1.2 PN Junction example	108
5. <i>UNIPOLAR Devices</i>	111
5.1 Technology and Workspace setting	112
5.2 Add Region	112
5.3 Mesh	117
5.5 Biasing	118
5.6 Start Simulation	118
5.7 Output Files	119
6. Optical Characterization	120
6.1. Optical Characterization	121
6.2 Photo Generation due to Light Absorption	121
6.3 Tutorial for Device Optical Characterization	122
6.4 Optical Output data	125
7. Visualize Output data	126
7.1. Viewing and Analyzing Output data	127
7.2 Electric Field Profile of MESFET	129
7.3 Carrier velocity along device length	130
7.4 Current Analysis	131

## References

# CHAPTER 1

## INTRODUCTION



## 1.1 Need of MC Particle Device Simulator

We are living in semiconductor era, the semiconductor devices technologies are shrinking towards nanometer scale regime. With the scaling down the transistor sizes, many technological challenges are faced by the industry for future device technologies developments. Like at advance node device geometries, velocity saturation restricts the carrier mobility in form of pronounced intervalley scattering mechanism, random doping fluctuations (RDF), line error roughness (LER) effects etc. Also, the device dimensions scaled down to 60 nm and below, the carrier velocity overshoots start to dominate, in turn changing the device performance in terms of larger ON-state currents and other physical phenomenon responsible for device performance degradation. Low dimensional geometries devices also suffer with shortening issues etc.

The application of nanotechnology techniques has paved way for development of new device technologies development scaled down to 5nm or below with improved characteristics. The geometry dimension scaling, increases the transistors density on the same chip in recent years and in turn reducing the cost of per device. The accurate prediction of the various pure physics-based effects with detection of the root causes responsible for the performance degradations and other physical phenomenon in these devices are still a big challenge for the semiconductor industry from existing and futuristic device technologies development point of view.

Only computation tools at atomistic scale able to detect and predict about the issues and challenges in device technology developments.

The incapability of the drift-diffusion model to demonstrates and predicts these entire physics-based phenomenons in these advance node devices poses lot of issues. The predicted current-voltage characteristics of the device through drift-diffusion model are not reliable. The drift-diffusion models are valid, in general, for large devices dimensions geometries, where applied electric field is not so high to causes the mobility degradation and the quantum confinement can be ignored. The modified drift-diffusion model with inclusion of field dependent mobility models and diffusion coefficients extends its validity up to a certain level of device dimensions when carrier velocity overshoot is negligible. The drift-diffusion model is popular for conventional device modeling relying under the assumption of equilibrium transport conditions; however, at high biasing conditions the results obtained from drift diffusion model also differed significantly even in big dimensional geometry devices due to the prominent ballistic transport effects.

On the other hand, the hydrodynamic model has been proposed as an alternate model to demonstrate the unanswered issues poses by the drift-diffusion model. It also suffers with the several discrepancies e.g.; the velocity overshoot can't be predicted accurately. The velocity overshoot depends upon the choice of the energy relaxation time. The energy relaxation time is dependent upon material properties, device geometry and doping parameters. For smaller device geometries, the larger deviation in velocity overshoot has been measured with hydrodynamics model hence the accuracy of predicted results are still questionable.

The drift diffusion and hydrodynamics transport models are derived from Boltzmann Transport Equation (BTE) by the method of moments by assuming several assumptions. These models are most popular method to handle carrier transport due to its simplicity, flexibility, and fast computing times, despite their limited range of validity. For the next generation nanometer scale device dimension geometries, the clear and accurate picture of the carrier transportation is impossible through drift diffusion or hydrodynamic models which are based on deterministic approaches. The physics is lumped into parameterized mobilities, diffusion constants, and lifetimes which are the essential incapability of these computational models.

There is urgent requirement for the simulation tool which can handle electronic transportation at the atomistic scale with inclusion of real nonlinear scattering events under non-equilibrium carrier dynamics conditions.

The solution of seven dimensions ( $x, y, z, k_x, k_y, k_z, t$ ) Boltzmann transport equation (BTE) with inclusion of non-linear scattering mechanisms are impossible through any numerical technique. Ensemble Monte Carlo (EMC) method has received much attention for the solution of Boltzmann transport equation (BTE) including non-linear scatterings. Under non-equilibrium carrier dynamics conditions for accurately predicting the carrier transportation on few valleys or full electronic band structure, EMC method has appeared best suited technique. The method is capable to explain the most of the physical effects associated with the non-linear carrier transportation mechanism in the conventional and advance node CMOS technology without using any initial assumptions or guess. The method resolves most of the unanswered key questions relating to different device technologies where understanding and insight of the device physics are crucial for the accurate prediction of I-V characteristics at atomistic scale.

The TNL-PDS provides generalized particle-based device simulation software capable to handle most of the semiconductor device technologies. The solution of BTE through the EMC



method for the prediction of the accurate non-linear carrier dynamics solution on few or various valleys of full electronic band structure is included by default.

## 1.2 Nature of electron

The simulation study of semiconductor devices provides current voltage (I-V) characteristics prediction through electronic transportation. The accurate prediction of the nature of electrons under semi-classical or quantum transport regimes are a tedious task. The few experiments e.g. Wilson chamber, single-slit diffraction experiment etc. give a clear description about the particle and wave nature of an electron which resembles dual nature of light. It helps to understand the limits of the two transport regimes formalisms.

An electron is represented by a particle in classical physics which also known as Newtonian physics. It assumes that an electron is a tiny small object having a mass and whose dimensions are negligible. A particle in phase space is described, in any time, by two vectors, i.e. the position

$$\vec{r} = (x, y, z) \quad (1.1)$$

And the velocity

$$\vec{v} = (v_x, v_y, v_z) \quad (1.2)$$

The particle dynamics can be described by,

$$m \frac{d^2 \vec{r}}{dt^2} = -\nabla U \quad (1.3)$$

Here  $m$  is the mass of the electron and  $U = U(x, y, z)$  is a function known as the potential that represents the forces acting over the particle.

An electron in the quantum regime is described by a mathematical object called a wave function  $\psi = \psi(x, y, z)$  which is a complex function similar to a wave and which square module tell us the probability of finding an electron at that point. The dynamics of this wave function is described by the solution of Schroedinger equation

$$i\hbar \frac{d\psi}{dt} = H\psi \quad (1.4)$$

Equations (1.3) describe the evolution of position and velocity of an electron, whereas and (1.4) describes the evolution of the probability of finding an electron in a given point. Thus, the both approaches have some analogies (being both deterministic) but differ for the evolving

quantities they describe. The distinction between both approaches can be visualized through application of particle based simulation analysis.

### 1.3 TNL Particle Device Simulator (TNL-PDS) Overview

TNL-PD simulator is an unmatched innovative particle device simulator (PDS). It uses ensemble Monte Carlo (EMC) technique for the solution of the Boltzmann transport equation coupled with quantum confinement effects, whereas Poisson equations is solved through successive over relaxation (SOR) method with the inclusion of different non-linear scattering mechanisms. It is also equipped with parallel computing feature to minimize the simulation time. TNL-PD (particle device) simulator considers the transport of Monte Carlo particles (also known as super particles) with or without inclusion of the quantum confinement effects under influence of applied external field, determined self-consistently through the solution of coupled Poisson's and BTE equation over a suitably small time-step on the electronic band structure. The time step is taken typically less than the inverse plasma frequency obtained with the highest carrier density in the device. The Poisson equation solution ( $V$ ) is generated over the node points on the meshes. The carrier transport solution is obtained using ensemble Monte Carlo (EMC) on the full range of space coordinates (few valleys or full electronic band structure) in accordance with the particle distribution itself.

Three types of particle-mesh (PM) coupling schemes are used for the assignment of the carrier charges (super particles) at different nodes and for the calculation of the force on each charge.

- 1 Carrier charge assign at the mesh nodes through Charge in Cloud (CIC), Nearest Grid Point (NGP) and Nearest Element Center (NEC) schemes
- 2 Solution of Poisson's equation on the mesh points through Successive Over Relaxation (SOR) method
- 3 Calculation of the mesh defined electric field components
- 4 Interpolation of forces at the particle positions.
- 5 Calculation of drift velocity of each carrier
- 6 Averaging the drift velocity components for getting I-V data

TNL-PDS has two simulators inbuilt for device simulator.

- a. Unipolar (TNL-NanoMOS) for nano electronics devices simulator (MOSFET, FDSOI, DSOI, GAA, FinFET, Nanowire etc.) and conventional MOSFET in 2D & 3D FET geometries.
- b. Bipolar (TNL-PDS) for power & conventional devices e.g. p-n, PIN, n-n junctions, HEMT, MESFET, Optical Devices etc. (2D geometries).

#### **1.4 Features**

TNL-PDS software is a graphical user interface (GUI) based software tool which run on the Windows platform with full capabilities.

- No need for initial assumptions & Solution for non-equilibrium transport conditions
- Transportation of carriers over various valleys of full electronic band structure in 2D and 3D device geometries under non equilibrium conditions
- Monte Carlo particles in cloud, no limit for use of particles (5000000)
- Various particle-mesh (PM) coupling schemes, available for assignment of carrier charge on different nodes
- Charge assignment at the mesh nodes through charge in cloud (CIC), nearest grid point (NGP) and nearest element center (NEC) schemes
- 2D and 3D Poisson Solvers equipped with Successive Over Relaxation (SOR) Technique
- Carriers mobility prediction based on applied external field, without using any model into account
- Boundary conditions include Neumann (Insulating) and Dirichlet (Ohmic & Schottky) conditions.
- Accuracy up to a single carrier/particle

#### **1.5 Comprehensive details of Modeling Capabilities**

TNL- PD simulator includes a comprehensive solution of various coupled equation's, including;

- Boltzmann transport Equation
- Monte Carlo (MC)
- Randomness
- Valley Deformation Potential

- Direct and Indirect Band gap materials
- Quantum Confinement
- Effective potential (Carrier Quantum Transport)
- Density Gradient (Carrier Quantum Transport)
- Bohm quantum potential (Carrier Quantum Transport)
- Poisson Equation
- Nonlinear Scatterings
- Acoustic Scattering (Lattice heating due to phonons)
- Intervalley Scattering
- Carrier-carrier (Coulomb) scattering
- Polar Scattering
- Surface Roughness Scattering
- Impact ionization Scattering
- Piezoelectric Scattering
- Defects Scattering (Traps, Impurity, Dislocations and Dynamic)
- Non-local Band to band Tunneling
- Graded and abrupt heterojunctions
- Ohmic, Schottky, and insulating contacts
- Charge in cloud (CIC) model for carrier distribution
- Nearest grid point (NGP) model for carrier distribution
- Nearest element center (NEC) model for carrier distribution
- Successive Over Relaxation (SOR)
- DC, AC small-signal, and full time-dependency

### **1.6 Integrated Capabilities**

TNL- PD simulator works well with other family of TNL simulator software from Tech Next Lab. For example, PDS

- Runs in the TNL Framework interactive run-time environment equipped with GUI capabilities.
- Interfaced to TNL-Plot, an interactive graphics, contours and analysis package.

- Accept inputs from the TNL-FB (Full Band) simulator.
- Different device technologies examples are inbuilt.
- Various material data base inbuilt e.g. group IV, III-V and II-VI semiconductors etc.
- Flexibility to accommodate user define materials and properties

### ***1.7 Numerical Implementation***

TNL- PD simulator uses powerful numerical techniques, including:

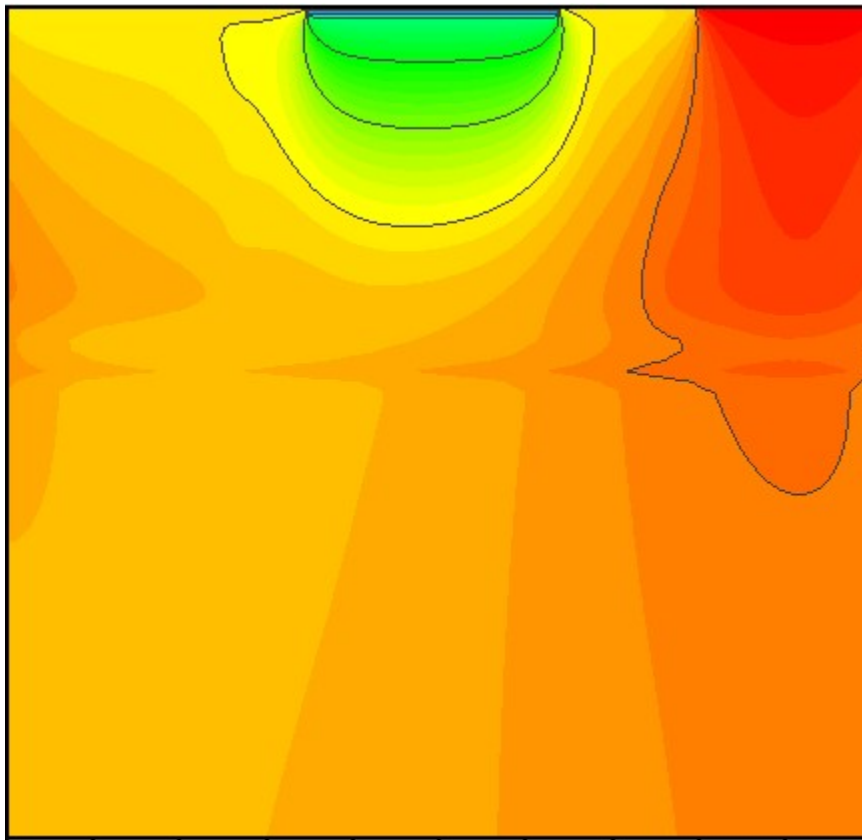
- Accurate and reliable techniques.
- Monte Carlo technique for solution of Boltzmann transport equation
- Carrier distribution as super particles.
- Solution with coupled non-linear scattering mechanisms.
- SOR nonlinear iteration strategies.
- Iterative efficient solver without requirement of initial guess.

## 1.8 Benefits can be realized

- World's fastest particle device simulator
- Equipped with Parallel Computing feature
- Based on Ensemble Monte Carlo Technique
- No need for initial assumptions like in Drift-Diffusion model
- Various material specific scattering processes inbuilt by defaults
- Number of Carrier's Initialization depends on user's hardware configuration
- Quantum Confinement effect can be analyzed with:
  - Density Gradient model
  - Effective Potential Method
  - Bohm Quantum Potential
- Transportation on parabolic & nonparabolic energy bands
- Coupled Boltzmann -Poisson solver
- Self low and high field mobility extraction
- Accurate device I-V prediction
- Trace single carrier's physical properties under various operating conditions
- Extract exact carrier position & energy before & after free flight
- CMOS, HEMT, BJT, MEMORY and other technology applications
- PN devices, MOSFET, MESFET, FinFET, GAA, TunnelFET, PDSOI, FDSOI, HEMT, Detectors etc.

# Chapter 2

## Start using MCPDS



## 2.1 Getting Started with Unipolar (NanoMOS) device simulator

To use the TNL Particle Device (TNL-PD) simulator user must have the official license. They can verify it by opening the TNL-Framework. At framework user will see a tick mark on the side of the name MC Particle Device Simulator (2D Poisson Solver) in green color which confirms the license for same as represented in Fig. 1. The 2D Poisson Solver means, 3D Boltzmann transport equation (2D device geometry with fixing width 1  $\mu\text{m}$  in z-direction) coupled with 2D Poisson's equations solution. But if a cross mark in red color is seen then user might not use valid license (user may contact on [info@technextlab.com](mailto:info@technextlab.com)).

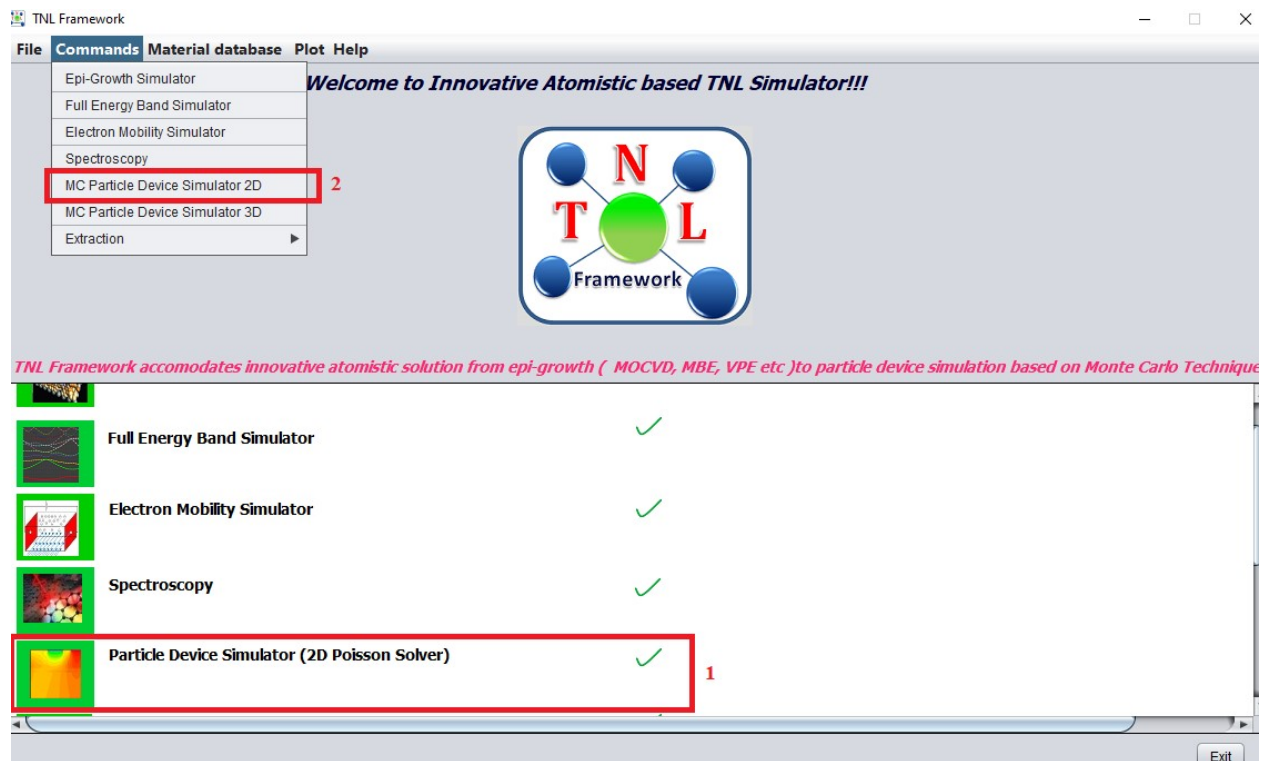


**Fig.2.1:** TNL-Framework

There are two ways to open the TNL-PD simulator from the Framework shown in Fig. 1. Those ways are shown in red rectangular boxes (box1 and box2).

1. This box1 contains PD simulator's icon and name. By a single click on icon or name user gets access to use the simulator
2. This box2 contains sub menu named as MC Particle Device Simulator 2D and 3D. By clicking on the *Command* menu various sub-menus containing the names of TNL family of simulators are there. By a single click on name user gets access to use the simulator.

Any of the above two methods will start the TNL-PD simulator window frame PDS simulator as shown in Fig.2.



## 2.2 TNL-PD SIMULATOR window frame

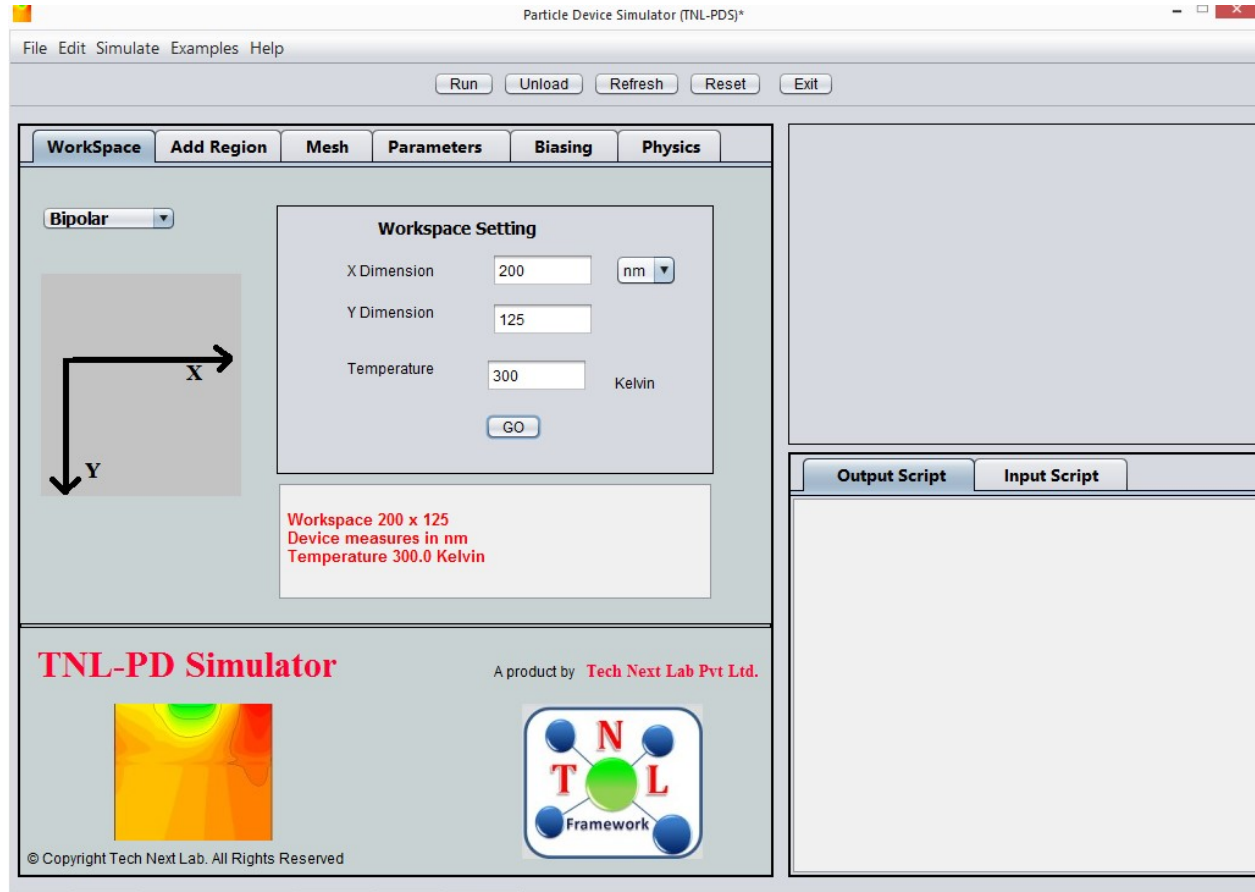


**Fig. 2.2:** Particle Device Simulator window frame.

TNL-PD simulator window frame in Fig. 2 contains two part i.e. left and right part of the frame. There are several tabs for the dedicated functions for various inputs.

Left part contains:

- i. Technology
- ii. Add Region
- iii. Mesh
- iv. Material Parameters
- v. Physics
- vi. Biasing

Right part contains:

- vii. Structure
- viii. Run Output Script
- ix. Input Script

The TNL-PD simulator GUI feature utilizes the essential information provided by users to define a device structure.

- The selection of *Technology*, i.e. UNIPOLAR (nanoMOS devices) or BIPOLAR (for conventional node, optical & power devices) to make enable the users to select their device technology applicable.
- The work space selection is the starting point to design device geometries choosing appropriate physical mechanisms, applied external voltages and running the simulations. Following sections will demonstrate step by step tutorial. Before starting the simulation, the device type and its dimensions are essential requirements.

### 2.2.1 Technology tab

The latest version of the TNL-PD simulator is structured with the two types of device technologies inbuilt as shown in Fig. 3,

#### i. Select Technology

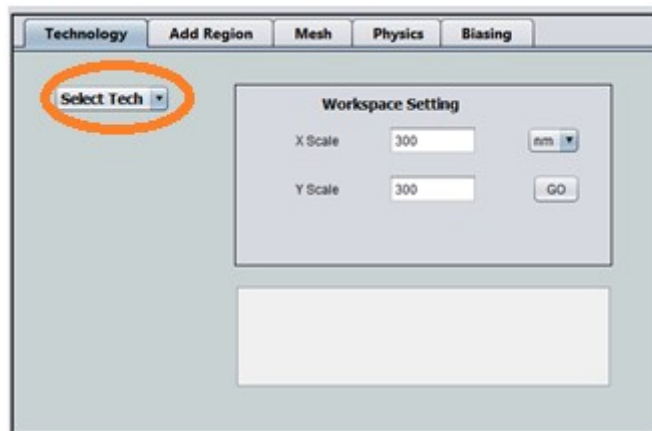


**Fig. 2.3:** Technology tab.

#### 2.2.1.1 Select Technology

The device technology tab consists of two simulators:

##### 2.2.1.1.1 UNIPOLAR

Metal oxide semiconductor type of structure for advance and conventional node devices i.e. FETs can be simulated on three valleys over full electronic band structure with inclusion of various nonlinear scattering mechanisms under UNIPOAR simulator tab e.g.:

- i. PDSOI, FDSOI (Fully or Partially Depleted Silicon on Insulator)
- ii. MOSFET (Metal Oxide Semiconductor Field Effect Transistor)

### 2.2.1.1.2 BIPOLAR

Any device geometry including

- i. PN Junctions devices
- ii. Diodes
- iii. BJT
- iv. MESFET
- v. TFET
- vi. HEMT (High Electron Mobility Transistor)
- vii. TFET (Tunneling FETs)

are simulated on single valley with inclusion of Acoustic (phonon), optical and impurity scattering mechanisms by solution of BTE through Monte Carlo techniques.

### 2.2.1.2 Workspace Setting

After selection of the specific device technology, workspace dimensions need to fill for generation of the device structure. *Workspace* will decide the various device geometries/dimensions in ‘*Add Region*’ section.

*Workspace* setting contains X scale and Y scale fields with unit. After filling the maximum numbers for X- and Y- values along with the operating temperature value, user need to click on GO button.

X Scale stands for setting maximum working Area in the X- & Y- scales. “GO” button is used for set initial working space as per device geometry requirement.

The information of the device technology selected and workspace dimensions will be displayed in the blank text-field below the workspaces setting. TNL-PD simulator initiates the selected workspace and device structure environment by the users.

Users may now define their device geometries by defining its different regions with selection of appropriate materials with doping and dimensions etc in the simulator. The user defined materials can also be used, in that case users need to provide all require material database. With the selection of various regions one by one, GUI feature creates the graphical image of the device at right hand side box of the TNL-PDS frame under Structure tab.

The Workspace Setting is common for both type of UNIPOLAR and BIPOLAR particle device simulators. In next version both simulators will be unified.

## 2.2.2 Add Region tab in NanoMOS Simulator (UNIPOLAR device simulator selected by users under Select Tech Tab)

The graphical user interface (GUI) feature is user friendly to define the device structure. The structure is created by a set of regions with different coordinates, material and doping etc. Refer to Fig. 2.4,



**Fig. 2.4:** Add Region

Under this tab, various materials, regions and contacts can be defined and added to the device structure. The elemental and compound semiconductor materials by default inbuilt are added to current version of simulator. An oxide region with dielectric constant can be added separately, Al and Al-Au alloy can be used as metal contacts. The other insulators e.g.  $\text{SiO}_2$ ,  $\text{Si}_3\text{N}_4$  can be defined at appropriate position in the device structure.

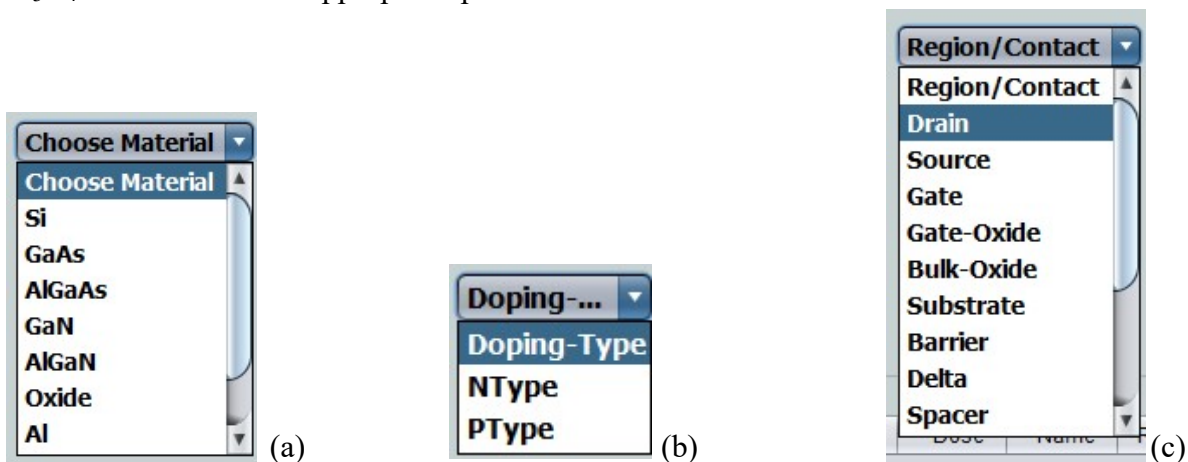


**Fig. 2.5:** Feasibility to choose (a) material (b) type of doping and (c) region or contact of device from various options.

- (i) The semiconductor materials from Choose Material drop box can be selected for a specific region in the device structure.
- (ii) The type of acceptor or donor doping can be chosen by selecting P-type or N-type respectively.

- (iii) The name of the semiconductor, metal and insulator regions are essential requirement to identify the particular region in UNIPOLAR simulator, selecting one of the options e.g. source, drain, gate etc. and ohmic or Schottky contacts etc.

**Fig. 2.6:** Fields to define the concentration and boundaries of a region

- (iv) The doping density is defined at the concentration text field as shown in fig. 2.6.
- (v) The four fields named Xmin, Xmax, Ymin, Ymax represent the minimum and maximum boundaries in x and y dimensions of a 2D structure.
- (vi) Oxide dielectric field shown in which user need to fill the dielectric constant of the oxide, e.g. dielectric constant  $\text{SiO}_2$  of 3.9 is selected by default.
- (vii) Width field is for defining the width of the device is essential requirement for running 2D simulation under UNIPOLAR technology selection. The Boltzmann Transport Equation solves 3D carrier transportation, whereas Poisson equation is solved over 2D node points. By-default it is 1 $\mu\text{m}$ , user may edit and can choose other value as per requirement, but user need to be careful in choosing the value of dielectric constant, doping concentrations and the mesh sizes (will talk about this later on).

**Fig. 2.7:** Add and Delete button. Table for complete data of every single region

- (viii) Every information filled by user for each material is added in the device structure by clicking add button. After adding every region, users need to click refresh button. Every time you click on add button the information of material,  $x_{\min}$ ,  $x_{\max}$ ,  $y_{\min}$ ,  $y_{\max}$ , doping type, dose, name of region and region will be printed on a next row of the table shown in Fig. 7.
- (ix) In case user finds some wrong information about any region has been chosen, they can eliminate that particular row by selecting the particular row in the table and clicking on the Delete button and then click on refresh button

- (x) User have flexibilities to click Add or Delete buttons, the pane in Structure tab at the simulator main frame will display to add or delete operation of that particular region graphically.

### 2.2.3 Mesh tab

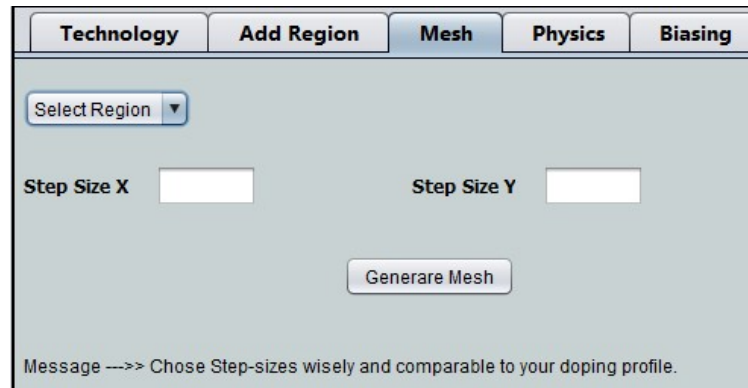


**Fig. 2.8:** Mesh tab.

Next tab on main frame is Mesh. The mesh or node points are selected over the device structure geometry by filling step size x and y values. In case of two dimensional (2D) structures, the intersection point of mesh in x and y dimension will be used for assigning super particles or charge in cloud (CIC) and calculation of potential by Poisson's equation over these node points. Step Size X defines the distance between two consecutive mesh lines in X direction and Step Size Y defines the distance between two consecutive mesh lines in Y direction. The Step Size X and Y are in the nanometer by default. After inserting suitable values in both of the above fields, click on *Generate Mesh* button. It will automatically generate mesh on device structure pane and also create number of node points in x and y directions which are essential requirement for the simulation.

For more accurate simulation user need to take notice of the following;

- i. Try to take square mesh.
  - ii. Smaller the mesh size, the simulation complexity will be more and simulation time will be longer.
  - iii. To avoid any error user need to be careful during defining the meshes in both directions.
- E.g.

There is a trade-off between doping concentrations and the cell volume in the device.

$$\text{cell volume} = \text{step size x} * \text{step size y} * \text{device depth}$$

To avoid error, doping concentrations of each region MUST be comparable or greater than the cell volume.

$$\text{Doping concentration} * \text{cell volume} \geq 1$$

The latest version of TNL-PD (UNIPOLAR) simulator, the uniform rectangular mesh option is enable, in next version of the simulator will be loaded with the capability of non-uniform and triangular meshes.

## 2.2.4 Parameters

Refer to Fig. 2.19, before proceeding for providing biasing at various device edges

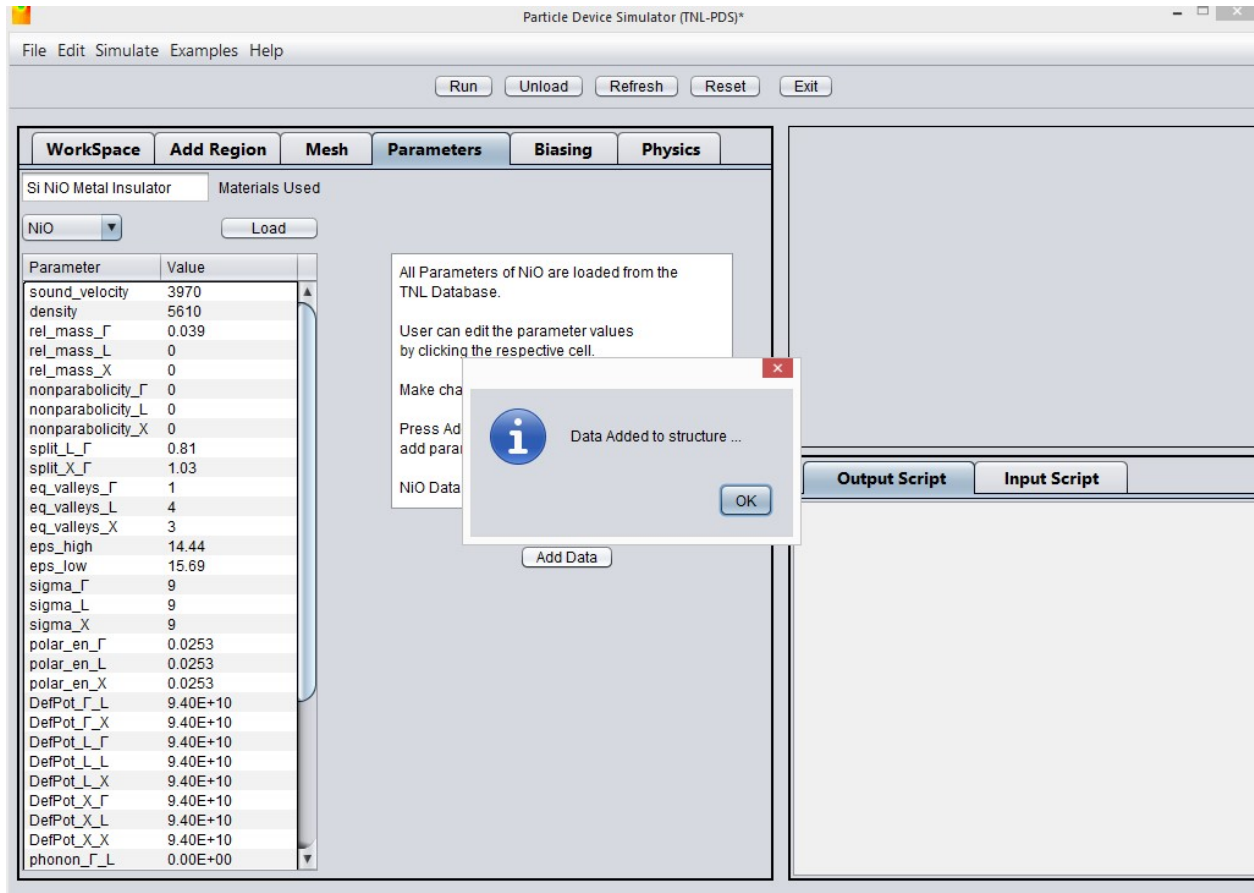


**Fig. 2.9:** Parameters Tab at GUI Frame

The various semiconductor materials name chosen during device structure design are automatically shown at Materials Used box. Users need to select one by one each semiconductor material at drop down menu and click load button, all the prerequisite material properties loaded at table below in the frame. All the parameters are editable, users may edit it as per his knowledge.

Each semiconductor material's properties used in device MUST be added to device structure by click on Add Data button, a popup message will be appeared that data is added to the structure, click OK and perform same steps for each and every material of the drop down box.

## 2.2.5 Physics tab

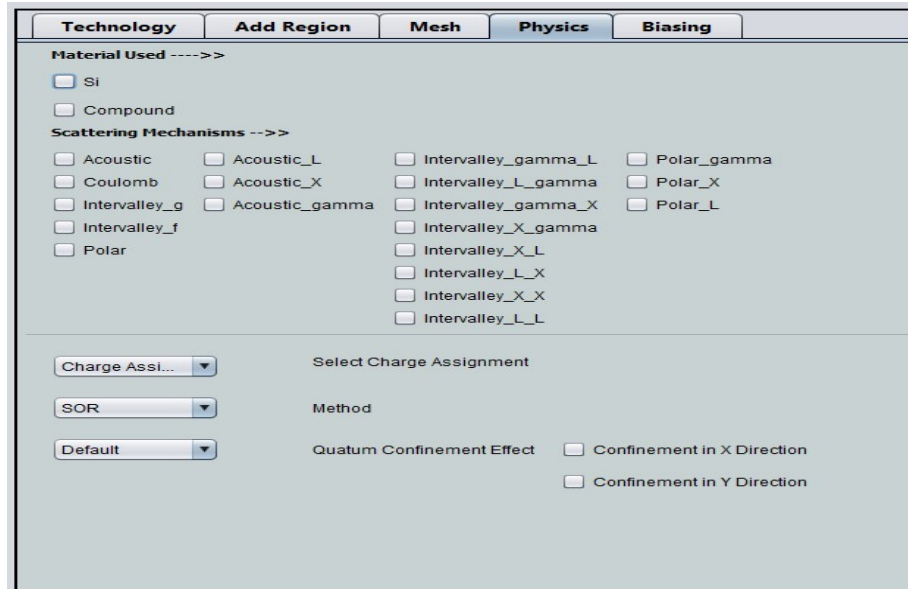


**Fig. 2.10:** Physics tab

Under Physics tab users, various material specific scattering mechanisms are given and user may chose as per their requirement.

The charge assignment techniques i.e. (CIC, NEC, NGP) are implemented for creation of super particles, all three techniques generate similar results. User need to one of them.

The solution of Poisson equation is carried out through Successive Over Relaxation (SOR) numerical method.

The quantum confinement effect can be invoke by make it enable and choosing carrier confinement direction.

### 2.2.5.1. Scattering Mechanism

To start simulation, user needs to select at least one of the scattering mechanisms which are essential requirement for running device simulation. The Acoustic and Coulomb scatterings are universal scattering mechanisms in the real samples. All types of scattering mechanisms are given for both single element and compound materials. Selection of various material specific scatterings can be used for calibration of experimental I-V data.

There are two ways to select the scattering mechanism. First, if you select Si or compound semiconductors placed under material used name, all the respective mechanisms will automatically get selected. Second, users can select one by one many of the available mechanisms per their requirements.

### 2.2.5.2. Select Charge Assignment

Next option is for selection of type of charge assignment techniques over the node points or mesh. Three types of charge assignment techniques have been implemented in the



TNL-PD (UNIPOLAR) simulator. All three charge assignment techniques produce similar results.

**(a) Charge in Cloud (CIC)**

In the CIC scheme a better approximation can be obtained assigning the charge of a super particle to the two nearest neighbor cell points.

**(b) Nearest Element Center (NEC)**

The NEC charge assignment force interpolation scheme attempts to reduce self-forces and increase the spatial accuracy in the presence of non-uniformly spaced tensor-product meshes and/or spatially-dependent permittivity.

**(c) Nearest Grid Point (NGP)**

In the NGP scheme all the charge from a given particle is assigned to the nearest grid point. The force on the particle is also taken as the one calculated on the nearest grid point.

### **2.2.5.3 Method**

Next tab is Method, use for solution of Poisson equation on node points for the super particles. The Succession Over Relaxation (SOR) method has been implemented to improve the rate of convergence for solution of Poisson equation. SOR method uses a weighted average of the results of the two most recent estimates to obtain the next best guess of the solution. If the solution is converging, this might help extrapolate to the real solution more quickly.

### **2.2.5.4 Quantum Confinement Effect**

For invoking quantum confinement effect over the transportation of the carriers in one, two or three directions an approach of an effective potential for consideration of quantum confinement effects in x-, y-, and z-directions separately have inbuilt in TNL-PD (UNIPOLAR) simulator. Here, the natural non-zero size of an electron wave packet, in the quantized system, is used to introduce a smoothing of the local potential (found from Poisson's equation). This approach naturally incorporates the quantum potentials, which are approximations to the effective potential. The effective potential is related to the self-consistent potential through an integral smoothing relation.

By-default this effect is disabled, if user want to include of quantum confined carriers transportation in to their device structure for simulation, they may chose enable option and also select one check box between confinement in x or confinement in y directions.

### **2.2.6. Biasing**

- The biasing tab in main frame is use to provide input voltages at different electrode terminals through "Solve" tab. Four types of terminals are Source, Drain, Gate and Substrate defined under UNIPOLAR technology. Click on insert button number of times as per the electrodes defined in the device structure for providing the voltage ramping information on each electrode.

- Users may choose constant voltage or ramping voltage conditions on a particular electrode along with the voltage boundary condition.
- Fill the initial, step and final biasing point. Suppose user gives initial value 0, step value 0.1V and final value 1V. Then the simulation will first start at the 0 then it will proceed to 0.1, 0.2, 0.3, ... and so on, up to final value 1V.
- During the simulation all respective results will be saved at these voltages (we will talk about it later in this tutorial).
- Then click on load button on the main frame under solve tab. The given voltage will be added to particular electrode.
- A field named 'Barrier voltage for Schottky contact, if users add any contact electrode terminal of Schottky type then they need to give the barrier voltage here. The barrier voltage ( $\Phi_B$ ) is defined as difference between the work function of metal ( $\Phi_M$ ) and the electron affinity ( $\chi$ ) of semiconductor. Unit is in Volt.

$$\Phi_B = \Phi_M - \chi$$

Once all the information has been provided by user, the structure is ready for start running the simulation, there are three ways:

- i. Click on '*RUN*' button present above.
- ii. Go to *Simulate* menu, then click on Run submenu.
- iii. Go with the key combination of Shift+F6.

## 2.2.6 Structure Tab

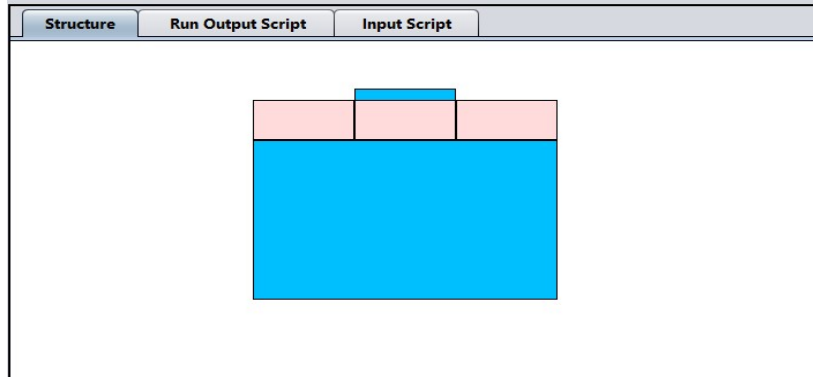


**Fig. 2.11:** Structure tab showing graphics of device

The window shows the graphics of the device structure defined with all the regions geometries added in the Add Region section. The users may select XScale and YScale values in work space setting, the blank space in Structure tab as shown in Fig. 2.11 allot that ranges and becomes ready to draw the 2D or 3D device structure graphics of the desired structure. Users provide dimensions and other data of a region and click on ADD button, the area will be shown with its material color in the workspace. In case some wrong information has been filled which can be visualized graphically, the user can easily delete that particular region. Users need to select that row from the table present in Add Region tab and then click on 'Delete' button. To see the change in graphics user need to click on the 'Refresh' button.

TNL-PD (UNIPOLAR) simulator's GUI capabilities provide feasibility to view and verify device structure from table which contains the database of the designed structure or through the structure graphics. Through GUI feature it can be easily checked that at the time of input whether there is some unnecessary spaces remains in consecutive regions or region overlapping have been made or not which can be removed easily.

### 2.3. Add Region tab in BIPOLAR Simulator (BIPOLAR device simulator selected by users under Select Tech Tab)

The GUI enabled feature provides flexibilities to define device structure geometries under BIPOLAR Technology selection in PDS simulator. The structure is created by a set of regions with different coordinates, semiconductor, insulator, metal materials, doping and contact information. First user need to define the Workspace Setting i.e. providing the total X-Dimension and Y-Dimension along with the operating Temperature as shown in below graphics.

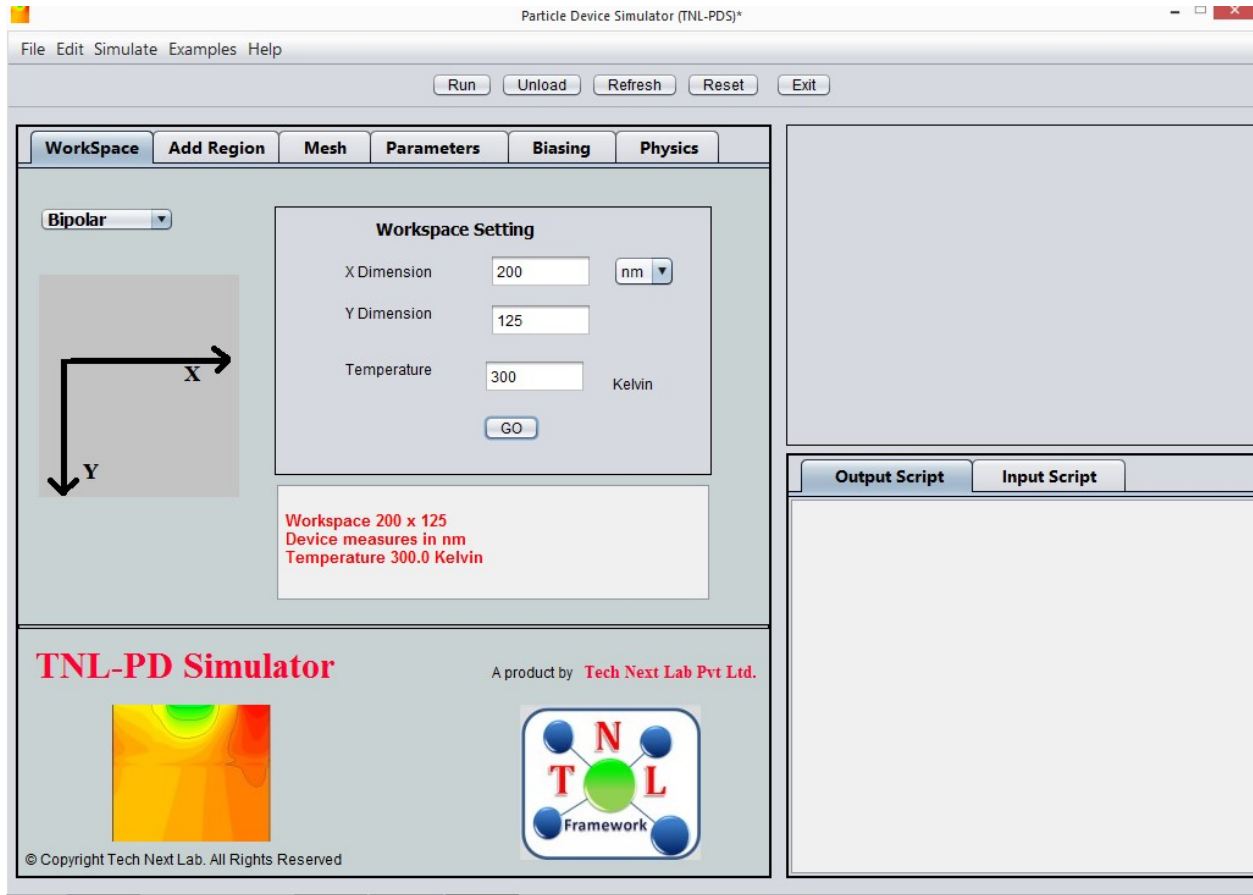


**Fig. 2.12** After setting the workspace dimensions users may proceed for adding regions.

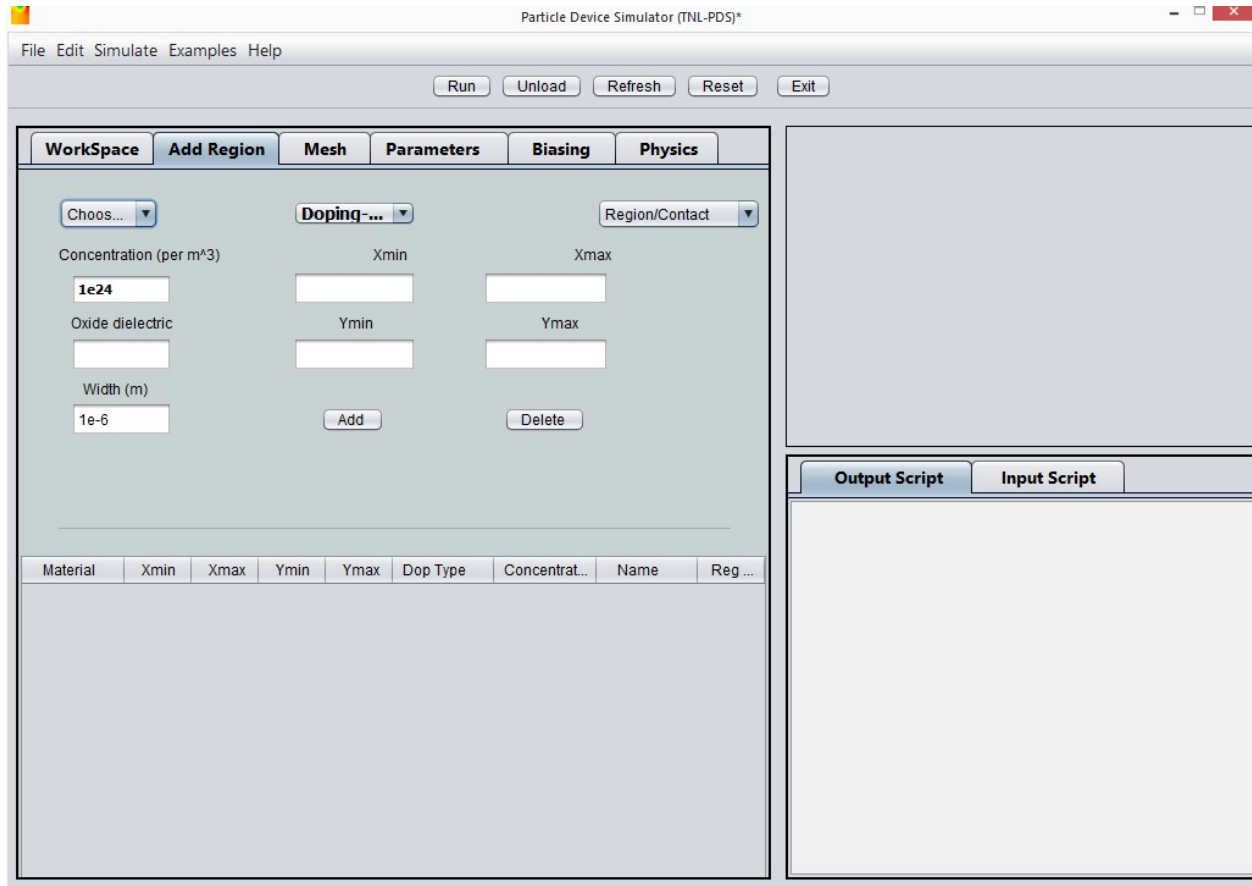
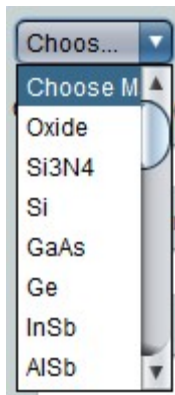
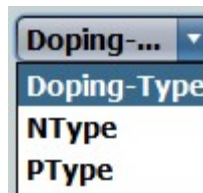


**Fig. 2.12:** Add Region

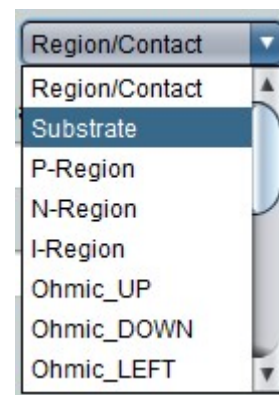
Under Choose Materials, Doping and Region/Contact tabs as shown in Fig. 2.12 various materials with doping profiles and contacts are defined and added to the device structure. The elemental and compound semiconductor materials database is added by default in current version of simulator. The contacts must be carefully chosen for all the device edges with appropriate ohmic, Schottky, insulators type by setting UP, DOWN, LEFT, RIGHT options respectively. No Edge boundaries should be left open. It will generate error.



(a) Materials



(b) ) type of doping



(c) region/contact of device

- i. User can choose semiconductor materials from database to define a specific region of the device structure.
- ii. User may select either acceptor or donor type doping for semiconductors materials for material chosen in step i.
- iii. During selection of Metal under Choose Material tab for defining contacts at device edges, the doping must be N-TYPE to make Ohmic contacts working as carrier reservoir and doping concentration magnitude must be equal to the maximum N-Type doping density of any of semiconductors chosen in the device structure geometry.
- iv. For Schottky electrode, users need to select Metal with no doping and 0 doping Concentration.
- v. To make insulating edge of the device structure, users need to select Insulator material with no doping and 0 doping Concentration.
- vi. The name of the materials are essential requirement to identify the boundary conditions in the device e.g. selecting one of the options like ohmic or Schottky, Insulator contacts etc.

Concentration	Xmin	Xmax
<input type="text"/>	<input type="text"/>	<input type="text"/>
Oxide dielectric	Ymin	Ymax
<input type="text" value="3.9"/>	<input type="text"/>	<input type="text"/>

**Fig. 2.13:** Fields to define the concentration and boundaries of a region

- vii. The concentration field shown in fig. 2.13 is to fill the doping density magnitude ( $/m^3$ ) of the selected materials.
- viii. The four fields named  $X_{min}$ ,  $X_{max}$ ,  $Y_{min}$ ,  $Y_{max}$  define the geometries of each region in the device structure.
- ix. Users may choose different regions dimensions with setting minimum and maximum x and y coordinates values after clicking on add button. After adding every region, users need to click refresh button. Every time you click on add button the information of material,  $X_{min}$ ,  $X_{max}$ ,  $Y_{min}$ ,  $Y_{max}$ , doping type, dose, name of region and region will get print on a next row of the table shown in Fig. 2.14.
- x. In case user locate some wrong information about any region chosen, it is easy to eliminate that particular row by clicking on the Delete button and then click on refresh button.
- xi. Any time users have flexibilities to click Add or Delete buttons in the left pane. To visualize add and delete operations by click on refresh button.

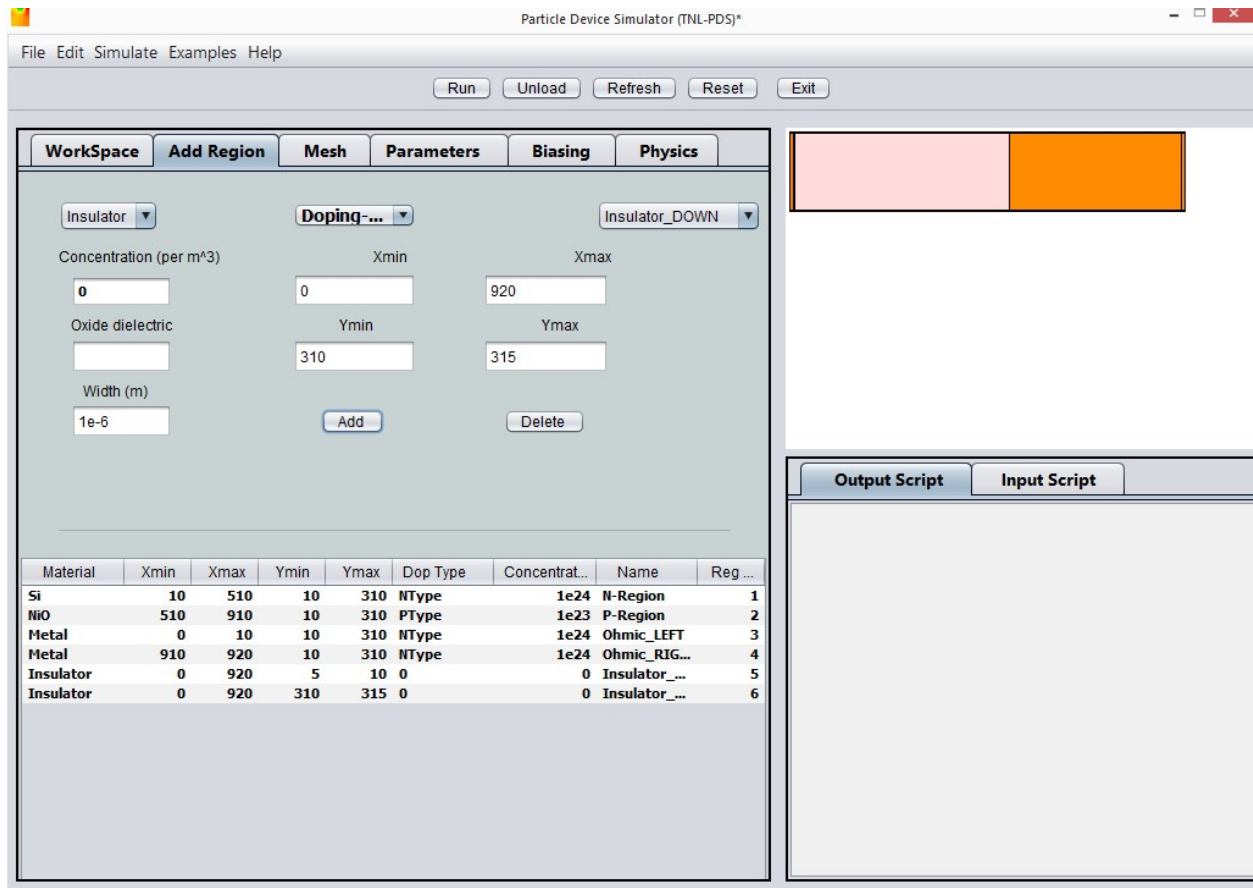


**Fig. 2.14:** Add and Delete button.  
Table for complete data of every single region

### 2.3.1 Mesh tab

Next tab on main frame is Mesh. To define mesh over the two dimensional (2D) structures, the intersection point of mesh in x and y dimension which are used as node points for charge distribution in form of super particle through charge assignment techniques (CIC, NGP, NEC) techniques and calculation of potential on each super particles. Step Size X defines the distance between two consecutive mesh lines in X direction and Step Size Y defines the distance between two consecutive mesh lines in Y direction. The Step Size X and Y are in the nanometer by default. After filling suitable values in both of the above fields, click on *Generate Mesh* button. It will automatically generate mesh on device structure pane and also create number of node points in x and y directions which are essential requirement for the simulation.

For more accurate simulation user must be careful of the following;

- iv. Define rectangular mesh spacing i.e. step X= step Y or step X> step Y or step X< step Y.

- v. Smaller the mesh size, the simulation complexity will be more and the simulation time will be longer.
- vi. To avoid error users need to be careful during defining the meshing in both directions.

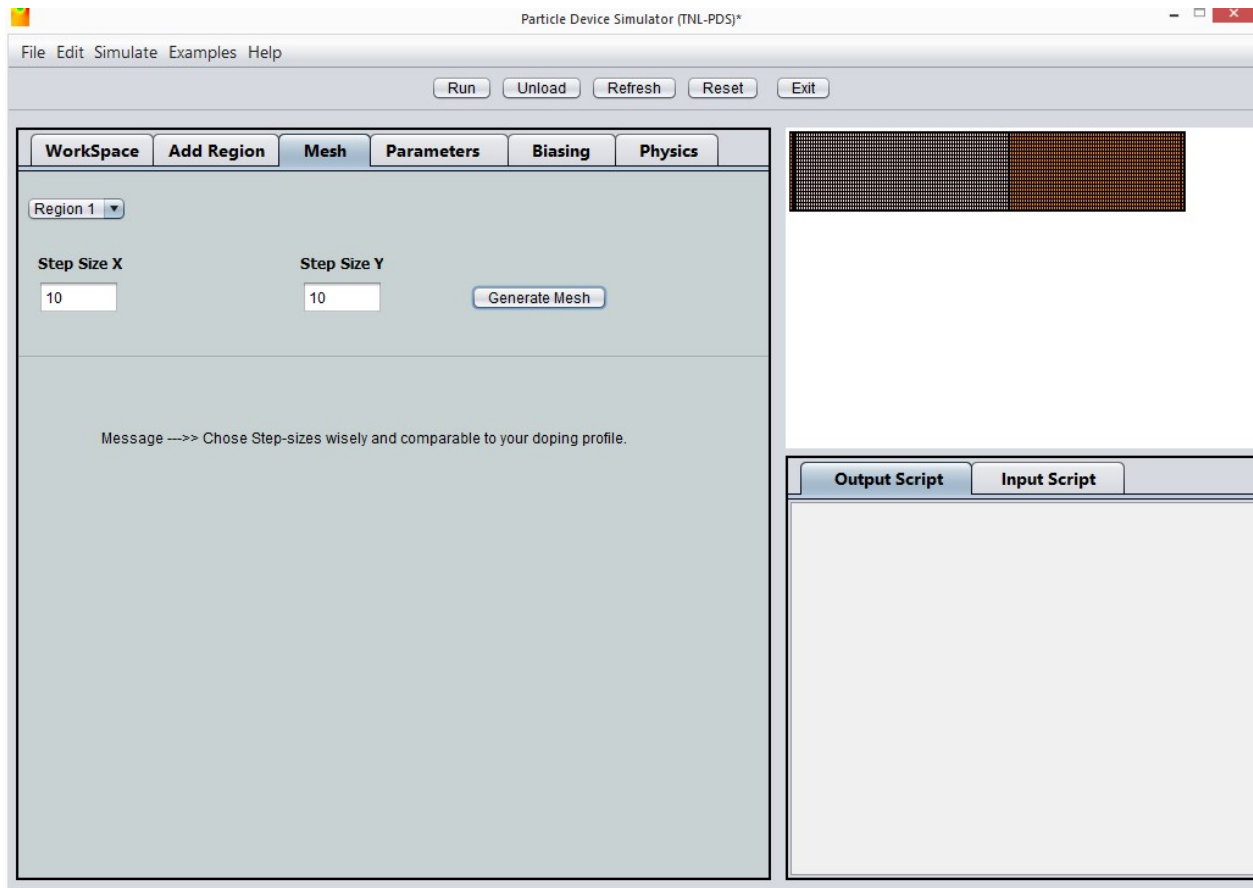


**Fig. 2.15:** Mesh tab.

### 2.3.2 Physics Tab

Under Physics tab users must filled various information require to initiate the simulation as shown by Fig. 2.16.

- Appropriate scattering mechanisms need to be chosen by user to invoke the specific scattering mechanism into simulation. User must be clear that acoustic scattering is universal fundamental scattering event independent of any aspect.

Under UNIPOLAR technology, there types of the scattering mechanisms i.e. Acoustic, Impurity and Optical scatterings are inbuilt in the current version. Scattering rates will decide the material quality of the device structure and can be used as experimental I-V data calibration.



- The total time for simulation will be provided by user. By default it is 0.5 ps (pico second) filled. The user must be careful during filling the total time as it must be  $< 1$  ps.
- Total time steps must be filled by user which will decide the total number of iterations.
- Band Structure drop down box contains three options i.e. parabolic and Kane. Parabolic Band Structure consider parabolic type of conduction band structure, Kane defines the nonparabolicity of band structure with nonparabolicity factor of the band structure.
- X-Device Length and Y-Device Length are the parameters automatically calculated and filled in the boxes based on the device geometries defined in the Add Regions section. Users have no need to worry about the same.
- Similarly X-Mesh and Y-Mesh automatically calculated and filled in the boxes from Mesh section.
- To invoke Quantum Confinement effects into simulation to calculate quantum confinement potential on each super particles, user need to check the box. After checking the box user will select the quantum model i.e. Density Gradient, Bohm, Bohm Calibrated and effective potential (Ferry).
- Lattice Temperature defines the operating device temperature, by default it is 300K.
- Statistical Weight basically used here to normalize the (initial) number of super-particles in a cell containing the maximum doping concentration of the device. The cells that have a lower doping density will be filled consequently.

E.g. suppose Statistical Weight is taken 350 (by default)

The cells that have the maximum doping will have 350 super-particles.

- Media term is used for fixing the (integer) number of final steps over which the observables are averaged over in order to smooth out the natural spurious oscillations intrinsic to the Monte Carlo method.

E.g. suppose Media is taken 500 (by default), i.e. the observables will be averaged over the 500 last final steps of the simulation.

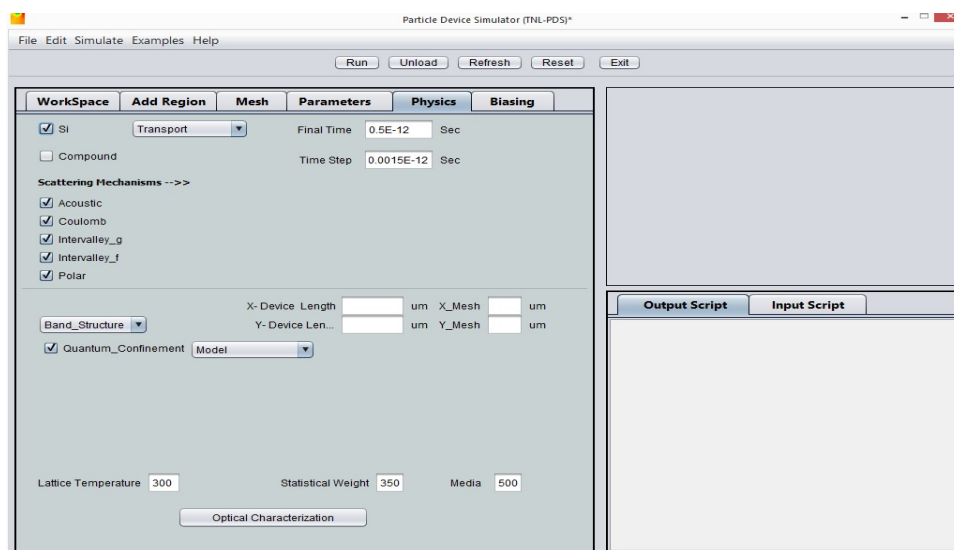
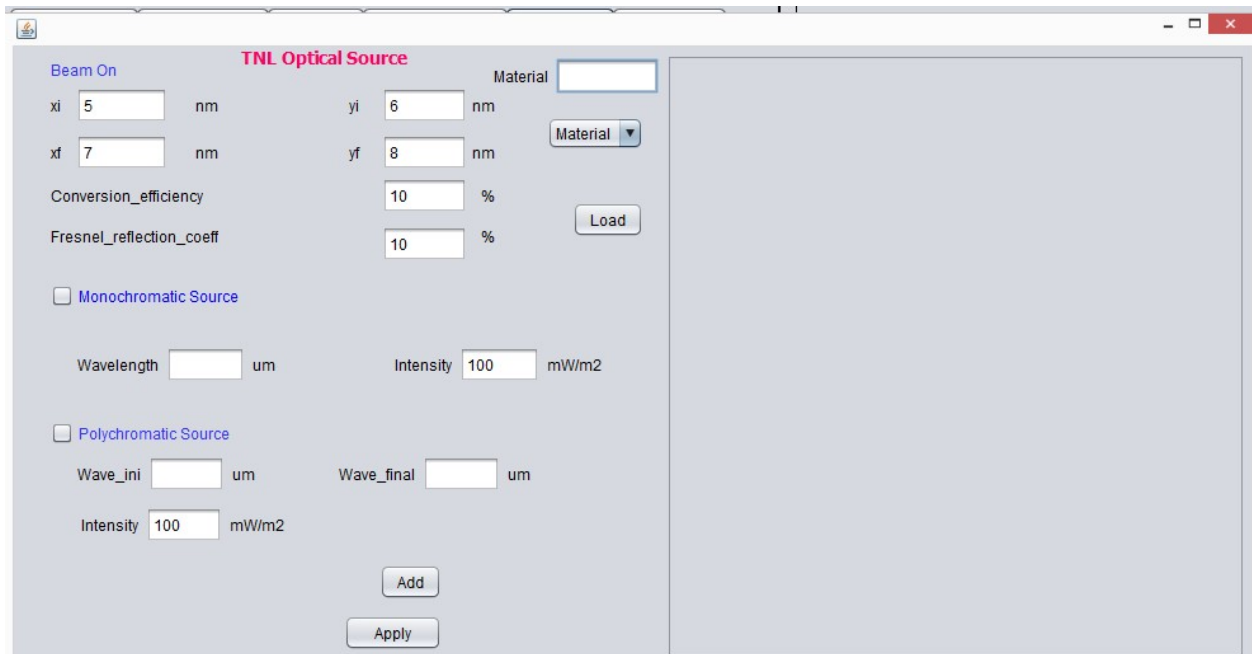


Fig. 2.16: Physics tab

### 2.3.3 Optical Characterization

The optical characterization of semiconductor devices through light propagation and absorption program integrated under the BIPOLAR technology in the TNL-PD simulator. It calculates optically carrier generation profiles within the semiconductor device geometry which is directly integrated into the Boltzmann transport equation. This unique coupling of optical carrier generation and BTE allows user to simulate current-voltage (I-V) responses for the monochromatic and polychromatic optical beams of constant intensity for applications of a broad range of optical detectors.

After clicking the Optical Characterization button, a new TNL Optical Source window will be opened. User need to fill all the appropriate require physical parameters values.



**Fig. 2.17:** TNL Optical Source

The Device can be illuminated either from top or bottom

- xi and xf are initial and final location on the device top or bottom edge where the beam incident. User must be careful during providing the values i.e.  $x_i < x_f$ .
- yi and yf are the y-axis locations on the device, it must be either top or back illumination, i.e.  $y_i = y_f$  in both cases either top or bottom illumination.
- Photon to electron hole pair conversion is defined through Conversion Efficiency factor and is taken in %.  
Suppose 100 photons incident on the device and conversion efficiency is 10%, means from the absorbed photons only 10 photons are converted into EHP.
- Impact of Fresnel Reflection coefficient is considered through coefficient R, user need to fill the value of R, and it may use as important parameter during photocurrent calibration.
- The Materials used in device structure are automatically selected in the Material box.

- f) User need to load the material index file by selecting material name in drop down box and click on load button. It will load index file on the right panel in TNL Optical Source frame.

In case users have no idea about wavelength at which optical absorption will be occurred in any specific material, the index data may provide information regarding wavelength and imaginary refractive indices. Users have flexibility to choose single wavelength as in case of monochromatic source or multiple wavelengths as in case of polychromatic source from the table. For more details refer to Fig. 2.18.

- g) Optical source information is implemented through monochromatic and polychromatic sources.
- h) Under Monochromatic Source option selection, user needs to fill single value of optical wavelength ( $\mu\text{m}$ ) with light intensity ( $\text{mW}/\text{cm}^2$ ) value at appropriate boxes.

$\lambda$ (nm)	n	k	$\alpha$ ( $\text{cm}^{-1}$ )
276.38	2.468212	0.920225	418405.3983
277.97	2.481301	0.936785	423498.4889
279.55	2.496806	0.951265	427613.9704
281.14	2.514458	0.963603	430710.4084
282.73	2.534003	0.973749	432797.7512
284.31	2.555201	0.98166	433889.1835
285.9	2.577822	0.987297	433953.8303
287.49	2.601644	0.99063	433010.669
289.08	2.626452	0.991632	431064.592
290.67	2.652035	0.990284	428123.8434
292.25	2.678182	0.986571	424212.7228
293.84	2.704684	0.980486	419314.9489
295.43	2.731332	0.972032	413462.2198
297.02	2.757912	0.961223	406675.7949
298.6	2.784211	0.948082	398993.6298
300.19	2.81001	0.932652	390421.0895
301.78	2.835093	0.914992	381010.2916
303.37	2.859243	0.895179	370806.3118
304.96	2.882245	0.873316	359863.9992
306.54	2.903894	0.849527	348257.0343
308.13	2.923994	0.823963	336034.2852
309.72	2.942366	0.796794	323285.8294
311.31	2.958849	0.768219	310100.0503
312.9	2.973307	0.738454	296570.3626
314.48	2.985635	0.707731	282803.6772
316.07	2.995756	0.676296	268883.038
317.66	3.003629	0.644398	254918.5951
319.25	3.009247	0.612292	241011.3765

**Fig. 2.18:** TNL Optical Source

- i) Under Polychromatic Source selection, user needs to fill initial and final values of optical wavelength ( $\mu\text{m}$ ) with light intensity ( $\text{mW}/\text{cm}^2$ ) values at appropriate boxes.

The optical carrier generation rate is defined as;

$$G = \frac{\eta_0(1 - R)I}{E} e^{-\alpha y}$$

Here,  $\eta_0$  - Conversion Efficiency

$R$  – Fresnel Reflection Coefficient

$I$  - Light intensity

$E = \frac{hc}{\lambda}$ , Photon Energy

$$\alpha = \frac{4\pi}{\lambda} k_i, \text{ Absorption Coefficient,}$$

$k_i$  is the imaginary part of refractive index of the material. Sopra material database has been included with the TNL PD (BIPOLAR) simulator. Users have flexibilities to include their wavelength dependent refractive index data.

### 2.3.4 Charge Assignment

The Charge in Cloud charge assignment technique on the node points of the meshes in BIPOLAR PDS simulator is chosen by default. **Charge in Cloud (CIC)**, the CIC scheme a better approximation can be obtained assigning the charge of a super particle to the two nearest neighbor cell points.

### 2.3.5 Parameters

Refer to Fig. 2.19, before proceeding for providing biasing at various device electrode edges

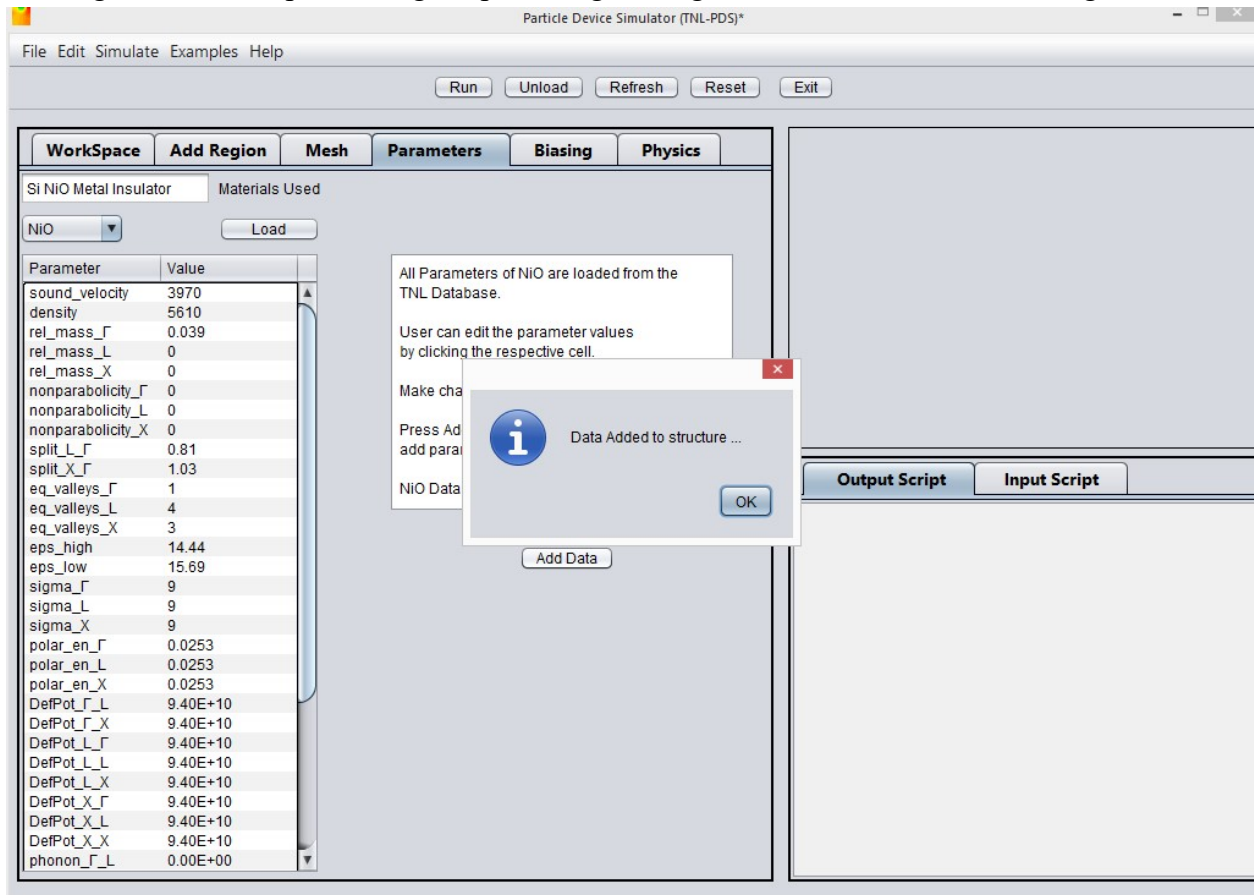


**Fig. 2.19:** Parameters Tab at GUI Frame

The various semiconductor materials chosen during device structure design is automatically store at Materials Used box. Users need to select one by one each material at drop down menu and click load button, all the prerequisite material properties loaded at table below in the frame. All the parameters are editable users may fill their material parameters values.

Then users need to click on Add Data button, a popup message will be generated that data added to the structure, click OK and perform same steps for each and every material reside at drop down box.

### 2.3.6 Biasing

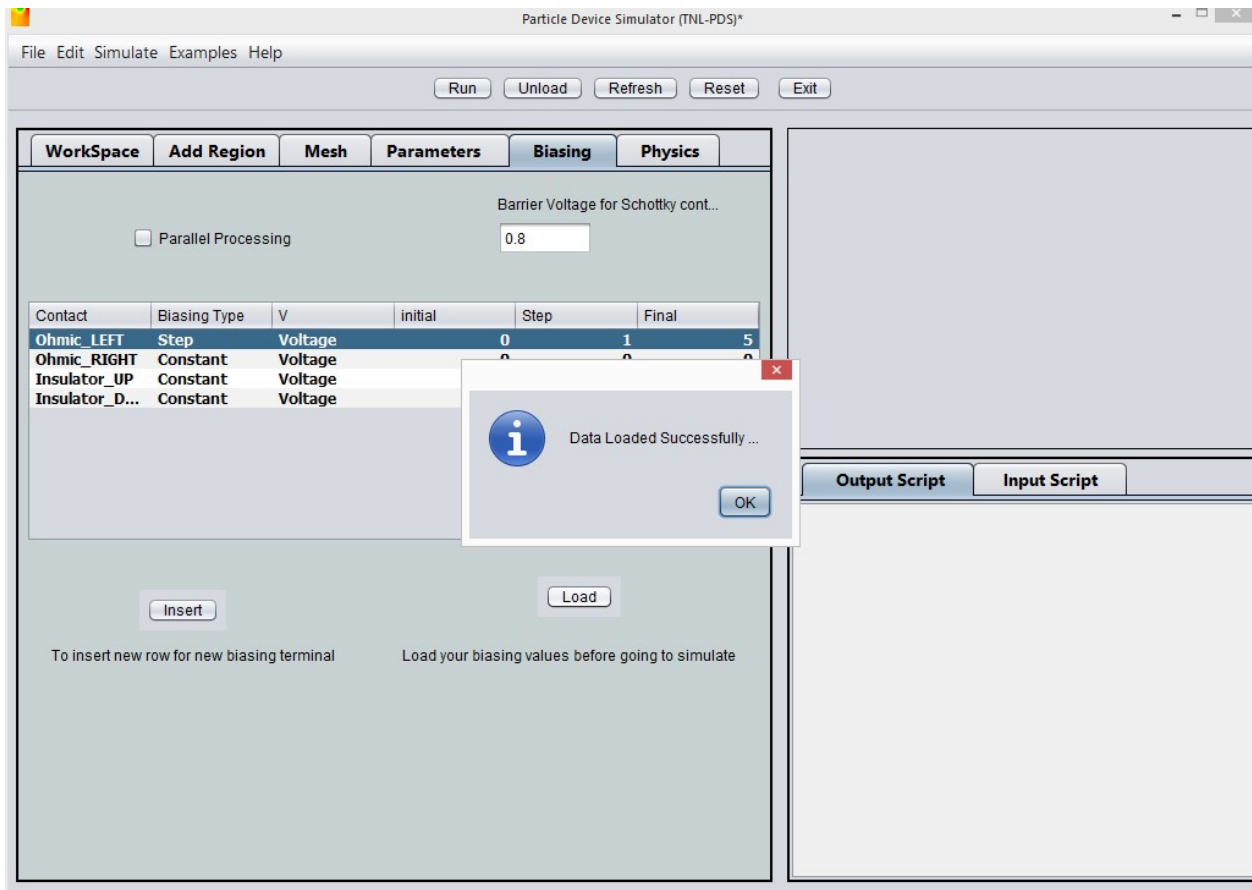


**Fig. 2.20:** Biasing Tab at GUI Frame

- Insert button is used to increase number of rows as per the electrodes added in the device structure for providing the voltage information.
- Users may choose constant or ramping voltage conditions on a particular electrode.
- Give the initial, step and final biasing point. Suppose user gives initial value 0, step value 0.1V and final value 1V. Then the simulation will first start at the 0 then it will proceed to 0.1, 0.2, 0.3, ... and so on, up to final value 1V.
- During the simulation all respective results will be saved at these voltages (we will talk about it later in this tutorial).
- Then click on load button on the main frame under solve tab. The given voltage will be added to particular electrode.
- The biasing tab in main frame in BIPOLAR PDS simulator is use to provide input voltages at all different edges of the device even in case, it is zero as well.
- User need to carefully choose the contact of terminal as defined in Add region section. E.g. Case of PN junction:
  1. Suppose in a pn junction device user has added Metal at left and right edges and insulator material at up and down edges.

2. User need to select Ohmic\_LEFT and Ohmic RIGHT to provide constant or ramping voltages at either contact or at both the contacts. The voltage will be uniformly distributed at whole edge of each side. On the other hand, user needs to provide zero potential at UP and DOWN insulator edges as shown in Fig. 13.

Case of MESFET:

1. In case of MESFET all three contacts exist at upper edge and three Metals have added at upper edge in Add region section with different x positions.
2. User may select Ohmic\_UP, Ohmic\_UP and Ohmic\_UP or Schottky electrodes to provide constant or ramping voltages at either contact to satisfy the Dirichlet boundary conditions. While the other remaining device edges are selected as Insulator\_LEFT, Insulator\_RIGHT, Insulator\_DOWN etc to satisfy Neumann boundary conditions. For isolation between Ohmic\_UP electrodes, user may choose Insulator\_UP at appropriate location during Add Region information fill.

After filling all above mentioned information by user in TNL-PD frame, the structure is ready for start running the simulation, there are three ways:

- iv. Click on 'RUN' button present above.
- v. Go to Simulate menu, then click on Run submenu.
- vi. Go with the key combination of Shift+F6.

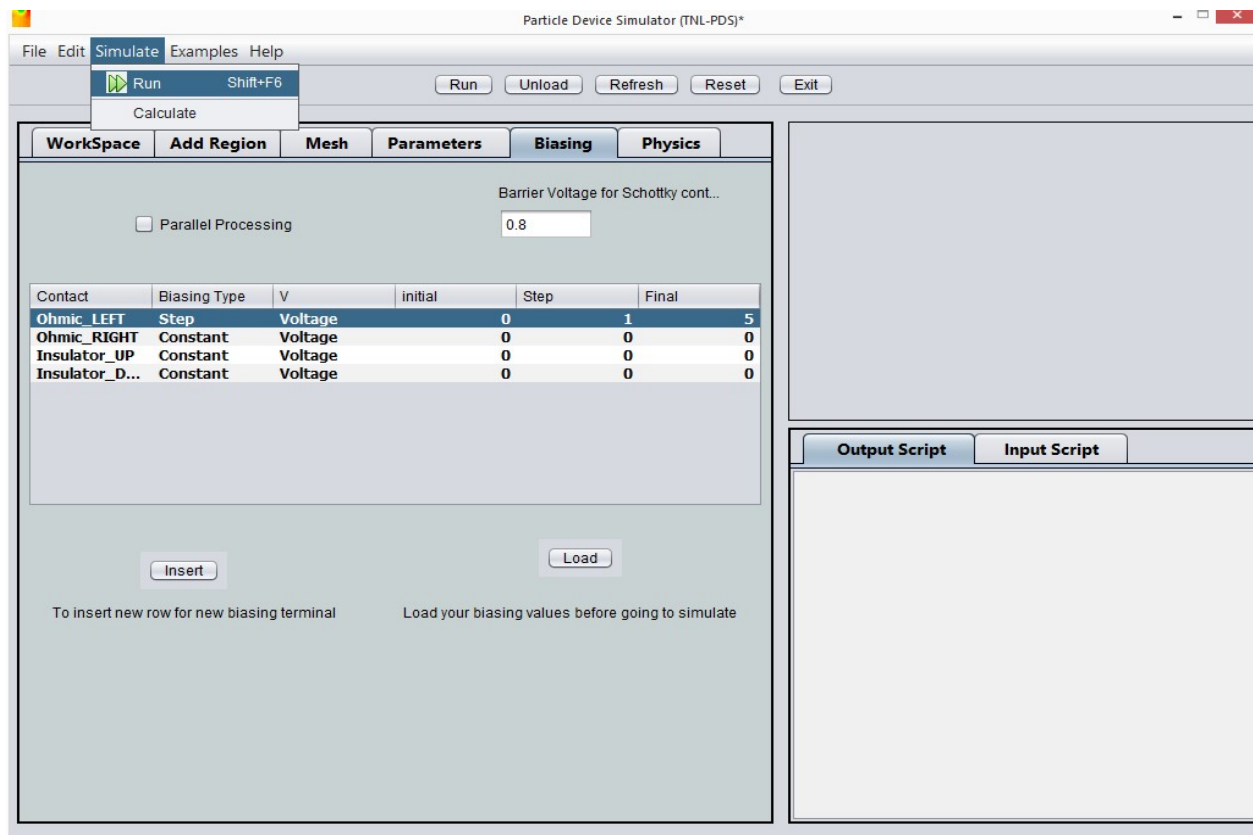
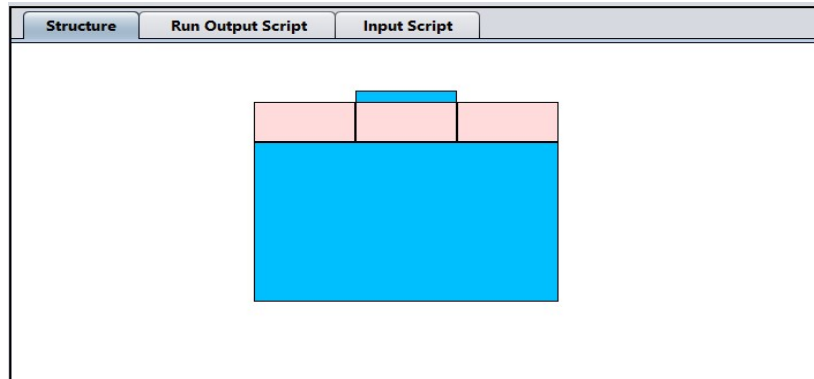


Fig. 2.21: Run Simulation from GUI Frame

### 2.3.7 Structure Tab



**Fig. 2.22:** Structure tab showing graphics of device

The tab shows the graphics of the device structure with all the regions geometries added in the Add Region section.

TNL-PD (BIPOLAR) simulator's GUI capabilities provide feasibility to view and verify device structure from table for each and every region/material/contact added to device geometry which contains the database of the designed structure or through the structure graphics. Through this it can be easily checked that at the time of input whether there is some unnecessary spaces in consecutive regions or region overlapping have been made or not and can be removed easily.



## 2.4 Run Output Script

It will provide all the output data information. Once the simulation will be completed it will show the message SIMULATION COMPLETED.

```

Structure Run Output Script Input Script
*          #          #          #          #          *
*          #          #          #          #          *
* TECH NEXT LAB FAMILY OF SIMULATORS
* ALL SIMULATORS ARE PROPRIETARY PRODUCTS OF TECHNEXT LAB PVT LTD.
* ALL SIMULATORS ARE TRADEMARK OF TECHNEXT LAB PVT LTD
* USER AGRE TO ALL TERMS & CONDITIONS TO RUN ANY TNL SIMULATORS.
* TNL FRAMEWORK LIC INFO NO OF USERS
* EPIGROW
* FULL BAND
* HALL MOBILITY
* MC PARTICLE DEVICE
* STRVIEWER
* TNL PLOT
*****
Simulation Starts...
02/09/2021 12:32:32

Working Directory C:\Users\fanis\Documents\device1\device1\Gate_vtg-3.0\drain_vtd0.0
Mechanisms in the gamma valley = 6
Mechanisms in the L valley = 8
Mechanisms in the X valley = 8
Mechanisms in the gamma valley = 6
Mechanisms in the L valley = 8
Mechanisms in the X valley = 8
Mechanisms in the gamma valley = 6
Mechanisms in the L valley = 8
Mechanisms in the X valley = 8
Mechanisms in the gamma valley = 6
Mechanisms in the L valley = 8
Mechanisms in the X valley = 8
Number of electrons initialized =43391
Number of electrons in use = 43391

Calculation starts at Drain voltage = 0.0 and Gate voltage = -3.0
Number of time steps for averaging =1000
Total number of time steps = 40000

11/26/2020 11:21:37
##### 11_26_quant1 #####
row\col 8 9
Material X min x max y min y max doping type conc Region
Si 50 75 5 15 NType 1e25 Source 1
Si 100 125 5 15 NType 1e25 Drain 2
Si 75 100 5 15 PType 2e24 Gate 3
Oxide 75 100 2 5 0 0 Gate-Oxide 4
Oxide 50 125 15 55 0 0 Bulk-Oxide 5
Al-Au_alloy 50 75 5 5 0 0 Ohmic 6
Al-Au_alloy 100 125 5 5 0 0 Ohmic 7
Al-Au_alloy 75 100 2 2 0 0 Ohmic 8
FD SOI
mesh_sizeX 1.0E-9
mesh_sizeY 1.0E-9
mult_factor 1.0E-9
acoustic ON
intervalley_g ON
intervalley_f ON
coulomb ON
charge_Assignment CIC
Parallel_Processing OFF
row\col2 2 6
Contact Biasing-Type Volt/Current Int Step Final
Gate Step Voltage -0.3 0.1 0.4 1
Drain Constant Voltage 0.6 0.6 0.6 2

```

Fig. 2.23: (a) Output script tab

(b) Input Script tab

## 2.5 Input Script

The tab consists of information about all the input information provided to initiate simulation from all the tabs on the left column of the main frame in script form. Users may have flexibility to load an example (.txt) file, then that whole script can also be printed here.

## 2.6 Menu

### i. File

When users click on File menu option, Open sub-menu will be opened. Click on Open a pop-up window will float on user's screen. From this users may go to specific directory and then to that folder in which users script file for their device structure input is present. Select that .txt file and click on open button below of the pop-up window. (See Section 1.3)

### ii. Simulate

The menu contains Run option click on this users may click to start the simulation after giving the path to save simulation.

*iii. Example*

Several examples are inbuilt to start working with the simulator under UNIPOLAR and BIPOLAR technologies options. Simulator can load with an example script of each device technology. Users can select any on and run the simulation.

*iv. Help*

Here three options named About, TNL-PDS Manual and TNL-PDS Tutorial are provided.

Clicking on about or by giving shortcut-key combination of Ctrl+H will transfer you the [TechNext Lab Pvt. Ltd.](https://www.technextlab.com) official website <https://www.technextlab.com>. Clicking on above options TNL-PDS Manual and TNL-PDS Tutorial, manual and tutorial file will be opened.

**2.7 Other**

- i. Run Button: This button is use to start the simulation.
- ii. Unload Button: The button is use to unload or delete all the input information given previously. The button is necessary when users need to input their data from the script file.
- iii. Refresh Button: The button is to refresh the graphics of device structure when there is some editing needed.
- iv. Reset Button: The button delete each and every thing and brings it to null value.
- v. Exit Button: This button closes the simulator GUI window.

## 2.8 Simulation of Examples (Script)

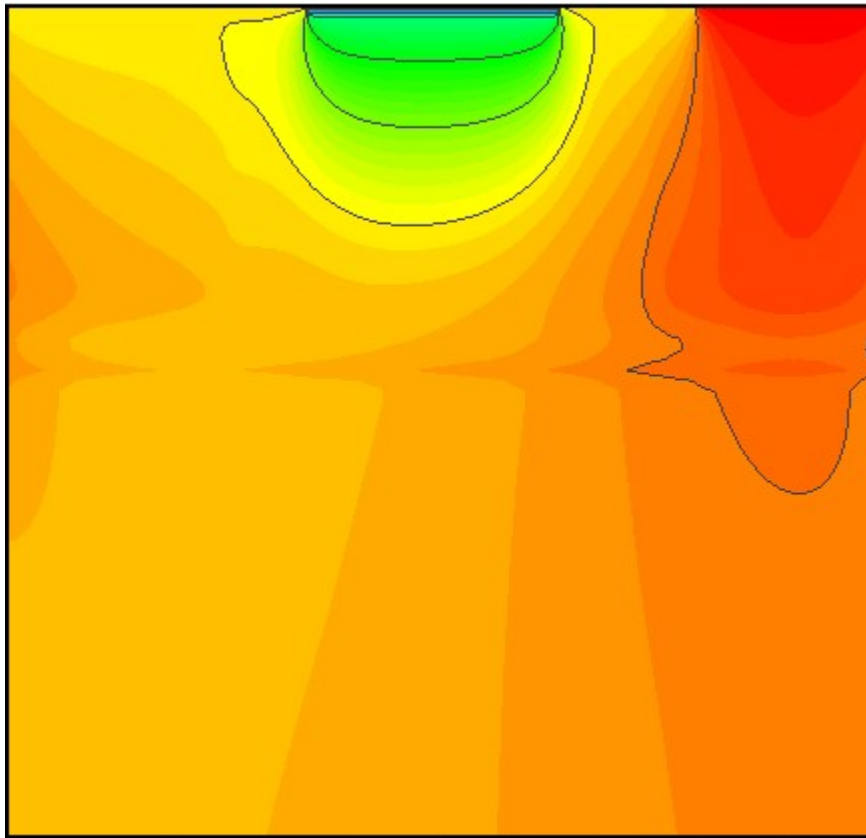
TNL-PD simulator provides flexibility to do device simulation through the script file as by using the GUI feature as described in the previous section. To start learning and working over TNL-PD simulator with inbuilt Examples, go through following steps:

- 1) Click on Unload button
- 2) Click on Technology drop box, select technology.
- 3) Fill Work Space dimension along with Temperature.
- 4) Give the workspace (X and Y scale) comparable to the device dimension written in the Example script file. User can see this in the Input Script tab.
- 5) Click on the Example menu and then select any of on technology name.
- 6) Click on Refresh button. User's device structure defined in script file will be loaded on GUI frame under Structure tab.
- 7) Check Mesh and Physics tabs.
- 8) Click on Material tab, load material and add parameters to device structure.
- 9) Click on Run button and select any directory or folder or path and give the name of your simulation output file, then click on save button, thus simulation will be started of the examples.
- 10) After some time scroll the Run Output Script pane and see the progress of your simulation. At the time of completion 'Simulation Completed Successfully' message will be shown in Run Output Window.
- 11) See output results by going through the directory as described in Step 6.

Same steps will be taken if you select a script file from Open option of File menu.

# Chapter 3

# Physics



The study of electronic transportation in the nanometer scale semiconductor devices involves several additional complications as compared to handle carrier transport in larger structures. The electronic band structure depends on the size and geometry of the device itself. In addition, the formulation of charge carrier dynamics on the electronic band structure must be beyond the equilibrium transport conditions. The structure and size of device itself may dictate the physics of the collision processes due to the presence of localized phonons, of interfacial excitations, of non-ideal surfaces and interfaces, etc.

Here we outline a possible scheme to tackle the problems mentioned above. Regarding the electronic band structure of the system, empirical local pseudopotentials details given and show that qualitatively and, often, quantitative generates accurate results which can be obtained in a variety of systems of interest, such as thin semiconducting (group VI, IV-IV, III-V and II-VI) bodies, hetero-layers, nanowires, and also even for carbon-base structures (graphene, graphene nanoribbons, carbon nanotubes). The reasons for focusing on ‘empirical’ pseudopotentials are twofold:

1. First, to develop a general scheme based on accurate k-space band-structure methods leading to the solution of electronic quantum transport in small dimensional devices. From this perspective, empirical or ab-initio pseudopotentials are equivalent algorithmically and numerically.
2. Second, while clearly ab-initio methods may provide the most accurate picture since ionic and charge redistribution can be accounted for. However, on the other hand their significant computational cost and questionable quantitative accuracy (remember that charge transport is often sensitive to energy changes of the order of the thermal energy,  $k_B T$ ) may render them unsuitable in most of the cases.

‘Empiricism’ may allow users to calibrate input parameters in order to fit experimental data, when available.

### 3.1 Electronic Band Structure

Monte Carlo method exploits mathematical technique and based on selection of random numbers. In principle, the Monte Carlo (MC) method can be considered as a very general mathematical tool for the solution of a great variety of problems. The method is exploited for solution of seven (07) phases Boltzmann transportation equation (BTE) in MC Particle Device simulator (TNL-PDS) on the single valley, three valleys or full electronic band structure.

Electrons in a perfect crystal can be described in terms of Bloch states, whose wave functions can be written as (3.1)

$$\psi_{nk}(r) = u_{nk}(r)e^{ik \cdot r} \quad (3.1)$$

where,  $n$  is a band index,  $\hbar k$  is the quasi momentum of the electron, and  $u_{nk}(r)$  is a function of the space coordinate  $r$  with the periodicity of the crystal.

For each band  $n$ , a value of the electron energy  $\varepsilon_n(k)$  is associated to the electron state  $k$ . The set of functions  $\varepsilon_n(k)$  and its values demonstrate the band structure of the material. The plane waves and empirical pseudopotentials methods have proven useful method to gain insight to calculate the full electronic band structure of most of the semiconductors (and other crystals). It also provides information regarding the electronic excitation spectrum within the solids. The ‘empirical’ nature implies loss of strong predictive power and ‘portability’ of ionic (pseudo) potentials, but it results in a vast simplification of the numerical problem (compared to ab-initio methods) and the small degree of fitting allowed by the technique affords – by definition – excellent agreement with experimental data [Cohen]. Since in TNL-PD simulator, our focus is on electronic transport, not on structure calculations, it represents the best choice to perform accurate calculations. The knowledge of the band structure of a solid is the starting point for the study of any electronic property. The full band structure of the thin / thick films can be simulated using **TNL-FB (FullBand)** simulator, a proprietary product of TNL family of simulators. The details of band structure calculation are given in user manual of FullBand (TNL-FB) simulator.

At zero temperature, the valence band of a semiconductor is entirely occupied by electrons, and the conduction band is entirely empty. The most of the group IV, III-V and II-VI semiconductors exists in  $sp^3$  hybridization, i.e., electrons are partially filled only up to p-orbital whereas higher orbital are deficient of electrons. In full band structure, the energy bands represent p-orbital is known as valance band and all above energy bands are known as conduction bands.

For temperature  $T > 0$ , few electrons leave the valence band and occupy some states in the conduction band due to change in their energies. In such a case the transport properties of the semiconductors are due to an equal number of electrons and holes.

### 3.1.1 Energy Bands

From computational point of view, two types of band structures exist i.e. parabolic and non parabolic. Both type of band structures are implemented in TNL-PD simulator.

#### 3.1.1.1 Parabolic Band

The parabolic band, as the name itself suggests, approximate the energy band in the minimum energy valley (for GaAs, for example, it is the point named  $\Gamma$  in figure 3.1) where the vast majority of electrons are (though this approximation is not valid in some cases, as we will see latter on)

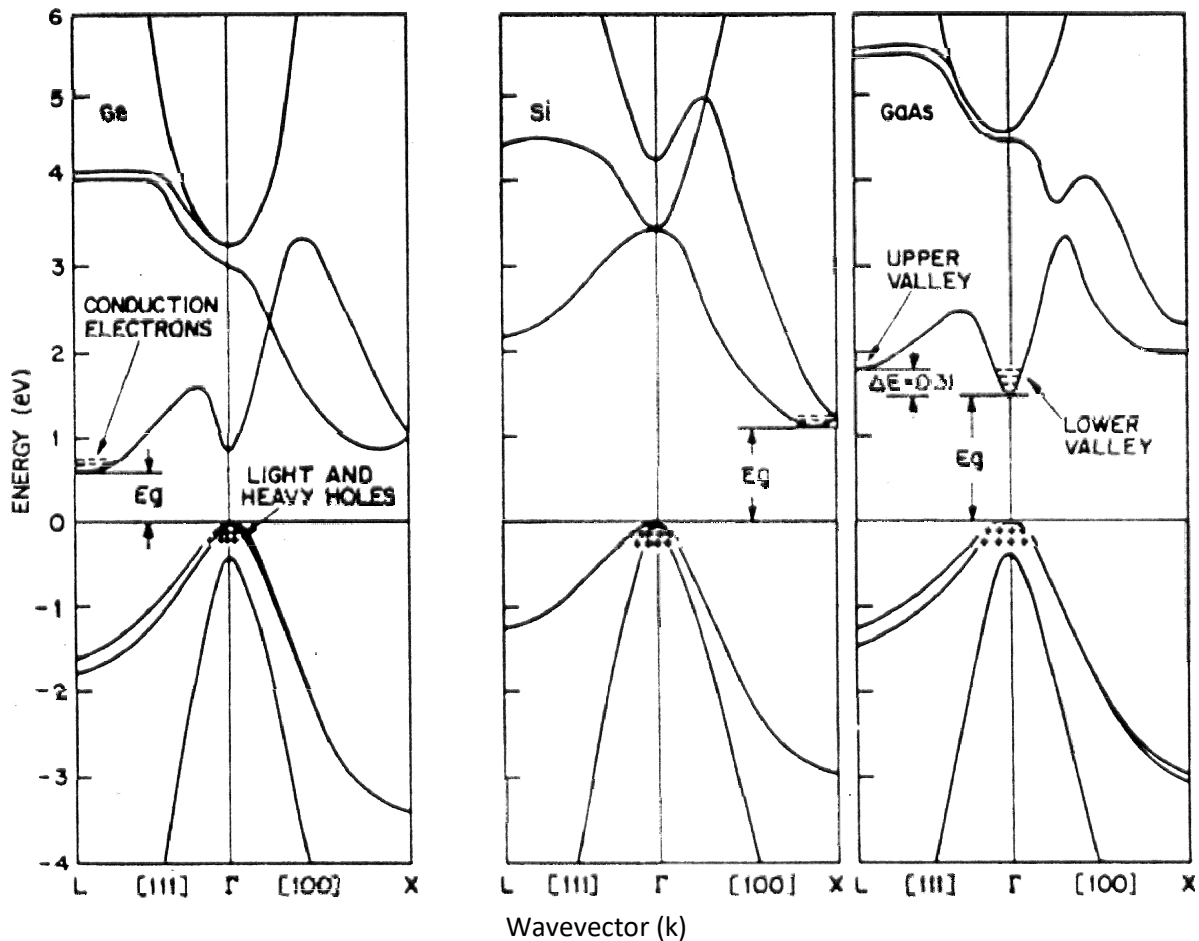


Figure 3.1 - Energy bands for Germanium, Silicon and Gallium Arsenide

Around the maximum of the valence band and the minimum of the conduction band the function  $\varepsilon(k)$  can be approximated with a parabolic function of  $k$  and for a high symmetry situation it reduces to

$$\varepsilon(k) = \frac{\hbar^2 k^2}{2m^*} \quad (3.2)$$

### 3.1.1.2 Nonparabolic Band

The most used non-parabolic approximation of the energy band is the so called Kane approximation. Away from conduction band minima, the non-parabolicity of bands dominates and  $\varepsilon(k)$  may be approximated as

$$\varepsilon(1 + \alpha\varepsilon) = \frac{\hbar^2 k^2}{2m^*} \quad (3.3)$$

Here  $m^*$  is the effective mass of the electrons and  $\alpha$  is the non-parabolicity factor associated with the band.

Finally, once the energy band is fixed, an important relation is the following (that is extremely useful for calculating the electron velocity)

$$\vec{v} = \frac{\nabla_k \varepsilon(\vec{k})}{\hbar} \quad (3.4)$$

The relation will be very useful during the carrier velocity computation of an electron in the Monte Carlo method implemented in TNL-PD simulator.

### 3.1.2 Nonparabolicity Factor ( $\alpha$ )

For values of  $k$  far from the minima of the conduction band and/or from the maxima of the valence band, the energy deviates from the simple quadratic expressions and nonparabolicity observed. For the conduction band, a simple analytical way of introducing nonparabolicity is to consider an energy-wave vector relation of the type as given in equation 3.9 and nonparabolicity parameter  $\alpha$  is;

$$\alpha = \frac{1}{E_g} \left(1 - \frac{m^*}{m_0}\right) \quad (3.5)$$

$E_g$  is the energy gap and  $m_0$  is the electronic rest mass.

### 3.1.3 Effective Masses

A simple parabolic band described by the energy-wave vector relationship in Eq. (3.2), is completely characterized by its effective mass  $m$ . Such a parameter plays a fundamental role in several physical problems of different nature: the acceleration of an electron in a crystal subject



to an external force, the ratio of the electron momentum to its velocity, the electron effective mass in energy space is

$$\frac{1}{m_{ij}^*} = \frac{1}{\hbar^2} \frac{\partial^2 \varepsilon}{\partial k_i \partial k_j} \quad (3.6)$$

Here  $m_{ij}$  is the inverse effective-mass tensor. The  $(1/m_{ij})$  is in general a function of  $k$ .

### 3.1.4 Conductivity Effective Mass

The conductivity effective mass is defined as ratio of the electron momentum to its velocity.

$$\frac{\hbar k}{m_c} = \frac{1}{\hbar} \frac{\partial \varepsilon}{\partial k} \quad (3.7)$$

In the simple case,  $m_c = m$ . For a parabolic, ellipsoidal band  $m_c^{-1}$  is the inverse effective-mass tensor. This indicates that  $v$  and  $k$  are not, in general, parallel in non-spherical bands. In this case a spherical approximation can be obtained by averaging over all possible directions. The resulting scalar conductivity inverse effective mass is

$$\frac{1}{m_c} = \frac{1}{3} \left( \frac{1}{m_l} \right) + \frac{2}{3} \left( \frac{1}{m_t} \right) \quad (3.8)$$

For a cubic semiconductor, this is also the conductivity effective mass at any given direction, averaged over the valleys equivalent by symmetry.

### 3.1.5 Density-of-States Effective Mass

In the evaluation of the number of carriers in the conduction band, the effective mass plays again a role due to its influence on the electron density of state in energy space. In fact, the electron density  $n$  is given by

$$n = \int f(\varepsilon) g(\varepsilon) d\varepsilon \quad (3.9)$$

Here  $f(\varepsilon)$  and  $g(\varepsilon)$  are the electron distribution function and density of states in energy space.

$$N(\varepsilon_k) = (2m^*)^{\frac{3}{2}} \gamma^{\frac{1}{2}}(\varepsilon_k) \frac{d\gamma(\varepsilon_k)}{d\varepsilon_k} \quad (3.10)$$

Where function  $\gamma$  is dependent on the energy.

$$\gamma(\varepsilon_k) = \varepsilon(1 + \alpha\varepsilon) = \frac{\hbar^2 k^2}{2m^*} \quad (3.11)$$

For a parabolic, ellipsoidal band, density of states mass  $m_d$  can be written as;

$$m_d = (m_l m_t^2)^{1/3} \quad (3.12)$$

The band parameters of zincblende (Zb) and wurtzite (Wz) binary semiconductors are listed in Table I & II as below;

**Zincblende (ZB)**

Material	Bandgap (eV)	$m_l/m^*$	$m_t/m^*$	$m_\Gamma/m^*$	$m_L/m^*$	$m_X/m^*$	$\alpha_\Gamma$	$\alpha_L$	$\alpha_X$
Si	1.12	0.98	0.19	-	-	-	0	0	0.5
Ge	0.7	1.59	0.08	-	-	-	0	0.5	0
GaAs	1.424	-	-	0.063	0.17	0.58	0.62	0.5	0.3
InP	1.34	-	-	0.08	0.25	0.32	0.83	0.23	0.38
AlAs	2.67	-	-	0.15	0.19	0.6	0	0.4	0.36
InAs	0.35	-	-	0.023	0.29	0.64	1.39	0.54	0.9
GaP	2.26	-	-	0.15	0	0.5	0	0	0
GaN	3.28	-	-	0.2	0.6	0.4	0.189	0.076	0.029
3C-SiC	2.36	0.68	0.25	-	-	-	0.323	0.323	0

Here,  $m_l$  and  $m_t$  are the electron's mass in the lateral and transverse directions of the lowest lying valley in the conduction band of the material. The  $m_\Gamma$ ,  $m_L$  and  $m_X$  are the electronic masses at  $\Gamma$ , L and X valleys in the conduction band whereas  $m^*$  is the rest mass of electron i.e. ( $9.31 \times 10^{-31}$ kg).

**Wurtzite (WZ)**

Material	Bandgap (eV)	$m_l/m^*$	$m_t/m^*$	$m_\Gamma/m^*$	$m_U/m^*$	$m_{\Gamma_3}/m^*$	$\alpha_\Gamma$	$\alpha_U$	$\alpha_{\Gamma_3}$
GaN	3.47	-	-	0.2	0.4	0.6	0.189	0.076	0.029
AlN	6.20	-	-	0.48	1	1	0.044	0	0
InN	0.7	-	-	0.04	0.25	1	1.32	0.23	0
ZnO	3.43			-	-	-			
4H-SiC	3.23	0.29	0.42	-	-	-	0.323	0.323	0
6H-SiC	2.86	0.20	0.42	-	-	-	0.323	0.323	0

Here,  $m_l$  and  $m_t$  are the electron's mass in the lateral and transverse directions of the lowest lying valley in the conduction band of the material. The  $m_\Gamma$ ,  $m_L$  and  $m_X$  are the electronic masses at  $\Gamma$ , L and X valleys in the conduction band whereas  $m^*$  is the rest mass of electron i.e. ( $9.31 \times 10^{-31}$ kg).

In case of the ternary semiconductor materials, the option to choose ternary material is enabled and user need to provide mole fraction value with selection of two binary materials to interpolate the ternary material properties.

### 3.1.6 Ternary and Quaternary semiconductors

The ternary and quaternary semiconductors material's parameters can be obtained through interpolation of the parameters of the binary semiconductors material's parameter.

E.g.

$$E_g = xE_g^A + (1 - x)E_g^B - bx(1 - x) \quad (3.13)$$

where A and B represent band gap values for binary semiconductors and b is bowing parameter with x is the mole fraction. By default the value of bowing parameter in TNL-PD simulator is taken unity.

Similarly, nonparabolicity factor and other parameters, effective mass, density of states masses can be interpolated.

### 3.2 Carrier Scattering Mechanisms

The justification for using a semi-classical approach for non-linear carrier dynamics for nanometer scale devices is rooted in the Heisenberg Uncertainty Principle. Within the aforementioned constraints of feature sizes and temperature, the uncertainty in a carrier's momentum  $p$  and position  $r$  of an ensemble of such carriers can be shown to be typically much less than the average momentum and the mean free path respectively. Under these circumstances, the carrier can be considered to behave as a narrow wave packet. The average momentum of a carrier ensemble is then given by the de Broglie relation as  $\mathbf{p} = \hbar\mathbf{k}$ , where  $k$  is the average wavevector of the ensemble. The mean free path is determined from the mean time between collisions or scattering, which is nearly equal to the inverse of the average scattering rate. The interactions of carriers (e.g., electrons) with each other and with the lattice of crystal introduce a variety of scattering processes responsible for relaxing the momentum and the energy of the particle. During scattering mechanisms, the energy of carriers remain conserved which is termed as **Fermi-Golden rule**. For carrier kinetic energies less than about 1.0eV, scattering occurs at a sufficiently low rate to satisfy the Uncertainty Principle and validate the semi-classical approach.

The standard scattering processes with **Fermi's Golden Rule** are implemented in the TNL-PD (Particle Device) simulator are given below. User has flexibility to choose any or more scattering processes appropriate for different semiconductor materials. To avoid the error user must select at least one scattering mechanism to run the simulation.

## Types of Scattering Mechanisms

### ***a. Lattice scattering***

1. Intravalley
  - i. Acoustic (Deformation and Piezoelectric)
  - ii. Optical (Polar and Non-polar)

### ***b. Defect scattering:***

1. Impurity
2. Alloy
3. Dislocation

### ***c. Piezoelectric***

### ***d. Carrier-carrier scattering***

### ***e. Impact Ionization***

### ***f. Surface Roughness***

### 3.2.1 Fermi's Golden Rule

The scattering rate, per unit time of a carrier in state  $\Psi_n(\mathbf{k}, \mathbf{r})$  to a state  $\Psi_n(\mathbf{k}', \mathbf{r})$  due to a perturbation of the Hamiltonian of magnitude  $H'$ , is given, within first-order, time dependent perturbation theory as

$$S(k', k) = \frac{2\pi}{\hbar} |\langle k' | H' | k \rangle| \delta(\varepsilon_{k'} - \varepsilon_k \mp \hbar\omega) \quad (3.14)$$

where the Dirac bra and ket variables  $\mathbf{k}$  and  $\mathbf{k}'$  denote the corresponding state wave vectors. The Kronecker delta function  $\delta$  in (3.12) enforces conservation of energy between the initial and final energy states,  $\varepsilon_{\mathbf{k}}$  and  $\varepsilon_{\mathbf{k}'}$ , respectively, accounting for the emission or absorption of a phonon of energy  $\hbar\omega$  in the scattering process, where  $\hbar$  is the Planck constant and  $\omega$  denotes the phonon frequency. This famous result is known as the *Fermi Golden Rule*. It is important to note that (3.12) assumes that momentum scattering occurs instantaneously, and that the real-space position of the particle remains constant during the collision.

The particular form of  $H'$  depends on the relevant scattering mechanism in question for the material of interest, and will be discussed in subsequent subsections of this chapter. Furthermore, the form of the Bloch function as given by (3.1) needs to be modified if the motion of the particle is dimensionally restricted due to quantization in a particular direction in the device.

### 3.2.2 Acoustic Deformation Potential Scattering

The acoustic phonons are responsible for the maximum energy transfer in an electronic interaction. In acoustic scattering process the phonons energies are much smaller than the electron energy, and thus very often acoustic scattering is treated as an elastic process. Acoustic scattering pave way to understand the exchange of an infinitesimal amount of energy between the electrons and the crystal. Under high temperatures or high field conditions, the average electron energy is larger than the optical-phonon energy, and this kind of phonon will be responsible for the task of exchanging energy between the electrons and the crystal.

As mentioned in section (3.1), the physical quantity of interest is the interaction potential resulting from the induced strain. Hence,

$$H'(\mathbf{r}, t) = \Xi_{ac} \nabla \cdot \mathbf{u}(\mathbf{r}, t) \quad (3.15)$$

where  $\Xi_{ac}$  denotes the acoustic deformation potential and  $\mathbf{u}(\mathbf{r}, t)$  is given as

$$\mathbf{u}(\mathbf{r}, t) = \sum_{\mathbf{q}} \left( \frac{\hbar}{2\rho\Omega\omega_{\mathbf{q}}} \right)^{\frac{1}{2}} \mathbf{e}_{\mathbf{q}} (a_{\mathbf{q}} + a_{-\mathbf{q}}^{\dagger}) e^{i\mathbf{q}\cdot\mathbf{r}} \quad (3.16)$$

Here  $\mathbf{q}$  is all phonon wave vectors (modes) summation and  $\omega_{\mathbf{q}}$  is the angular frequency,  $\Omega$  is the crystal volume,  $\mathbf{e}_{\mathbf{q}}$  is the unit polarization vector, and  $a_{-\mathbf{q}}^{\dagger}$  and  $a_{\mathbf{q}}$  are the quantum mechanical raising and lowering operators, respectively.

At  $T=300\text{K}$ , the energy  $\hbar\omega \ll k_{\text{B}}T$ , assuming the equi-partition approximation  $N_0(\omega_0) = \frac{k_{\text{B}}T}{\hbar\omega}$ , so that  $N_0(\omega_0) = N_0(\omega_0) + 1$  and  $\hbar\omega \approx 0$ . The acoustic scattering rate is

$$\Gamma(\varepsilon_k) = \frac{2\pi\Xi_{ac}^2 k_{\text{B}}T}{\hbar C_1} N(\varepsilon_k) \left( \frac{(1+\alpha\varepsilon_k)^2 + \frac{1}{3}(\alpha\varepsilon_k)^2}{(1+2\alpha\varepsilon_k)^2} \right) \quad (3.17)$$

where  $T$  is the lattice temperature,  $C_1$  is the material dependent elastic constant dependent on the mass density  $\rho$  and velocity of sound in material  $v_s$  and defined as

$$c_1 = \rho v_s^2 \quad (3.18)$$

The density of states,  $N(\varepsilon_k)$  for a carrier in a non-parabolic band is given above. The acoustic deformation potential scattering is isotropic for spherical and parabolic bands. The final wavevector can be chosen at random since all scattering angles are equally probable.

In the case of non-parabolic bands, the scattering is not strictly isotropic.



### 3.2.3 Non-Polar Optical Scattering

The optical phonons are assumed to remain at constant equivalent temperature as the dispersion relation of such kind of phonons is observed quite flat for the  $q$  values involved in electronic intravalley transitions. This kind of scattering is isotropic. This kind of scattering is dependent on the interaction potential is proportional to the displacement as compared to the case of acoustic deformation potential scattering where induced strain is of importance. The phonon energies at higher optical frequencies are of the order of the thermal energy involved in these interactions.

Therefore, for non-polar optical phonons near the zone center the interaction potential is given as

$$H'(\mathbf{r}, t) = D_{ij} \cdot \mathbf{u}(\mathbf{r}, t) \quad (3.19)$$

Here  $D_{ij}$  is a valley dependent deformation potential

At near to the edge of the Brillouin zone, the non-polar optical phonons that contribute to intervalley scattering are at slightly lower energies (on the order of a few meV) than those at the zone center.

$$\Gamma(\varepsilon_k) = \left( \frac{\pi D_{ij}^2 Z_j}{\rho \omega_{ij}} \right) \left( N_o(\omega_o) + \frac{1}{2} \mp \frac{1}{2} \right) \left( \frac{(2m_d)^{3/2} \sqrt{\varepsilon_f(1+\alpha\varepsilon_f)}}{4\pi^2 \hbar^3} \right) (1 + 2\alpha\varepsilon_f) \quad (3.20)$$

with,  $\varepsilon_f = \varepsilon_k \pm \hbar\omega_{ij} - \Delta\varepsilon_{ij}$  (3.21)

where,  $\Delta\varepsilon_{ij}$  and  $\omega_{ij}$  denote the energy offset and intervalley phonon frequency, respectively, between the  $i^{\text{th}}$  and  $j^{\text{th}}$  valleys in the 3-valley model employed.  $Z_j$  denotes the number of equivalent  $j$  valleys due to crystal symmetry and  $\rho$  is the mass density.

### 3.2.4 Polar Optical Phonon Scattering

The electrostatic nature of the interaction is strongly anisotropic in nature. The treatment of this scattering is again simplified by the constancy of the phonon energy in the transition similar to *Non-Polar Optical Scattering*. At high electron energies the total scattering rate for polar optical scattering decreases with increasing energy, owing to the electrostatic nature of the interaction. The scattering rate is

$$\Gamma(\varepsilon_k) = \left( \frac{\sqrt{m_d} e^2 \omega_{LO}}{4\sqrt{2}\pi\hbar\epsilon_p} \right) \left( N_o + \frac{1}{2} \mp \frac{1}{2} \right) \left( \frac{1+2\alpha\varepsilon_{k'}}{\gamma(\varepsilon_k)} \right) F(\varepsilon_k, \varepsilon_{k'}) \quad (3.22)$$

where,

$$N_o = \frac{1}{e^{\frac{\hbar\omega_{LO}}{k_B T} - 1}}, \quad \frac{1}{\epsilon_p} = \frac{1}{\epsilon_{high}} - \frac{1}{\epsilon_{low}} \quad \text{and} \quad F(\varepsilon_k, \varepsilon_{k'}) = \frac{\sqrt{\gamma(\varepsilon_k)} + \sqrt{\gamma(\varepsilon_{k'})}}{\sqrt{\gamma(\varepsilon_k)} - \sqrt{\gamma(\varepsilon_{k'})}}$$

Here,  $\omega_{LO}$  is the longitudinal optical phonon frequency,  $m_d$  is density of states mass,  $\epsilon_{high}$  and  $\epsilon_{low}$  are the high frequency and low frequency dielectric constant of the material.  $\gamma(\varepsilon_k)$  is defined as a function dependent upon nonparabolicity of the bands refer to equation (3.5).

### 3.2.5 Ionized Impurity Scattering

In highly doped semiconductors (doping density greater than  $\sim 10^{17}/\text{cm}^3$ ), the resulting ionized impurities create coulombic potentials that scatter the carriers. These potentials are screened by the free carriers in the vicinity of the ions. A screening model that is typically used, which is employed here, is the Brooks-Herring model. This type of collisions is elastic in nature and therefore it cannot alone control the transport process in the presence of an external field. It must be accompanied by some other dissipating scattering mechanism if the proper energy distribution of electrons is to be derived from theory. Owing to the electrostatic nature of the interaction, the efficiency of ionized impurity scattering decreases as the temperature of the crystal increases. In TNL-PD simulator, the screened perturbation potential is given by

$$V(r) = \frac{Zen_o}{4\pi\epsilon_s r} e^{-q_D r} \quad (3.23)$$

where  $Ze$  denotes the charge of the ion,  $r$  the distance of the carrier from the ion, and  $n_o$  is the equilibrium density (i.e., the density of free carriers that would exist in the vicinity of the impurity if it were not ionized). The screening factor,  $q_D$ , is taken as the Debye wavevector given by

$$q_D = \sqrt{\frac{e^2 n_o}{\epsilon_s k_B T}} \quad (3.24)$$

The perturbed Hamiltonian is

$$H' = \frac{Zen_o}{4\pi\epsilon_s r} e^{-q_D r} \quad (3.25)$$

From Fermi Golden rule, the scattering rate is

$$\Gamma(\epsilon_k) = \left[ \frac{2\pi e^4 N_i Z^2}{\epsilon_s^2 \hbar^4} \right] N(\epsilon_k) \left[ \frac{1}{q_D^2 (q_D^2 + 4k^2)} \right] \quad (3.26)$$

The scattering rate given in equation (3.24) is valid within the Brooks-Herring model so long as  $q_D$  in the denominator is large enough so that the scattering rate does not diverge.

### 3.2.6 Alloy Scattering

In the group IV-VI, III-V and II-VI compound intrinsic semiconductors, the introduction of alloys cause an additional disruption to the periodic potential of crystal. In TNL-PD simulator the alloy scattering rate is implemented as

$$\Gamma(\varepsilon_k) = \frac{3\pi m^*}{8\sqrt{2}\hbar^4} [x(1-x)] [\gamma(\varepsilon_k)]^{3/2} \frac{d\gamma(\varepsilon_k)}{d\varepsilon} \Omega |\Delta V|^2 \quad (3.27)$$

where  $x$  is the molar fraction, the volume of the unit cell  $\Omega$  is given by  $a_o^3/4$  where  $a_o$  is the lattice constant, and  $\Delta V$  characterizes the strength of the perturbing potential.

### 3.2.7 Piezoelectric Scattering

The piezoelectric scattering should dominate deformation potential scattering at low enough temperatures in crystals having the piezoelectric effect. The scattering rate, in the elastic and the equi-partition approximation, is then of the form;

$$\Gamma(k_0) = \frac{m^* k_B T}{4\pi\hbar^3 k \rho} \left( \frac{e e_{pz}}{\epsilon v_s} \right)^2 \ln \left( 1 + 4 \frac{k^2}{q_D^2} \right) \quad (3.28)$$

Here, the screening factor,  $q_D$ , is taken as the Debye wavevector (see equation 3.24) and  $e_{pz}$  is the piezoelectric constant of the semiconductor material.

### 3.2.8 Dislocation Scattering

The abrupt changes in the periodic arrangements of atoms along a line in the lattice are defined as dislocation e.g. the epitaxial growth of GaN on Si has a 17% lattice mismatch whereas on Al<sub>2</sub>O<sub>3</sub>, it has a 13.8% lattice mismatch and a 34% mismatch in the thermal expansion coefficient. Dislocations are typically formed due to the large lattice mismatch of GaN with the substrates on which it is epitaxially grown (SiC and Sapphire). Under these situations, dislocation scattering mechanism becomes the dominant one at doping levels equivalent with the volume concentration of traps introduced by dislocations. The scattering rate can be expressed as

$$\Gamma(\varepsilon_k) = \left[ \frac{e^4 N_{dis} m_d}{\varepsilon_s^2 \hbar^3 c^2} \right] \left[ \frac{\lambda^4}{\left( 1 + \frac{8\lambda^2 m_d (1 + \alpha \varepsilon_k)}{\hbar^2} \right)^{3/2}} \right] \left( 1 + \frac{4\lambda^2 m_d \varepsilon_k (1 + \alpha \varepsilon_k)}{\hbar^2} \right) (1 + 2\alpha \varepsilon_k) \quad (3.29)$$

Here  $c$  is the velocity of light,  $N_{dis}$  is the line dislocation density and  $\lambda$  is the screening factor and is given by

$$\lambda = \sqrt{\frac{\varepsilon k_B T}{e^2 n_s}} \quad (3.30)$$

Where,  $n_s$  is the effective screening concentration.

### 3.2.9 Carrier-Carrier Scattering

Carrier-carrier interactions, apart from degeneracy effects, may be treated as a scattering process within the Monte Carlo algorithm on the same footing as other mechanisms. The two-body coulomb interaction can still be represented by a screened potential. It starts from the realization that a sum over the distribution function associated with each electron is simply an ensemble average of a given quantity. The individual carrier-carrier interaction via a screened Coulomb potential of the form is given by

$$V(r) = \frac{e^2}{\epsilon r} e^{-\beta} \quad (3.31)$$

Here,  $\beta$  is inverse Debye screening length and the transition probability of two electrons from the wave-vectors  $k$  and  $k_0$  to  $k'$  and  $k'_0$  is obtained using the *Fermi Golden rule*. Thus, the scattering rate due to carrier-carrier scattering can be expressed as

$$\Gamma(k_0) = \frac{2m^*e^4}{\hbar^3\epsilon^2V} \sum_k \frac{|k-k_0|}{|k-k_0|^2+\beta^2} \quad (3.32)$$

Here  $m^*$  is the electronic effective mass depends upon the position of electron on phase space,  $e$  is the electronic charge,  $V$  is the screened potential refers to equation (3.29) and  $\epsilon$  is the dielectric constant of the material.

### 3.2.10 Impact Ionization Scattering

The impact ionization scattering rate depends on the volume of the available phase space and the average squared transition matrix element  $|M_{ii}|^2$  within that phase space. The importance of the impact ionization rate around the threshold energy depends on the high energy tail of the carrier distribution and the ratio of the impact ionization rate to the phonon scattering rates. A carrier, being able to impact ionization, has to survive to energies above the threshold, emitting less phonon than the bulk of the particles. The carrier distribution above the threshold energy therefore strongly depends on the dissipation processes below the threshold energy. If the carrier has survived to impact ionization enabling energies, the occurrence of impact ionization has to be relevant compared to phonon scattering. The impact ionization rates are given by the below equation which validate the Keldysh formulas in modified form,

$$\Gamma(\varepsilon_k) = \Lambda^{ii}(\varepsilon_k - \varepsilon_{th}) \quad (3.33)$$

Here,

$$\Lambda^{ii} = \frac{2\pi}{\hbar} |M_{ii}|^2 \frac{\Omega^3}{N_{cell}} \quad (3.34)$$

Here,  $\varepsilon_k$  and  $\varepsilon_{th}$  are the electron energy and material specific threshold energy at which impact ionization initiate.  $M_{ii}$  is the multiplication factor for electrons,  $N_{cell}$  is the number of cells and  $\Omega$  is the volume.

### 3.2.11 Interface Roughness Scattering

This scattering mechanism also known as surface scattering is results due to the corrugation of interfaces. It becomes active when an electron travels in their vicinity. For this reason it is clear that the effect of such a mechanism is more pronounced when the transport phenomenon under investigation occurs in a narrow channel close to the oxide interface. Furthermore, the effect is comparatively stronger at low temperatures when the phonon contribution is smaller. Surface scattering is usually considered elastic.



The material parameters used in computation of scattering rates are;

**Zincblende (ZB) Material parameters used in various scattering mechanisms between three valley i.e.  $\Gamma$ , L and X**

Parameters	Si	Ge	GaAs	InP	AlAs	InAs	GaP	GaN(ZB)	3C-SiC
$\epsilon_{\infty}$	11.7	16.2	10.92	9.61	12.5	12.3	9.11	5.3	6.52
$\epsilon_s$	11.7	16.2	12.9	12.5	14.6	15.15	11.1	9.7	9.72
<b>M (kg/m<sup>3</sup>)</b>	2329	5320	5370	4810	3720	5680	4140	6087	3200
$v_s$ (m/s)	5220	5400	5220	5220	4280	5500	5220	5220	10000
$D_{a\Gamma}$ (eV)	1.2	2.5	7.01	5	7	5.8	5	8.3	14
$D_{aL}$ (eV)	1.7	2.5	9.2	5	7	5.8	5	8.3	14
$D_{aX}$ (eV)	1.7	2.5	9	5	7	5.8	5	8.3	14
$\hbar\omega_{L\Gamma}^{\uparrow}$ (eV)	0.063	0.037	0.03536	0.043	0.015	0.03	0.051	0.0873	0.12
$\hbar\omega_{L\Gamma}^{\downarrow}$ (eV)	0.063	0.037	0.03536	0.043	0.015	0.03	0.051	0.0873	0.12
$\hbar\omega_{L\Gamma}^{\times}$ (eV)	0.063	0.037	0.03536	0.043	0.015	0.03	0.051	0.0873	0.12
$D_{\Gamma\rightarrow L}$ (eV $m^{-1}$ )	0	2.00E+10	1.80E+10	5.06E+10	7.02E+10	5.59E+10	5.10E+10	1.80E+10	9E10
$D_{\Gamma\rightarrow X}$ (eV $m^{-1}$ )	0	1.00E+11	1.00E+11	4.98E+10	7.30E+10	6.35E+10	5.86E+10	1.00E+11	9E10
$D_{L\rightarrow\Gamma}$ (eV $m^{-1}$ )	0	2.00E+10	1.80E+10	5.06E+10	7.02E+10	5.59E+10	5.10E+10	1.80E+10	9E10
$D_{L\rightarrow L}$ (eV $m^{-1}$ )	2.63E+10	3.00E+10	5.00E+10	5.75E+10	8.02E+10	6.35E+10	5.86E+10	5.00E+10	9E10
$D_{L\rightarrow X}$ (eV $m^{-1}$ )	2.34E+10	4.10E+10	1.00E+10	4.68E+10	6.63E+10	5.59E+10	5.10E+10	1.00E+10	9E10
$D_{X\rightarrow\Gamma}$ (eV $m^{-1}$ )	0	1.00E+11	1.00E+11	4.98E+10	7.30E+10	6.35E+10	5.86E+10	1.00E+11	9E10
$D_{X\rightarrow L}$ (eV $m^{-1}$ )	2.34E+10	4.10E+10	1.00E+10	4.68E+10	6.63E+10	5.59E+10	5.10E+10	1.00E+10	9E10
$D_{X\rightarrow X}$ (eV $m^{-1}$ )	2.26E+10	9.00E+10	1.00E+11	2.80E+10	3.57E+10	3.36E+10	2.77E+10	1.00E+11	9E10
$\hbar\omega_{\Gamma\rightarrow L}$ (eV)	0	2.32E-02	0.0278	2.22E-02	2.51E-02	1.75E-02	2.56E-02	0.0278	0.0854
$\hbar\omega_{\Gamma\rightarrow X}$ (eV)	0	2.30E-02	0.0299	2.19E-02	2.51E-02	1.92E-02	2.86E-02	0.0299	0.0854
$\hbar\omega_{L\rightarrow\Gamma}$ (eV)	0	2.32E-02	0.0278	2.22E-02	2.51E-02	1.75E-02	2.56E-02	0.0278	0.0854
$\hbar\omega_{L\rightarrow L}$ (eV)	3.89E-02	2.40E-02	0.029	2.43E-02	2.70E-02	1.92E-02	2.86E-02	0.029	0.0854
$\hbar\omega_{L\rightarrow X}$ (eV)	3.72E-02	2.28E-02	0.0293	2.09E-02	2.32E-02	1.75E-02	2.56E-02	0.0293	0.0854
$\hbar\omega_{X\rightarrow\Gamma}$ (eV)	0	2.30E-02	0.0299	2.19E-02	2.51E-02	1.92E-02	2.86E-02	0.0299	0.0854
$\hbar\omega_{X\rightarrow L}$ (eV)	3.72E-02	2.28E-02	0.0293	2.09E-02	2.32E-02	1.75E-02	2.56E-02	0.0293	0.0854
$\hbar\omega_{X\rightarrow X}$ (eV)	5.09E-02	3.07E-02	0.0299	2.57E-02	2.63E-02	1.93E-02	2.66E-02	0.0299	0.0854
$E_L - E_{\Gamma}$ (eV)	0.88	-0.14	0.29	0.59	0.1	0.73	0.18	1.4	1.4
$E_X - E_{\Gamma}$ (eV)	0.08	0.635	0.48	0.85	0.25	1.02	0.52	1.2	2.24
$ee_{pz}$	0	0	0	0	0	0	0	0.375	0
$\Delta_{Alloy}$	0	0	0	0	0	0	0	0	0
$N_{dis}$	0	0	0	0	0	0	0	0	0
$N_i$	0	0	0	0	0	0	0	0	0
$\epsilon_{th}$ (eV)	1.23	1.2	1.42	3.1			7.5E6		

**Material parameters used in various scattering mechanisms between three valley i.e.  $\Gamma$ , U and  $\Gamma_3$**

**Wurtzite (WZ)**

Parameters	GaN	AlN	InN	ZnO	2H-SiC	4H-SiC
$\epsilon_\infty$	5.28	4.77	8.4	3.7	6.5	6.5
$\epsilon_s$	9.7	8.5	15.3	8.2	9.7	9.66
M (kg/m <sup>3</sup> )	6087	3230	6240	5600	3200	3200
$v_s$ (m/s)	7620	9060	3780	6400	1373	1373
$D_{a\Gamma}$ (eV)	8.3	6.2	2.05	14	15	17.5
$D_{aU}$ (eV)	8.3	6.9	4.76	14	15	17.5
$D_{a\Gamma_3}$ (eV)	8.3	7.2	3.83	14	15	17.5
$\hbar\omega_{LO}^\Gamma$ (eV)	0.090811	0.0992	0.073	0.072	0.12	0.12
$\hbar\omega_{LO}^U$ (eV)	0.090811	0.0992	0.073	0.072	0.12	0.12
$\hbar\omega_{LO}^{\Gamma_3}$ (eV)	0.090811	0.0992	0.073	0.072	0.12	0.12
$D_{\Gamma \rightarrow U}$ (eVm <sup>-1</sup> )	1.80E+10	1.00E+11	1.00E+11	1.80E+10	7E10	6E10
$D_{\Gamma \rightarrow \Gamma_3}$ (eVm <sup>-1</sup> )	1.00E+11	1.00E+11	1.00E+11	1.00E+11	7E10	6E10
$D_{U \rightarrow \Gamma}$ (eVm <sup>-1</sup> )	1.80E+10	1.00E+11	1.00E+11	1.80E+10	7E10	6E10
$D_{U \rightarrow U}$ (eVm <sup>-1</sup> )	5.00E+10	1.00E+11	1.00E+11	5.00E+10	7E10	6E10
$D_{U \rightarrow \Gamma_3}$ (eVm <sup>-1</sup> )	1.00E+10	1.00E+11	1.00E+11	1.00E+10	7E10	6E10
$D_{\Gamma_3 \rightarrow \Gamma}$ (eVm <sup>-1</sup> )	1.00E+11	1.00E+11	1.00E+11	1.00E+11	7E10	6E10
$D_{\Gamma_3 \rightarrow U}$ (eVm <sup>-1</sup> )	1.00E+10	1.00E+11	1.00E+11	1.00E+10	7E10	6E10
$D_{\Gamma_3 \rightarrow \Gamma_3}$ (eVm <sup>-1</sup> )	1.00E+11	1.00E+11	1.00E+11	1.00E+10	7E10	6E10
$\hbar\omega_{\Gamma \rightarrow U}$ (eV)	0.073	0.0992	0.0278	0.073	0.0854	0.0854
$\hbar\omega_{\Gamma \rightarrow \Gamma_3}$ (eV)	0.073	0.0992	0.0299	0.073	0.0854	0.0854
$\hbar\omega_{U \rightarrow \Gamma}$ (eV)	0.073	0.0992	0.0278	0.073	0.0854	0.0854
$\hbar\omega_{U \rightarrow U}$ (eV)	0.073	0.0992	0.029	0.073	0.0854	0.0854
$\hbar\omega_{U \rightarrow \Gamma_3}$ (eV)	0.073	0.0992	0.0293	0.073	0.0854	0.0854
$\hbar\omega_{\Gamma_3 \rightarrow \Gamma}$ (eV)	0.073	0.0992	0.0299	0.073	0.0854	0.0854
$\hbar\omega_{\Gamma_3 \rightarrow U}$ (eV)	0.073	0.0992	0.0293	0.073	0.0854	0.0854
$\hbar\omega_{\Gamma_3 \rightarrow \Gamma_3}$ (eV)	0.073	0.0992	0.029	0.073	0.0854	0.0854
$E_U - E_\Gamma$ (eV)	1.34	0.7	2.71	2.1	1.5	2.5
$E_{\Gamma_3} - E_\Gamma$ (eV)	2.14	1	1.78	2.9	2.27	0
$ee_{pz}$	0.375	0.92	0.375	0.375	0	0
$\Delta_{Alloy}$	0	0	0	0	0	0
$N_{dis}$	0	0	0	0	0	0
$N_i$	1.00E+13	1.00E+13	0	1.00E+13	0	0
$\mathcal{E}_{th}$						

The ternary material parameters can be interpolated using binary material data.

Here,

- $\epsilon_s$  and  $\epsilon_\infty$  are the static relative permittivity and high-frequency relative permittivity.
- $M$  is density.
- $v_s$  is saturation velocity.
- $D_a$  is acoustic deformation potential.
- $D_{x-y}$  is intervalley deformation potential from x-valley to y-valley.
- $\hbar\omega$  is the polar optical phonon energy.
- $\hbar\omega_{x-y}$  is the intervalley transition optical phonon energy.
- $E_x - E_y$  is valley separation energy between X and Y valley,
- $e_{pz}$  is piezoelectric coefficient.
- $\Delta_{Alloy}$  is alloy disorder factor.
- $N_{dis}$  is line dislocation factor.
- $N_i$  is ionized impurity.

### 3.3 Ensemble Monte Carlo Device Simulator

The details of the Ensemble Monte Carlo (EMC) algorithms implemented in the TNL-PD simulator with the salient features of each algorithm are discussed in subsequent subsections. First though, an overview of the entire process is presented as depicted in Figure 3.1.

#### Flow Chart for program implementation

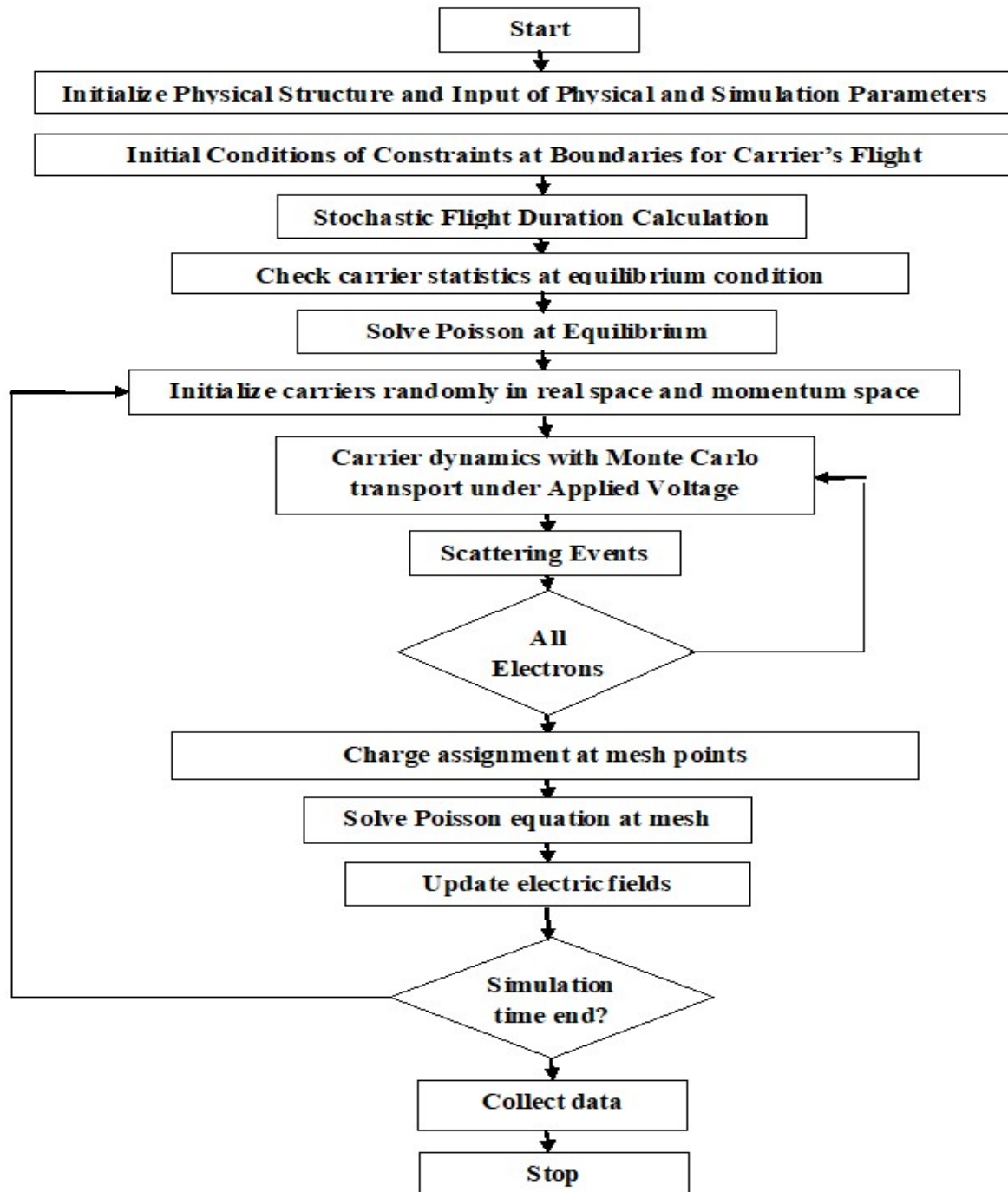


Figure 3.1: A schematic Algorithm flow chart of TNL-PD Simulator

### 3.3.1 Carrier Transport Equation

The TNL-PD simulator considers carrier dynamics defined through carrier transport theory which is used for treatments of hot-electron effects. The charge carriers are considered to travel according to classical mechanics between two successive scattering events (see section 3.2), while the scattering cross-sections, in the imperfect host crystal, are derived from the quantum theory of scattering. The charge carriers have been considered to move between two successive scattering events based on classical mechanics however the scattering cross-sections, in the imperfect host crystal, are derived from the quantum theory of scattering. The technique, semiclassical in nature is used here to solve carrier transportation classically as well as quantum mechanically [1]-[5]

The carrier distribution function is treated as a fundamental quantity in transport theory which is defined as proportional to the density of the electrons in the seven-dimensional space  $(\mathbf{r}, \mathbf{k}, t)$ , where  $\mathbf{r}$  indicates the position in the crystal and  $t$  is time in order of picosecond. The normalization constant can be chosen in such a way that

$$\frac{2}{(2\pi)^3} \int d\mathbf{k} \int d\mathbf{r} f(\mathbf{r}, \mathbf{k}, t) = N \quad (3.35)$$

Here,  $N$  denotes the total number of electrons in the crystal.

The Boltzmann transport equation (BTE) is used here to describe the carrier transport phenomena and can be written as

$$\frac{\partial f}{\partial t} + \mathbf{v} \cdot \nabla_{\mathbf{r}} f + \mathbf{F} \cdot \nabla_{\mathbf{k}} f = \left( \frac{\partial f}{\partial t} \right)_{scattering} \quad (3.36)$$

All the important quantity of interest related to carrier transport e.g. carrier drift velocity, carrier mean energy, carrier diffusion coefficient etc. as a function of external applied field, temperature, carrier concentration gradient etc. can be obtained from the distribution function. The basic knowledge required for the analysis for the transport phenomenon and information regarding the distribution function depend on the band structure  $\varepsilon(\mathbf{k})$  of the specific material.

It is assumed that under equilibrium conditions, the carrier distribution function follows Fermi-Dirac (FD) statistics and reduces to Maxwell-Boltzmann (MB) statistics when  $\varepsilon - \varepsilon_F \gg k_B T$ , where  $\varepsilon_F$  is the Fermi level energy. The equilibrium distribution function,  $f_o$  under MB distribution regime at equilibrium is accounted as

$$f_{MB} = K e^{-\left(\varepsilon/k_B T\right)} \quad (3.37)$$

Here,  $K$  is the normalization constant.

The right-hand side of equation (3.34) is showing dependence of the carrier distribution function on the scattering process and equals the difference between the in-scattering and the out-scattering processes, and is given as

$$\left(\frac{\partial f}{\partial t}\right)_{coll} = \sum_{k'} \{S(\mathbf{k}', \mathbf{k})f(\mathbf{k}')[1-f(\mathbf{k})] - S(\mathbf{k}, \mathbf{k}')f(\mathbf{k})[1-f(\mathbf{k}')] \} = \widehat{C}f \quad (3.38)$$

The  $(1 - f)$  coefficients account for the Pauli exclusion principle; in the approximation of Eq. (3.37) these factors do not contribute since it is always assumed that  $f \ll 1$ . The presence of  $f(\mathbf{k})$  and  $f(\mathbf{k}')$  in the collision integral makes the BTE rather complicated integro-differential equation for  $f(\mathbf{r}, \mathbf{k}, t)$ , whose solution requires a number of simplifying assumptions. In the absence of perturbing fields and temperature gradients, the distribution function must be the Fermi-Dirac (FD) function. In this case, the collision term must vanish and the principle of detailed balance gives for all  $\mathbf{k}$  and  $\mathbf{k}'$  and all scattering mechanisms

$$\frac{S(\mathbf{k}, \mathbf{k}')}{S(\mathbf{k}', \mathbf{k})} = \frac{f_0(\mathbf{k}') [1 - f_0(\mathbf{k})]}{f_0(\mathbf{k}) [1 - f_0(\mathbf{k}')]}. \quad (3.39)$$

Therefore, if the phonons interacting with the electrons are in thermal equilibrium, we get

$$\frac{S(\mathbf{k}, \mathbf{k}')}{S(\mathbf{k}', \mathbf{k})} = \exp\left(\frac{E_{\mathbf{k}} - E_{\mathbf{k}'}}{k_B T}\right). \quad (3.40)$$

This relation must be satisfied regardless of the origin of the scattering forces. If, for example, we assume  $E_{\mathbf{k}} > E_{\mathbf{k}'}$ , then  $S(\mathbf{k}, \mathbf{k}')$  which involves emission must exceed  $S(\mathbf{k}', \mathbf{k})$  which involves absorption. Note that the Boltzmann transport equation (BTE) is valid under assumptions of semi-classical transport and can be solved under conditions

1. Effective mass approximation (which incorporates the quantum effects due to the periodicity of the crystal);
2. Born approximation for the collisions,
3. In the limit of small perturbation for the electron-phonon interaction and instantaneous collisions,

It has no memory effects, i.e. no dependence on initial condition terms. The phonons are usually treated as in equilibrium, although the condition of non-equilibrium phonons may be included through an additional equation.

By substituting Eq. (3.38) into the Boltzmann transport equation (3.36), an integral-differential equation is obtained. The complexity of such an equation strongly depends on the used scattering mechanisms and on the band structure of the material. It is hard to find solutions to the Boltzmann equation through analytical (without linearizing BTE, where carrier transport phenomena are in the nonlinear regimes) and numerical techniques which require several approximations e.g. under use of simple scattering mechanisms, it converts to drift-diffusion model etc.

The iterative technique is the best suited technique which yields a solution of the Boltzmann equation by means of an iterative procedure. It processes the whole distribution function at each step of the procedure with physical phenomena that depend only on details of the distribution function. The Monte Carlo technique, as a direct simulation of the dynamics of charge carriers enables to extract any required physical information while the solution of the transport equation is being built up. Furthermore, it enables to simulate particular physical situations unattainable in experiments and even to investigate into non-existing advance materials. This use of Monte Carlo makes it similar to an experimental technique, and may be called as the simulated "experiment" which can in fact be compared with analytically formulated theories.

### 3.3.2 Formulation of Scattering Mechanisms

The total scattering rate  $\Gamma_j$  is a sum of all possible scattering rates. For the computational technical reasons each scattering mechanism is numbered sequentially from one to  $N_r$  in the TNL-PD simulator, the total number of such mechanisms are considered. Once the numbering is decided it should not change during simulation. The total scattering rate is defined as;

$$\Gamma[\mathbf{k}(t)] = \sum_{i=1}^{N_r} \lambda_i[\mathbf{k}(t)] \quad (3.41)$$

where  $t$  represents the time, which is related to the energy or wave vector of the scattering particle through Equations (3.11), and  $\lambda_i$  represents the rate of a particular scattering mechanism  $i$ . The scattering mechanism terminating the free flight is selected by means of a random number.

$$r_\gamma = \Gamma r_s \quad (3.42)$$

here,  $r_s$  represents a flat random number.

Free carriers (electrons and holes) interact with the crystal lattice, defects and with each other through a variety of scattering processes which relax the energy and momentum of the particle. Based on first order, time-dependent perturbation theory, and the transition rate from an initial state  $\mathbf{k}$  in band  $n$  to a final state  $\mathbf{k}'$  in band  $m$  for the  $j^{\text{th}}$  scattering mechanism is given by Fermi's Golden rule [11] refer to equation (3.14).

The delta function in equation (3.14) describes the conservation of energy, valid for long times after the collision is over, with  $\hbar\omega$  the energy absorbed (upper sign) or emitted (lower sign) during the process. The total scattering rate used to generate the free flight is

$$\Gamma_j[n, \mathbf{k}] = \frac{2\pi}{\hbar} \sum_{m, \mathbf{k}'} \left| \langle m, \mathbf{k}' | V_j(\mathbf{r}) | n, \mathbf{k} \rangle \right|^2 \delta(E_{\mathbf{k}'} - E_{\mathbf{k}} \mp \hbar\omega) \quad (3.43)$$

The scattering rates  $\Gamma[n, \mathbf{k}; m, \mathbf{k}']$  and  $\Gamma_j[n, \mathbf{k}]$  calculated using time dependent perturbation theory using Fermi's rule, equation (3.43), and the calculated rates are then tabulated in a scattering table in order to select the type of scattering and final state after scattering as discussed earlier. The scattering mechanism  $j$  is selected satisfying the inequality from the equation (3.42):



$$\sum_{i=1}^{j-1} \lambda_i[k(t)] \leq r_\gamma < \sum_{i=1}^j \lambda_i[k(t)] \quad (3.44)$$

with

$$\sum_{i=1}^0 \lambda_i[k(t)] = 0 \quad (3.45)$$

Thus, the various scattering mechanisms are passed through in the sequence they have been ordered until  $\sum \lambda_i$  exceeds  $r_\gamma$ . The search terminates sooner the smaller the value of  $r_\gamma$  which is why TNL-PD simulator is equipped with given the above-mentioned method on numbering of the various scattering mechanisms. This scheme makes a weighted selection such that, over a long period of time, the relative amount of scattering from a particular type equals its fractional part of the total scattering rate or cross-section. The various types of scattering mechanisms is implemented in the TNL-PD simulator are given [3], [7].

The basic formalisms used in TNL-PD simulator for scattering events are considered as:

- Fraction of all scattering events caused by polar optical phonons against the electric field for each separate minimum.  
e = phonon emission  
a = absorption
- Fraction of all scattering events during steady state causing transfer of carriers between conduction band minima in zincblende semiconductor materials against the electric field.

Carrier transfer in  $\Gamma \rightarrow X$ ,  $L \rightarrow X$  and  $\Gamma \rightarrow L$  valleys

Carrier transfer in the opposite direction, e.g.  $X \rightarrow \Gamma$ ,  $X \rightarrow L$  and  $L \rightarrow \Gamma$  valleys

e = phonon emission

a = absorption

- Fraction of scattering events during steady state causing transfer within the equivalent X and L minima in zincblende semiconductor materials.

e = phonon emission

a = absorption

### 3.3.3 Monte Carlo (MC) Technique

The Monte Carlo (MC) method, consists of a simulation of the motion of one or more electrons inside the crystal, subject to the action of external applied electric and of given scattering mechanisms. The durations of the carrier free flights between two successive collisions and the scattering events involved in the simulation are selected stochastically in accordance with some given probabilities describing the microscopic processes. As a consequence, the Monte Carlo method relies on the generation of a sequence of random numbers with given distribution probabilities.

In TNL-PD simulator, the details of each step of the procedure of the Monte Carlo program implemented are given in the following sections. The simulation starts with electrons in given initial conditions with wave vector  $k_0$ ; then the duration of the first free flight is chosen with a probability distribution determined by the scattering probabilities. During the free flight the external forces under the influence of applied electric field are;

$$F = \hbar \frac{\partial k}{\partial t} \quad (3.46)$$

$$F = -qE = q\nabla_k \phi \quad (3.47)$$

Here,  $\phi$  is the potential due to applied field.

#### 3.3.3.1 Free Flight Generation

In the TNL-PD simulator, particle motion is assumed to consist of free flights terminated by instantaneous scattering events, which change the momentum and energy of the particle after scattering event. The first task is to generate free flights of time duration selected randomly for each particle. This time duration is governed by total time of Monte-Carlo simulation divided in time steps  $dt$ , which gives total number of steps as a simulation points.

To simulate the carrier transportation process, the probability density,  $P(t)$ , function with the product of probability density and time step. The  $P(t)dt$  is introduced as the joint probability of a particle which will arrive at time  $t$  without any scattering event after a previous scattering event occurring at time  $t = 0$ , and then suffer a collision in a time interval  $dt$  around time  $t$ . The probability of scattering in the time interval  $dt$  around time  $t$  is written as  $\Gamma[k(t)]dt$ , where  $\Gamma[k(t)]$  is the scattering rate of an electron which is a function of wave vector  $k$ . The scattering rate,  $\Gamma[k(t)]$ , represents the sum of the contributions from each individual scattering mechanism as described in section 3.2, which are usually calculated quantum mechanically using perturbation

theory. The implicit dependence of  $\Gamma[\mathbf{k}(t)]$  on time reflects the change in  $\mathbf{k}$  due to acceleration by internal and external forces on the electron.

In case of electronic transportation, Eq. (3.45) may be integrated to give the time evolution of wave vector  $\mathbf{k}$  relation in the phase space between two successive collision events as

$$\mathbf{k}(t) = \mathbf{k}(0) - \frac{eE\Delta t}{\hbar} \quad (3.48)$$

where  $E$  is the external applied field.

The scattering rate,  $\Gamma[\mathbf{k}(t)]$ , the probability that a particle has not suffered a collision after a time  $t$  is given by

$$\exp\left(-\int_0^t \Gamma[\mathbf{k}(t')] dt'\right) \quad (3.49)$$

Thus, the probability of scattering in the time interval  $dt$  after a free flight of time  $t$  may be written as the joint probability

$$P(t)dt = \Gamma[\mathbf{k}(t)] \exp\left[-\int_0^t \Gamma[\mathbf{k}(t')] dt'\right] dt \quad (3.50)$$

Random flight times may be generated according to the probability density  $P(t)$  above using, for example, the pseudo-random number generator implicit on most modern computers, which generate uniformly distributed random numbers in the range  $[0,1]$ . Using a Direct method for random flight times generation sampled from  $P(t)$  according to

$$r = \int_0^{t_r} P(t) dt \quad (3.51)$$

where  $r$  is a uniformly distributed random number and  $t_r$  is the desired free flight time.

Integrating Eq. (3.49) with  $P(t)$  given by Eq. (3.48) above yields

$$r = 1 - \exp\left[-\int_0^{t_r} \Gamma[\mathbf{k}(t')] dt'\right] \quad (3.52)$$

Since  $(1 - r)$  is statistically the same as  $r$ , Eq. (3.52) may be simplified to

$$-\ln r = \int_0^{t_r} \Gamma[\mathbf{k}(t')] dt' \quad (3.53)$$

Eq. (3.53) is the fundamental equation used to generate the random free flight time after each scattering event, resulting in a random walk process related to the underlying particle distribution function. If there is no external driving field leading to a change of  $k$  between scattering events the time dependence vanishes, and the integral is trivially evaluated. In the general case where this simplification is not possible, it is expedient to introduce the so called self-scattering method in which introduction of a fictitious scattering mechanism whose scattering rate always adjusts itself in such a way that the total (self-scattering plus real scattering) rate is a constant in time [12].

$$\Gamma = \Gamma[\mathbf{k}(t')] + \Gamma_{self}[\mathbf{k}(t')] \quad (3.54)$$

where  $\Gamma_{self}[\mathbf{k}(t')]$  is the self-scattering rate. The self-scattering mechanism itself is defined such that the final state before and after scattering is identical. Hence, it has no effect on the free flight trajectory of a particle when selected as the terminating scattering mechanism, yet results in the simplification of Eq. (3.22) such that the free flight is given by

$$t_r = -\frac{1}{\Gamma} \ln r \quad (3.53)$$

The constant total rate including self-scattering ( $\Gamma$ ) must be chosen at the start of the simulation interval, there may be multiple such intervals throughout an entire simulation, so that it is larger than the maximum scattering encountered during the same time interval. In the simplest case, a single value is chosen at the beginning of the entire simulation (constant gamma method), checking to ensure that the real rate never exceeds this value during the simulation.

### 3.3.2.2 Choice of Scattering Angles

Defining a spherical coordinate system around the initial wave vector  $\mathbf{k}$ , the final wave vector  $\mathbf{k}'$  is specified by  $|\mathbf{k}'|$  (which depends on conservation of energy) as well as the azimuthal and polar angles,  $\varphi$  and  $\theta$  around  $\mathbf{k}$ . Typically, the scattering rate,  $\Gamma_j[n, \mathbf{k}; m, \mathbf{k}']$ , only depends on the angle  $\theta$  between  $\mathbf{k}$  and  $\mathbf{k}'$ . Therefore,  $\varphi$  may be chosen using a uniform random number between 0 and  $2\pi$  (i.e.  $2\pi r$ ), while  $\theta$  is chosen according to the angular dependence for scattering arising from  $\Gamma_j[n, \mathbf{k}; m, \mathbf{k}']$ . If the probability for scattering into a certain angle  $P(\theta)d\theta$  is integrated, the random angles satisfying this probability density may be generated from a uniform distribution between 0 and 1 through inversion of Eq. (3.51).

Once the scattering mechanism has been selected, the scattering angles have to be calculated in order to determine the initial direction of the next flight. TNL-PD simulator takes into account the polar angular dependence of the scattering rate of electrons in a prototypical polar semiconductor, due to polar optical phonon scattering. The probability density for scattering into an angle  $\theta$ , relative to the original trajectory of travel just before scattering, is given by

$$P(\theta)d\theta = \frac{\Gamma_{POP}(\theta)d\theta}{\int_0^\pi \Gamma_{POP}(\theta)d\theta} \sim \frac{\sin(\theta)d\theta}{(E + E' - 2\sqrt{EE'} \cos\theta)} \quad (3.56)$$

where  $\Gamma_{POP}(\theta)$  is the scattering rate into a small angle  $d\theta$  around the angle  $\theta$ ,  $E$  is the energy of the particle before scattering, and  $E' = E \pm \hbar\omega_o$  is the final energy corresponding to the emission (lower sign) or absorption (upper sign) of an optical phonon of energy  $\hbar\omega_o$ . The integral in the numerator is for normalization.

### 3.3.3.3 Time Step

As in the case of solution of full Maxwell's equations, a stable Monte Carlo device simulation can be achieved by selection of the appropriate time-step,  $\Delta t$ , and the spatial mesh size ( $\Delta x$ ,  $\Delta y$ , and/or  $\Delta z$ ). The time-step and the mesh size may correlate to each other in connection with the numerical stability. For example, as discussed in the context of solving drift-diffusion simulations, the time-step  $\Delta t$  must be related to the plasma frequency

$$\omega_p = \sqrt{\frac{ne^2}{\epsilon_s m^*}} \quad (3.57)$$

where  $\epsilon_s$  is the material permittivity and  $n$  is the carrier density. From the view point of the stability criterion,  $\Delta t$  must be much smaller than the inverse plasma frequency. The highest carrier density specified in the device model is used to estimate  $\Delta t$ . If the material is a multi-valley semiconductor, the smallest effective mass to be experienced by the carriers is used in Equation 3.57 as well.

### 3.3.3.4 Mesh Size

The mesh size for the spatial resolution of the potential is dictated by the charge variations. Hence, users need to choose the mesh size such that it must be smaller than the smallest wavelength of the charge variations. The smallest wavelength is approximately equal to the Debye length which is given as

$$\lambda_d = \epsilon_s m^* \sqrt{\frac{\epsilon_s k_B T}{ne^2}} \quad (3.58)$$

The highest carrier density specified in the multi-layer device should be used to estimate  $\lambda_d$  from the stability criterion in TNL-PD simulator. The smaller mesh size must be always chosen as compared to the Debye length value obtained by Equation 3.58.

Based on the discussion above, the time-step ( $\Delta t$ ) and the mesh size ( $\Delta x$ ,  $\Delta y$ , and/or  $\Delta z$ ) can be specified separately. However, the  $\Delta t$  chosen must be checked again by calculating the distance  $l_{max}$ , defined as

$$l_{max} = v_{max} \times \Delta t \quad (3.59)$$

In practice, choosing the time step and grid spacing is by trial-and-error, within these guidelines. A good rule of thumb is that the ratios of time step and grid spacing, to the plasma period and Debye length, respectively, should be on the order of unity.

### 3.4 Particle Mesh Coupling

The particle-mesh coupling method is a widespread technique for space charge calculations. The spatial distribution of potential and electric field is obtained through solution of Poisson equation in TNL Particle Device Simulator (TNL-PDS) for simulation of semiconductor devices with Monte Carlo (MC) technique. The accurate computation of particle dynamics under applied electric field requires accurate solution of Poisson's equation. The particle simulation means the assignation of the particle's charge on the rectangular mesh. In the TNL-PD simulator, three types of the most famous charge assignment schemes i.e. Nearest Grid Point (NGP) Nearest Element Center (NEC) and Cloud In Cell (CIC) are implemented [1]. All three schemes produce similar output results. The details of each charge assignment scheme are given below.

#### 3.4.1 Nearest Grid Point (NGP) Technique

The NGP technique considers all the charge from a given particle is assigned to the nearest grid points. The force on the particle is also taken as the one calculated on the nearest grid point.

The charge density at a mesh point is given by the total charge in the cell surrounding the mesh point  $p$  divided by the cell volume. The lowest order charge assignment function for a particle located at position  $\mathbf{r} = (x, y, z)$  is given by interpolation function as,

$$\omega(r) = \begin{cases} 1 & \text{for } -\frac{\Delta r}{2} \leq r \leq \frac{\Delta r}{2} \\ 0 & \text{otherwise} \end{cases} \quad (3.60)$$

Here  $\Delta r$  includes the variations in terms of  $\Delta x$ ,  $\Delta y$ , and  $\Delta z$ , which are minimum mesh spacing between two consecutive meshes respectively.

The charge assignment is defined as

$$\rho(r) = \frac{qN_s}{\Delta r} \sum_{i=0}^{N_p} \omega(r_i - r_p) + \rho_{init} \quad (3.61)$$

The NGP force interpolation follows the same scheme as the particle assignment. The force field in any point of a cell takes the value of the mesh point at the center of the cell. [1]

#### 3.4.2 Nearest Element Center (NEC) Technique

The NEC charge assignment or force interpolation technique attempts to reduce self-forces and increase spatial accuracy in the presence of non-uniformly spaced tensor-product meshes and/or spatially dependent permittivity, i.e., restriction ( $P$ ) is removed and ( $M$ ) is relaxed. In addition, the NEC scheme can be utilized in one axis direction (where local mesh spacing is non-uniform)



and the CIC scheme can be utilized in the other (where local mesh spacing is uniform). Such hybrid schemes offer smoother assignment/interpolation on the mesh compared with the pure NEC. The new steps of the pure NEC PM scheme are as follows [2], [6],

4. Charge assignment on the mesh is done by driving the charges  $\rho$  equally on the four mesh points of the element (i, j, k).
5. Computation of forces on the mesh points
6. Computation of fields
  - $\Delta_{i,l,k}^x$  where  $l = j, j + 1$ ,
  - $\Delta_{m,j,k}^y$  where  $m = i, i + 1$ , and
  - $\Delta_{i,j,n}^z$  where  $n = k, k + 1$
7. Interpolation on the charges to calculate forces as
  - $E^x = (\Delta_{i,j,k}^x - \Delta_{i+1,j,k}^x)/2$
  - $E^y = (\Delta_{i,j,k}^y - \Delta_{i,j+1,k}^y)/2$
  - $E^z = (\Delta_{i,j,k}^z - \Delta_{i,j,k+1}^z)/2$

### 3.4.3 Cloud-in-Cell (CIC) Technique

CIC scheme (a better approximation over NGP scheme) that gives smoother results and reduces errors, is used for charges assignment over rectangular mesh points. This assigns particle's charge to more than one mesh point to make super-particle in a way proportional to the distance of surrounding cells. The lowest order charge assignment function for a particle located at position  $\mathbf{r} = (x, y, z)$  is given by interpolation function as, [1]-[4]

$$\omega(r) = \begin{cases} \left\{ \left(1 - \frac{x}{\Delta x}\right) \left(1 - \frac{y}{\Delta y}\right) \left(1 - \frac{z}{\Delta z}\right) \right\} & \text{for } -\frac{\Delta r}{2} \leq r \leq \frac{\Delta r}{2} \\ 0 & \text{otherwise} \end{cases} \quad (3.62)$$

Here  $\Delta x$ ,  $\Delta y$ , and  $\Delta z$  are minimum mesh spacing between two consecutive meshes respectively.

The charge assignment is defined as

$$\rho(r) = \frac{qN_s}{\Delta r} \sum_{i=0}^{N_p} \omega(r_i - r_p) + \rho_{init} \quad (3.63)$$

The mesh size for the spatial resolution of the potential is dictated by the charge variations. The mesh size is chosen to be smaller than the smallest wavelength of the charge variations which must be equal to the Debye length and given as;

$$L_d = \sqrt{\frac{\epsilon k_b T}{e^2 N}} \quad (3.64)$$

Here  $\epsilon$  is the permittivity of energy band of material over which carrier is moving,  $e$  is the electronic charge,  $N$  is doping density and  $T$  is the temperature.

### 3.5. Boundary Conditions

Two boundary conditions are used for estimation of charge carrier dynamics and for solution of Poisson's equation. The carriers hit the edges of device, the reflective boundary conditions are implemented in the simulator by default known as Neumann condition while the carriers hit the contact region of the device it is assumed that carrier will be absorbed and immediately re-emitted from same contact with different wave vector or from other contact to follow carrier conservation principle inside the device and is known as Dirichlet boundary conditions.

The 2D and 3D Poisson solution with tracking the super-particle in all three dimensions real space and momentum space is always cost-effective solution for advance and conventional node device technologies. However, to address quantum mechanical phenomenon with advance node devices require accurate solution of Poisson's solver on each mesh point in three dimensions (3D). The 2D simulation skips many important physical mechanisms during the transport of carriers under influence of external electric field. The 3D Poisson solution is always cost expensive, however it helps for better understanding of real physical phenomenon associated with carrier transport. TNL-PD (Particle Device) simulator is taking ~8 CPU hours against reported simulation time 24 CPU hours in reference [11] ramping same voltage. Also, we have tested it for different applied voltage conditions, the reliability in computation time for 3D simulation reflect strong evidence for world's fastest 2D/3D Particle Device Simulator (PDS) equipped with parallel computing facility.

Note: In TNL-PD simulator under Bipolar technology selection, user need to careful to define the boundary conditions. The device edges should not leave without defining appropriate boundary conditions with appropriate voltage at each boundary condition.



Here Green boundary on respective edge on device, represents Neumann boundary i.e. insulating characteristics whereas black boundary represents Metal electrodes (Ohmic and Schottky contacts) i.e. Dirichlet boundary conditions.

### 3.5 Discretization of Poisson's Equation

A well-established Ensemble Monte Carlo (EMC) technique is used as a direct simulation of the dynamics of charge carriers inside the crystal under the applied electric field, enabling users to extract the required physical information. The solution of Boltzmann transport equation (BTE) under non-equilibrium includes rate change of distribution function, however under equilibrium, the distribution function resemble with the Fermi-Dirac function. The Monte Carlo program implemented for simulation of carrier transport process initiate with carriers under equilibrium conditions, the first free flight duration under external electrostatic force is chosen with a probability distribution determined by the scattering probabilities.[1]-[6],

From Maxwell's equation;

$$\nabla \cdot D = \rho \quad (3.65)$$

Here D is the electric displacement vector and  $\rho$  is the free charge density. The displacement vector in turn is given by the constitutive equation,

$$D = \epsilon \cdot E \quad (3.66)$$

where  $\epsilon$  is the dielectric permittivity and E is the electric field. In turn, the electric field is defined in terms of the gradient of the electrostatic potential as

$$E = -\nabla\phi \quad (3.67)$$

Substituting (3.13) into (3.12), using (3.14), yields (3.8), repeated for convenience:

$$\nabla \cdot \epsilon \cdot (-\nabla\phi) = \rho \quad (3.68)$$

After simplify equation (3.68) for the case of 1D,

$$\frac{d^2\phi}{dx^2} = \rho \quad (3.69)$$

In case of an equally-spaced meshes (with space step  $\Delta x$ ), the functions  $\phi(r)$  and  $\rho(x)$  can be replaced by vectors of elements  $\rho_j$  and  $\phi_j$  defined at the mesh points  $x_j$  with the condition  $1 \leq j \leq J$ . The total length L of the device region of interest is  $L = J\Delta x$ . Using a finite difference scheme, the second derivative  $\frac{d^2\phi}{dx^2}$  can be replaced by the difference operator as;

$$\Delta_x'' = \frac{\phi_{j+1} - 2\phi_j + \phi_{j-1}}{\Delta x^2} \quad (3.70)$$

The Poisson's equation is converted as;

$$\phi_{j+1} - 2\phi_j + \phi_{j-1} = \Delta x^2 \rho_j \quad (3.71)$$

Equation (3.69) is to apply at every internal point  $j$  on the mesh. Assuming for example that the boundary conditions specify the value of the potential at the end points,  $\phi_1 = w_1$  and  $\phi_j = w_j$  then

$$\begin{aligned}
 \phi_1 &= w_1 \\
 \phi_1 - 2\phi_2 + \phi_3 &= \Delta x^2 \rho_2 \\
 \phi_2 - 2\phi_3 + \phi_4 &= \Delta x^2 \rho_3 \\
 \phi_3 - 2\phi_4 + \phi_5 &= \Delta x^2 \rho_4 \\
 &\dots \dots \dots \dots \dots \dots \dots \\
 \phi_{j-2} - 2\phi_{j-1} + \phi_j &= \Delta x^2 \rho_{j-1} \\
 \phi_j &= w_j
 \end{aligned} \tag{3.72}$$

Converting equation 3.72 into matrix representation,

$$\mathbf{A}\boldsymbol{\phi} = \mathbf{w} \tag{3.73}$$

where, the matrix  $\mathbf{A}$  can be written in form

$$\mathbf{A} = \begin{vmatrix} 1 & 0 & 0 & \dots & 0 \\ 1 & -2 & 1 & 0 & 0 \\ 0 & 1 & -2 & 1 & \\ & & \dots & & \\ & & 1 & -2 & 1 \\ 0 & \dots & 0 & 0 & 0 \end{vmatrix} \tag{3.72}$$

$\mathbf{A}$  has non-zero elements only along the central three diagonals of the matrix (tridiagonal matrix). Because of the large number of zeros the matrix is called "sparse".

### 3.5.1 Uniform Mesh

The solution of equation (3.68) for the case of 2D can be represented on the an equally-spaced meshes (with space step  $\Delta$  in x-axis and y-axis) as,

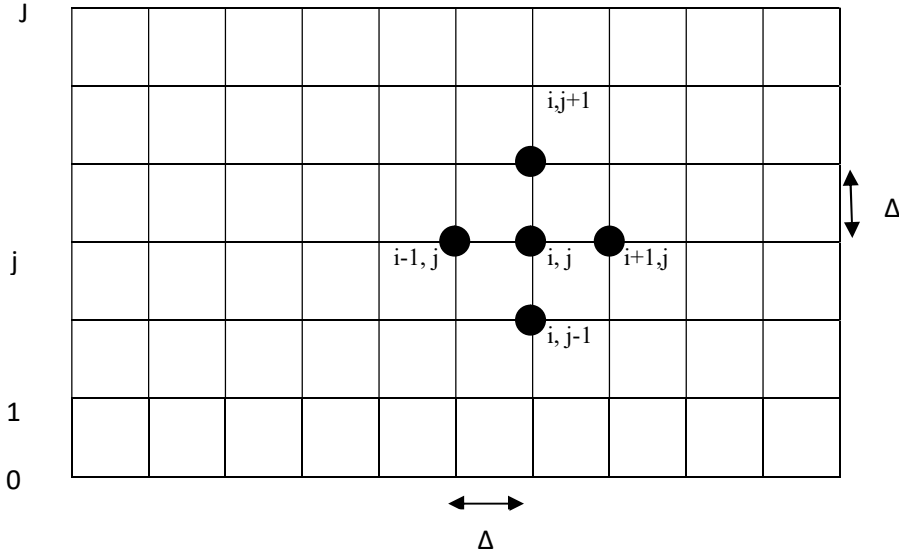


Figure 3.2: Mesh Grid to discuss boundary Conditions

The 2D Poisson equation is

$$\frac{d^2\phi}{dx^2} + \frac{d^2\phi}{dy^2} = \rho \quad (3.75)$$

The solution of 2D Poisson's equation on the rectangular meshes as shown in Figure 3.2 with grid points  $(i, j)$  where  $1 \leq i \leq I$  and  $1 \leq j \leq J$  under finite difference scheme can be written as;

$$\frac{\phi_{i+1,j} - 2\phi_{i,j} + \phi_{i-1,j}}{\Delta x^2} + \frac{\phi_{i,j+1} - 2\phi_{i,j} + \phi_{i,j-1}}{\Delta y^2} = \rho_{ij} \quad (3.76)$$

Here,  $\Delta x = \Delta y = \Delta$ , the equation (3.76) can be simplified as,

$$(\phi_{i+1,j} + \phi_{i-1,j} + \phi_{i,j+1} + \phi_{i,j-1}) - 4\phi_{i,j} = \Delta^2 \rho_{ij} \quad (3.77)$$

The scheme of five-point stencil in 2D is shown in figure 3.2. Here  $x$  and  $y$  represent the mesh spacing rather than the coordinates. It connects every grid point to the four nearest neighbor points. Higher level approximations that take into account a larger number of neighbors can be adopted.



### 3.5.3 Solution of Poisson's Equation in 2D

In TNL-PD simulator, the solution of Poisson equation depends on the type of regions of interest and material of the device structure. For example, case of MOS structure, oxide regions of the device, the concentration of electrons and holes are negligible that the free charge density is treated as zero. In semiconductor regions, free charges density consists of four parts: hole concentration, electron concentration, ionized donor concentration, and ionized acceptor concentration. Thus, the Poisson's equation (3.66) becomes of the following form:

$$\nabla \cdot \epsilon \cdot (-\nabla \phi) = \begin{cases} 0 & \text{In Oxide} \\ -e(n - p - N_D^+ + N_A^-) & \text{In Semiconductor} \end{cases} \quad (3.83)$$

where  $n$  and  $p$  are, respectively, the electron and hole densities and can be calculated from either Boltzmann or Fermi-Dirac statistics.,  $N_D^+$  and  $N_A^-$  the concentration of ionized donors and acceptors, and  $e$  the electron charge.

In case of non-degenerate semiconductors and under equilibrium conditions (i.e. following Fermi-Dirac statistics), the electron and hole densities can be written as;

$$p = N_i \exp\left(-\frac{\phi}{V_T}\right) \quad (3.84)$$

$$n = N_i \exp\left(\frac{\phi}{V_T}\right) \quad (3.85)$$

where  $N_i$  is the intrinsic carrier density and  $V_T$  is the thermal voltage.

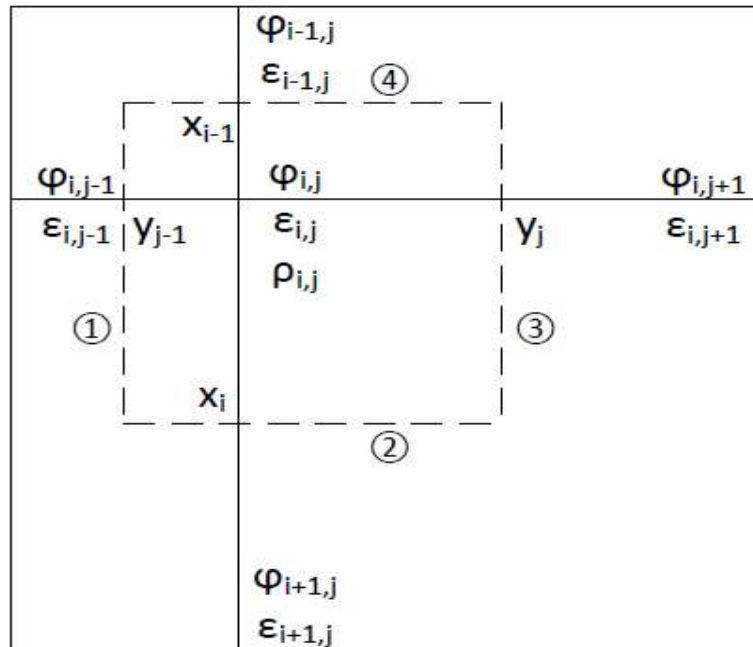


Figure 3.3: Scheme of 5-point Stencil in 2D.



In Figure 3.3,  $\epsilon_{i,j}$  are the dielectric constant of the respective materials regions in which mesh point is taken. Similarly  $\phi_{i,j}$  are the respective potentials at each node points.

The 5-point stencils (i.e. 1, 2, 3, 4 and center point) representation of Poisson equation can be simplified and written in equation form as;

$$1 + 2 + 3 + 4 = \rho_{ij} dx dy$$

Where the stencil points are;

$$\begin{aligned} 1 &= \frac{1}{2} (\epsilon_{i,j-1} + \epsilon_{i,j}) \frac{\phi_{i,j-1} - \phi_{i,j}}{y_{j-1}} dx \\ 2 &= \frac{1}{2} (\epsilon_{i-1,j} + \epsilon_{i,j}) \frac{\phi_{i-1,j} - \phi_{i,j}}{x_{i-1}} dy \\ 3 &= \frac{1}{2} (\epsilon_{i,j+1} + \epsilon_{i,j}) \frac{\phi_{i,j+1} - \phi_{i,j}}{y_j} dx \\ 4 &= (\epsilon_{i+1,j} + \epsilon_{i,j}) \frac{\phi_{i+1,j} - \phi_{i,j}}{x_i} dy \end{aligned} \quad (3.86)$$

Here, dx and dy are the mesh spacing is given by;

$$\begin{aligned} dx &= \frac{x_{i,j} - x_{i,j-1}}{2} \\ dy &= \frac{y_{i,j} - y_{i,j-1}}{2} \end{aligned} \quad (3.87)$$

With proper substitution and simplification, the final expression of discretized Poisson's equation (3.83) is

$$\begin{aligned} &\frac{(\epsilon_{i+1,j} + \epsilon_{i,j})}{x_i(x_i + x_{i-1})} \phi_{i+1,j} + \frac{(\epsilon_{i-1,j} + \epsilon_{i,j})}{x_{i-1}(x_i + x_{i-1})} \phi_{i-1,j} + \frac{(\epsilon_{i,j+1} + \epsilon_{i,j})}{y_j(y_j - y_{j-1})} \phi_{i,j+1} + \frac{(\epsilon_{i,j-1} + \epsilon_{i,j})}{y_j(y_j - y_{j-1})} \phi_{i,j-1} - \left[ \frac{(\epsilon_{i+1,j} + \epsilon_{i,j})}{x_i(x_i + x_{i-1})} + \right. \\ &\left. \frac{(\epsilon_{i-1,j} + \epsilon_{i,j})}{x_{i-1}(x_i + x_{i-1})} + \frac{(\epsilon_{i,j+1} + \epsilon_{i,j})}{y_j(y_j - y_{j-1})} + \frac{(\epsilon_{i,j-1} + \epsilon_{i,j})}{y_j(y_j - y_{j-1})} \right] \phi_{i,j} = -q \left( N_i \exp\left(-\frac{\phi_{i,j}}{V_T}\right) - N_i \exp\left(\frac{\phi_{i,j}}{V_T}\right) + dop_{i,j} \right) \end{aligned} \quad (3.88)$$

The final expression of discretized Poisson's equation is nonlinear because of the electron and hole concentration on the right-hand side. Common iterative methods cannot work with nonlinear system. Therefore, proper linearization is necessary for Poisson's equation. Taylor series is employed to linearize the exponential function;

$$e^x = 1 + \frac{x}{1!} + \frac{x^2}{2!} + \frac{x^3}{3!} + \dots, -\infty < x < \infty \quad (3.89)$$

Applying a small update  $\delta$  to current potential, the new potential is

$$\phi^{new} = \phi^{old} + \delta \quad (3.90)$$

The electron and hole densities are

$$N_i \exp\left(-\frac{\phi}{V_T}\right) \rightarrow N_i \exp\left(-\frac{\phi^{old} + \delta}{V_T}\right) = N_i \exp\left(-\frac{\phi^{old}}{V_T}\right) \exp\left(-\frac{\delta}{V_T}\right) \quad (3.91)$$

$$N_i \exp\left(\frac{\phi}{V_T}\right) \rightarrow N_i \exp\left(\frac{\phi^{old} + \delta}{V_T}\right) = N_i \exp\left(\frac{\phi^{old}}{V_T}\right) \exp\left(\frac{\delta}{V_T}\right) \quad (3.92)$$

Using the Taylor series of exponential function up to two terms only for the term  $\delta$ ,

$$\exp\left(-\frac{\delta}{V_T}\right) \approx \left(1 - \frac{\delta}{V_T}\right) \quad (3.93)$$

$$\exp\left(\frac{\delta}{V_T}\right) \approx \left(1 + \frac{\delta}{V_T}\right) \quad (3.94)$$

Substituting the linearized terms from equations (3.93) and (3.94) back to the electron and hole concentration, the new equations are

$$p = N_i \exp\left(-\frac{\phi^{old}}{V_T}\right) \left(1 - \frac{\phi^{new} - \phi^{old}}{V_T}\right) \quad (3.95)$$

$$n = N_i \exp\left(\frac{\phi^{old}}{V_T}\right) \left(1 + \frac{\phi^{new} - \phi^{old}}{V_T}\right) \quad (3.96)$$

Rearranging Poisson equation refer to equation (3.88)

$$\begin{aligned} & \frac{(\epsilon_{i+1,j} + \epsilon_{i,j})}{x_i(x_i + x_{i-1})} \phi_{i+1,j}^{old} + \frac{(\epsilon_{i-1,j} + \epsilon_{i,j})}{x_{i-1}(x_i + x_{i-1})} \phi_{i-1,j}^{old} + \frac{(\epsilon_{i,j+1} + \epsilon_{i,j})}{y_j(y_j - y_{j-1})} \phi_{i,j+1}^{old} + \frac{(\epsilon_{i,j-1} + \epsilon_{i,j})}{y_j(y_j - y_{j-1})} \phi_{i,j-1}^{old} - \frac{(\epsilon_{i+1,j} + \epsilon_{i,j})}{x_i(x_i + x_{i-1})} + \\ & \frac{(\epsilon_{i-1,j} + \epsilon_{i,j})}{x_{i-1}(x_i + x_{i-1})} + \frac{(\epsilon_{i,j+1} + \epsilon_{i,j})}{y_j(y_j - y_{j-1})} + \frac{(\epsilon_{i,j-1} + \epsilon_{i,j})}{y_j(y_j - y_{j-1})} \Big] \phi_{i,j}^{new} - q \left( N_i \exp\left(-\frac{\phi_{i,j}^{old}}{V_T}\right) + N_i \exp\left(\frac{\phi_{i,j}^{old}}{V_T}\right) \right) \frac{\phi_{i,j}^{new}}{V_T} = \\ & -q \left[ N_i \exp\left(-\frac{\phi_{i,j}^{old}}{V_T}\right) \left(1 + \frac{\phi_{i,j}^{old}}{V_T}\right) + N_i \exp\left(\frac{\phi_{i,j}^{old}}{V_T}\right) \left(1 - \frac{\phi_{i,j}^{old}}{V_T}\right) + doping_{i,j} \right] \end{aligned} \quad (3.97)$$

Thus, the Poisson's equation (3.97) is linear now for iterative solvers.

This linear system can either be solved as a matrix  $Ax = b$  or multiple scalar equations. Matrix form is ideal to isolate the mathematical problem from changing geometries and physical problems. However, scalar equations are coupled to a certain geometry, which makes it more intuitive.

### 3.6 Boundary Conditions

Before proceeding for solution of linear Poisson's equation (3.94), Users need to decide the boundary conditions of the device. TNL-PD simulator supports several boundary conditions: Ohmic contacts, Schottky contacts, insulated contacts, and Neumann (reflective) boundaries. Voltage boundary conditions are normally specified at contacts. Additional boundary conditions have been implemented to address the needs of specific applications.

In a semiconductor device, ohmic and Schottky contacts are treated as Dirichlet boundaries. Neumann boundary conditions are applied to the rest of device geometry. Boundary conditions can be implicitly buried in the coefficient matrix A. For scalar equations, treatment of boundary conditions is similar.

#### 3.6.1 Neumann and Dirichlet boundary conditions

In TNL-PD simulator, Neumann boundary condition is implemented and given by

$$\frac{\partial \phi}{\partial n} = f \quad (3.98)$$

where  $n$  is the normal to the boundary and  $f$  is a scalar function. In semiconductor device, scalar function  $f$  is set to zero, creating so called ghost point to help solving matrix problems.

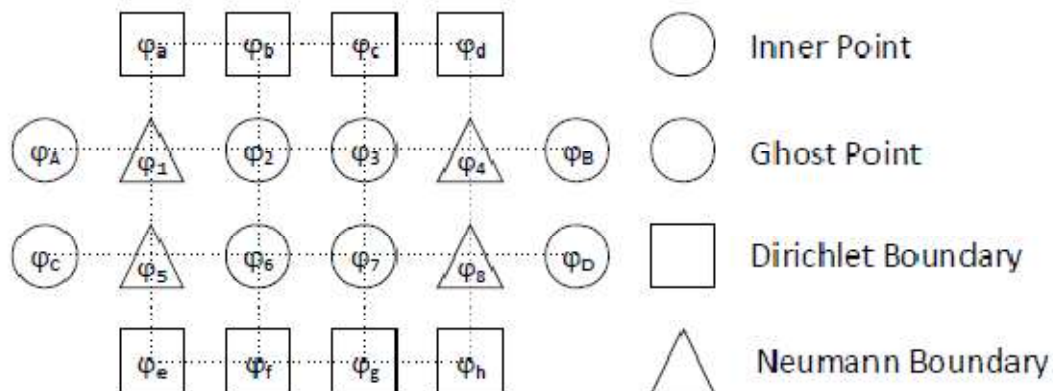


Figure 3.4: A schematic representation of 16 Points Mesh Grid to discuss boundary Conditions

A 16 points mesh grid containing inner points, Dirichlet boundary, and Neumann boundary is shown in figure 3.4. Therefore, only 8 points (from  $\phi_1$  to  $\phi_8$ ), including inner points and Neumann boundary points, need to be calculated.

With typical 5-point 2D stencil, Poisson's equation at point 2 is

$$a_2\phi_1 + b_2\phi_6 + e_2\phi_b + d_2\phi_3 - c_2\phi_2 = f_2 \quad (3.99)$$

In equation (3.96), the value of coefficient  $e_2$  and  $\phi_b$  are known. So it may be shifted to to right hand side of the equation (3.96), thus only unknown variables remain on the left-hand side of the equation;

$$a_2\phi_1 + b_2\phi_6 + d_2\phi_3 - c_2\phi_2 = f_2 - e_2\phi_b \quad (3.100)$$

Following this procedure, Dirichlet boundary points are eliminated from the coefficient matrix A and combined into forcing terms.

At point 1, Poisson's equation is;

$$a_1\phi_a + b_1\phi_5 + e_1\phi_A + d_1\phi_2 - c_1\phi_1 = f_1 \quad (3.101)$$

A ghost point A is introduced to help solve Neumann boundary problem. Neumann boundary conditions in semiconductor devices give zero value for the first order derivative of the potential, which ensures that  $a_1$  equals to  $d_1$  and  $\phi_A$  equals to  $\phi_2$ . So Poisson's equation at point 1 can be simplified together with the treatment for Dirichlet boundary as following:

$$a_1\phi_5 + 2d_1\phi_2 - c_1\phi_1 = f_1 - a_1\phi_a \quad (3.102)$$

Now only 8 unknown points are included in the Poisson's equation system. The matrix representation is

$$\begin{bmatrix} -c_1 & 2d_1 & b_1 & & & & & & \\ a_2 & -c_2 & d_2 & & b_2 & & & & \\ & a_3 & -c_3 & d_3 & & b_3 & & & \\ & & 2a_4 & -c_4 & & & b_4 & & \\ e_5 & & & -c_5 & 2d_5 & & & & \\ & e_6 & & a_6 & -c_6 & d_6 & & & \\ & & e_7 & & a_7 & -c_7 & d_7 & & \\ & & & e_8 & & 2a_8 & -c_8 & & \end{bmatrix} \begin{bmatrix} \varphi_1 \\ \varphi_2 \\ \varphi_3 \\ \varphi_4 \\ \varphi_5 \\ \varphi_6 \\ \varphi_7 \\ \varphi_8 \end{bmatrix} = \begin{bmatrix} f_1 \\ f_2 \\ f_3 \\ f_4 \\ f_5 \\ f_6 \\ f_7 \\ f_8 \end{bmatrix} - \begin{bmatrix} e_1\varphi_a \\ e_2\varphi_b \\ e_3\varphi_c \\ e_4\varphi_d \\ b_5\varphi_e \\ b_6\varphi_f \\ b_7\varphi_g \\ b_8\varphi_h \end{bmatrix} \quad (3.103)$$

Source and drain contacts are treated as Ohmic contacts (charge neutrality) and can be computed as:

$$\rho = (p - n + \text{doping}) = \left[ N_i \exp\left(-\frac{\phi}{V_T}\right) - N_i \exp\left(\frac{\phi}{V_T}\right) + \text{doping} \right] = 0 \quad (3.104)$$

With n-type doping, the potential is positive.

So,  $N_i \exp\left(-\frac{\phi}{V_T}\right)$  is a small value and can be ignored.

Then, the potential is

$$\phi = V_T \ln\left(\frac{\text{dop}}{N_i}\right) \quad (3.105)$$

On the contrary, p-doping makes the potential negative. The term  $N_i \exp\left(-\frac{\phi}{V_T}\right)$  can be ignored.

The potential is

$$\phi = -V_T \ln\left(\frac{-\text{dop}}{N_i}\right) \quad (3.106)$$

Under no external biasing applied either source or drain contacts, the equilibrium condition can be checked. In case of three contact terminal devices, the potential that results from the charge neutrality condition is used as Dirichlet boundary value at source and drain region. Gate voltage can be applied in equilibrium condition. A gate voltage is chosen to neutralize the potential barrier resulting in zero potential for Dirichlet boundary condition in the gate region. Similarly, substrate contact is simply set to zero or assume to be grounded.

For insulator region like gate oxide, the initial potential is set to zero. For semiconductor region, two initial guesses are used to test the robustness of the numerical solvers. One method is to set the potential to zero. The other method is to use charge neutrality to calculate the initial potential from doping profile.

### 3.7 Iterative Methods

Direct methods and iterative methods are two major category of matrix solver. The use of a direct method for the solution of a set of equations for the large systems might be too expensive in terms of the amount of storage and computational hardware requirements. Direct methods are based on Gauss elimination, which is intuitive but costs a large amount of time and computer memory. Therefore, iterative methods are typically used in computer solvers. The approaches based on an iterative procedure can minimize the storage and simulation time. An iterative approach starts with an initial guess procedure. This procedure may be simply represented by the matrix equation and is simple to apply. In particular, for sparse matrices, it involves only a small number of arithmetic operations at each iteration step. On the other hand, many iteration steps may be required before a reasonable solution is obtained. Two questions are of great relevance: first, is the convergences achieved for any solution guess and second, how rapidly the solution.

An iterative approach starts with an initial guess for the vector  $\mathbf{u}$ , say  $\mathbf{u}^{(0)}$  and proceeds in successive steps in an attempt to improve our inexact solution  $\mathbf{u}^{(p)}$ . In the simplest form, this procedure may be represented by the matrix equation,

$$\mathbf{u}^{(p+1)} = \mathbf{P}\mathbf{u}^{(p)} + \mathbf{c} \quad (3.107)$$

then the vector  $\mathbf{u}^{(\infty)}$  satisfies the matrix equation

$$(\mathbf{I} - \mathbf{P})\mathbf{u}^{(\infty)} = \mathbf{c} \quad (3.108)$$

Thus  $\mathbf{u}^{(\infty)}$  will be the solution we require if this matrix equation (3.108) is consistent with the equation of interest (3.82). It follows that if the vector  $\mathbf{c}$  is related to the known vector  $\mathbf{w}$  by the non-singular matrix  $\mathbf{T}$ , with  $\mathbf{c} = \mathbf{T}\mathbf{w}$ , then the iteration matrix must satisfy the condition

$$\mathbf{T}^{-1}(\mathbf{I} - \mathbf{P}) = \mathbf{A} \quad (3.109)$$

Or,

$$\mathbf{P} = \mathbf{I} - \mathbf{T}\mathbf{A} \quad (3.110)$$

The advantage of this procedure is that each improved value  $\mathbf{u}^{(p+1)}$  is obtained explicitly.

For the case of sparse matrices, it involves only a small number of arithmetic operations at each iteration step. On the other hand, many iteration steps may be required before a reasonable solution is obtained. Two questions are of great relevance: first, is the convergence achieved for any solution guess  $\mathbf{u}^{(0)}$  and second, how rapidly the solution vectors  $\mathbf{u}^{(p)}$  will converge. Rather

than considering the absolute solution vector  $\mathbf{u}^{(p)}$ , it is useful to examine the error vector  $\boldsymbol{\kappa}^{(p)}$  which remains at any step: thus, if  $\mathbf{u}$  is the exact solution of the matrix equation,

$$\boldsymbol{\kappa}^{(p)} = \mathbf{u}^{(p)} - \mathbf{u} \quad (3.111)$$

For reasons of consistency, the exact solution  $\mathbf{u}$  should satisfy the equation

$$\mathbf{u} = \mathbf{P}\mathbf{u} + \mathbf{c} \quad (3.112)$$

With the help of equation (3.107) and (3.111), the error vector at successive steps can be defined as

$$\boldsymbol{\kappa}^{(p+1)} = \mathbf{P}\boldsymbol{\kappa}^{(p)} \quad (3.113)$$

The requirement of getting convergence

$$|\boldsymbol{\kappa}^{(p+1)}| < |\boldsymbol{\kappa}^{(p)}| \quad (3.114)$$

For the case of the general five-point difference equation (Eq. 3.77) and (Eq. 3.78), the iterative procedure can be set up directly by solving for the value of the potential at the mesh point  $(i, j)$  in terms of its surrounding values as follows:

$$\phi_{i,j}^* = \frac{1}{e_{i,j}} (f_{i,j} - a_{i,j}\phi_{i+1,j} - b_{i,j}\phi_{i-1,j} - c_{i,j}\phi_{i,j+1} - d_{i,j}\phi_{i,j-1}) \quad (3.115)$$

$$\phi_{i,j}^{new} = \omega\phi_{i,j}^* + (1 - \omega)\phi_{i,j}^{old} \quad (3.116)$$

where  $f_{i,j} = \Delta^2\rho_{i,j}$  and  $\omega$  is a constant or variable relaxation factor chosen to optimize the convergence of the iteration.

### 3.7.1 The Gauss Seidel Method

In each iteration step, the equation (3.113), each component of the vector  $\phi_{i,j}^{new}$  is computed in the sequence. For example, in the calculation of the potential at (i, j), the new iteration values  $\phi_{i,j-1}^{new}$  and  $\phi_{i-1,j}^{new}$  have already been determined. Since they are an improvement on the old values, to enhance convergence it is reasonable to use the new values in the iteration procedure. As in the Jacobi method,  $\omega$  is equal to unity. It can be shown that the rate of convergence of the Gauss-Seidel method is greater than that of the Jacobi method, though only marginally so.

### 3.7.2 The Successive Over-Relaxation (SOR) Method

To further improve the rate of convergence of the Gauss-Seidel method, one might consider using a weighted average of the results of the two most recent estimates to obtain the next best guess of the solution. If the solution is converging, this might help extrapolate to the real solution more quickly. A linear combination of the old value  $\phi_{i,j}^{old}$  and the value given by Gauss-Seidel as expressed by rearranging equation (3.116) as

$$\phi_{i,j}^{new} = \phi_{i,j}^{old} - \omega \frac{R_{i,j}}{e_{i,j}} \quad (3.117)$$

where  $R_{i,j}$  is called residual and is given by

$$R_{i,j} = a_{i,j}\phi_{i+1,j} + b_{i,j}\phi_{i-1,j} + c_{i,j}\phi_{i,j+1} + d_{i,j}\phi_{i,j-1} - f_{i,j} \quad (3.118)$$

The relaxation factor  $\omega$  is taken in the range  $1 \leq \omega \leq 2$  and corresponds to an overcorrection on the value in order to anticipate future corrections.



### 3.8 Electric Field Calculation

Once the potential has been calculated on the grid, the value of the electric field

$$\mathbf{E}(\mathbf{r}) = -\nabla\phi(\mathbf{r}) \quad (3.119)$$

Using centered difference method on the mesh point, the x-component and y-component of electric field at mesh point (i, j) can be computed as;

$$E_x = \frac{\phi_{i+1,j} - \phi_{i-1,j}}{2\Delta x} \quad (3.120)$$

$$E_y = \frac{\phi_{i,j+1} - \phi_{i,j-1}}{2\Delta y} \quad (3.121)$$

Special care needs to be taken in determining the value at the boundaries. For example, in the case of Neumann's condition, in order to achieve normal derivatives of the potential equal to zero, an extra fictitious mesh is created outside the boundary. The values of the potential on the two points adjacent to the boundary (the one just outside and just inside, respectively) are set equal to each other, in order to have zero field on the boundary.

### 3.9 Quantum Confinement Effects

The quantum confinement effects are included in the TNL-PD simulator to explain quantization effects in modern down-scaled microelectronics devices through density gradient model and effective potential approach given by Ferry.

#### 3.9.1 Density Gradient model

The density gradient model allows a local representation of quantum confinement effect and shows more suitability for the implementation in device simulators compared to a coupled Schrodinger-Poisson solver, which is dependent on non-local quantities. The role of quantum confinement effects in narrow width advance node CMOS, FETs, TFETs, JLFET, power, and other nanodevices are studied successfully through the density gradient model on unstructured meshes to describe carrier confinement in arbitrary potential wells. In density gradient model, an additional term is included in the Boltzmann transport equation. The additional term is higher-order derivatives of the potential. It thereby introduces a limited degree of additional nonlocality into the equations which accounts for the impact of quantization effects. The model is simple and its ability to describe C–V characteristics and even tunneling currents are well established. The implementation of density gradient model contains the Jacobian of the system need to be modified, but it remains sparse. The model can be used in one or multidimensional by construction depending upon the requirements. Density gradient model is first-order quantum-correction model describe carrier confinement by locally modifying the electrostatic potential through a correction potential  $\gamma$ . The equations for the correction potential are derived from Wigner's equation, it is assumed that any effects associated with Fermi-Dirac statistics and many-body effects can be safely neglected. The effective mass and non-parabolic band approximations are used and it is assumed that the described electron gas has an infinite extent. The Wigner function is Fourier transform of the product of wave functions at two points in space [10]-[11]

$$f(r, k, t) = \frac{1}{\pi^3} \int \Psi(r - r', t) \Psi^*(r - r', t) \exp(2ir'k) dr' \quad (3.122)$$

The Boltzmann-Wigner transport equation can be derived as

$$\frac{\partial f}{\partial t} + v \cdot \nabla_r f - \frac{q}{\hbar} \sum_{\alpha=0}^{\infty} \frac{(-1)^{2\alpha}}{4^{\alpha}(2n+1)!} \nabla_k^{2n+1} V(\mathbf{r}) \cdot \nabla_k^{2n+1} f = \left( \frac{\partial f}{\partial t} \right)_{coll} \quad (3.123)$$

Here  $v$  is the carrier velocity and  $V$  is the external applied voltage. At  $\alpha = 0$  the equation (3.123), it converts into Boltzmann transport equation. For a parabolic E-k dispersion relation and term  $\alpha = 1$ , the equation yields transport equation with inclusion of density gradient model and given as,

$$\frac{\partial f}{\partial t} + \frac{\hbar k}{m^*} \nabla_r f - \frac{1}{\hbar} \nabla_r (V(\mathbf{r}) - \nabla_r^2 \phi) \nabla_k f = \left( \frac{\partial f}{\partial t} \right)_{coll} \quad (3.124)$$

The correction potential term in multidimensional space is included in term  $\nabla_r^2 \phi$  in the equation (3.124). The term can be defined as

$$\gamma(r, t) = \frac{\hbar^2}{12\lambda k_b T m^*} \left( \nabla_r^2 \phi(r, t) - \frac{1}{2k_b T} (\nabla_r \phi(r, t))^2 \right) \quad (3.125)$$

Here  $k_b$  is Boltzmann constant and  $T$  is the temperature,  $m^*$  is effective mass of carriers. The fitting parameter  $\lambda$  is determined by comparing the carrier density in a device structure to the carrier density obtained by the solution of Poisson Equation. The electric field is obtained as  $E = -\nabla \phi$ , which is undefined at abrupt potential steps, the electrostatic potential is replaced, in the equation (3.13) by  $\phi + \gamma$ , yielding

$$\gamma(r, t) = \frac{\hbar^2}{12\lambda k_b T m^*} \left( \nabla_r^2 \phi(r, t) + \nabla_r^2 \gamma(r, t) - \frac{1}{2k_b T} ((\nabla_r \phi(r, t))^2 + \nabla_r \gamma(r, t))^2 \right) \quad (3.126)$$

The second order correction potential is used to avoid the error and to calculate separately for each type of carriers and added in the external potential for respective charge carriers.

### 3.9.2 The Effective Potential

The natural nonzero size of an electron wave packet in the quantized system, is used to introduce a smoothing of the local potential which is found from Poisson's equation solution. This approach naturally incorporates the quantum potentials, which are approximations to the effective potential. The introduction of an effective potential follows two trends that have been prominent. These are the non-zero size of an electron wave packet and the use of a modified potential to describe quantum effects within classical statistical mechanics.

The effective potential primarily arise from the non-zero size of the electron wavepacket. The potential, in an inhomogeneous system enters the Hamiltonian as

$$H_V = \int dr V(r)n(r) \quad (3.127)$$

Using nonlocal form for charge;

$$V = \int dr V(r) \sum_i n(r) \quad (3.128)$$

It is also desirable to define a smooth quantum potential for use in particle-based simulation. Ferry [59] suggested an “effective potential” that is derived from a Gaussian wavepacket description of particle motion, where the extent of the wave packet is defined from the range of wave vectors established by the thermalized distribution function. The effective potential seen by electrons is given by the convolution of this wave packet with the physical potential

$$V_{eff} = \frac{1}{\sqrt{2\pi a_0}} \int_{-\infty}^{\infty} V(x') \exp\left(-\frac{(x-x')^2}{2a_0^2}\right) dx' \quad (3.129)$$

Here,  $V(x')$  is the actual potential and  $a_0$  is the spatial spread of the wave-packet. The effective potential accounts for the “size of the electron” and its associated wave-packet, which feels the presence of barriers etc., at a distance. The actual particle is treated as point-like in the presence of the effective potential associated with its wave-like nature, leading back to a classical particle simulation scheme.

The charge distribution by Poisson's equation is given as

$$-\nabla(\epsilon\nabla\phi) = 4\pi \quad (3.130)$$

The permittivity  $\epsilon$  in Eq. (3.127) is position dependent under the condition when various different materials form the device. The charge density  $\rho$  is given by

$$\rho = -e(n - p - N_D^+ + N_A^-) \quad (3.131)$$

where  $n$  and  $p$  are, respectively, the electron and hole densities,  $N_D^+$  and  $N_A^-$  the concentration of ionized donors and acceptors, and  $e$  the electron charge.

### 3.9.3 Bohm Quantum Potential

Mathematically the Bohm potential reads

$$V_{Bohm} = -\frac{\hbar^2}{2m} \frac{\nabla^2 n}{n} \quad (3.132)$$

where  $n$  is the electron density.

### 3.9.3 Calibrated Bohm Quantum Potential

The Calibrated Bohm potential can be considered as a generalization of (1.21). The potential reads:

$$V_{C.Bohm} = -\frac{\hbar^2}{2} \Upsilon \frac{\nabla(\frac{1}{m} \nabla n^\alpha)}{n^\alpha} \quad (3.133)$$

where  $\alpha$  and  $\gamma$  are two fitting parameters that can be calibrated by means of more sophisticated (and thus more computationally demanding) quantum models.

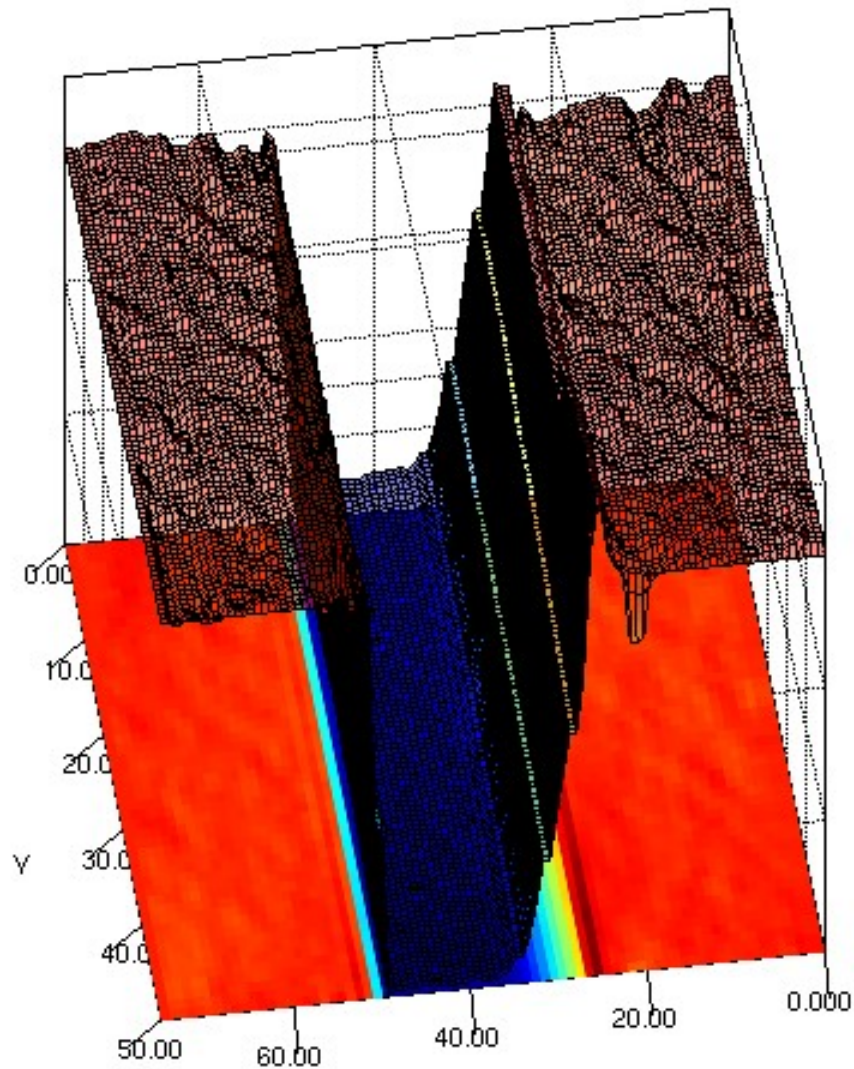
The full effective potential is

$$V_{full} = \alpha^2 \frac{d^2 V}{dx^2} \quad (3.134)$$

To use these effective potentials, basically, one calculates the classical potential by means of the Poisson equation (1.20) and add the selected effective potential to it.

# Chapter 4

## BIPOLAR Devices

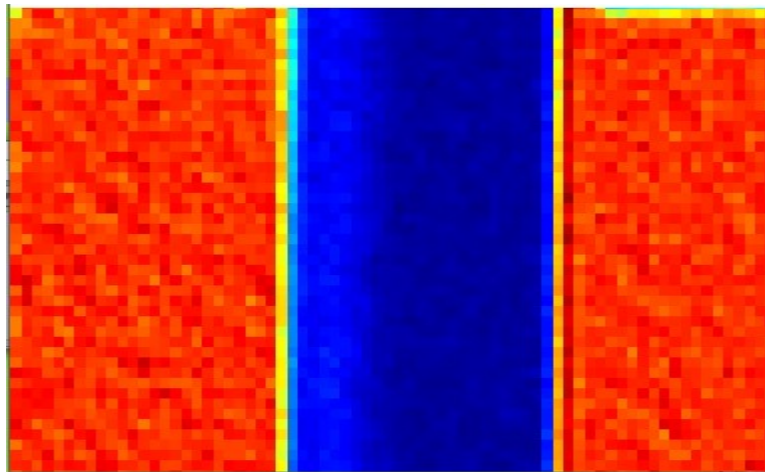


## 4.1 Introduction

TNL-PD (BIPOLAR) simulator is an user friendly GUI enabled simulation tool with very convenient way to describe a device geometries and structure that has to be simulated. The user can define a device by simply describing on GUI interfaced frame.

### 4.1.1 MESFET example to start

The best way to understand how to define a device is by first studying an example. The example we will study here is a MESFET, a silicon device well-known by engineers. The MESFET we want to define and simulate is a structure like the shown below.



A MESFET is a three terminal device, known as the source, the gate and the drain. Two contacts i.e. source and drain, are ohmic contacts, whereas the gate is a Schottky contact. This device has also two  $n^+$  zones and one  $n$  zone. The dimensions of the MESFET under consideration are  $d = 0.2 \mu\text{m}$ ,  $L_1 = 0.1 \mu\text{m}$ ,  $L_c = 0.4 \mu\text{m}$ ,  $L_2 = 0.1 \mu\text{m}$ ,  $L_G = 0.2 \mu\text{m}$  and  $W = 0.05 \mu\text{m}$ . The densities are  $n^+ = 3 \times 10^{23}/\text{m}^3$  and  $n = 10^{23}/\text{m}^3$ .

To simulate electron transport in a MESFET using the Monte Carlo method, user need to go through Chapter 2 carefully.

After starting the TNL-PD simulator, select the BIPOLAR technology from select Tech drop down menu and defining the working dimension and temperature.

Click on Add Region Tab,

1. Select Material Si
2. Doping Type NType
3. Region N-Region

4. Doping Concentration  $1E2 /m^3$

5. Fill  $x_{min} = 0$ ,  $x_{max} = 750$ ,  $y_{min} = 0$ ,  $y_{min} = 500$ ,

Here dimensions are in nm. User defines the total device length and height with back ground doping concentration. Click Add button

<i>Material</i>	<i>x<sub>min</sub></i>	<i>x<sub>max</sub></i>	<i>y<sub>min</sub></i>	<i>y<sub>min</sub></i>	<i>DopingType</i>	<i>Conc</i>	<i>Region</i>	<i>No.</i>
Si	0	250	0	500	NType	1e22	N-Region	1

Similarly select Si with different geometries and doping concentrations and add. User will see the below lines in the table

Si	0	750	0	500	PType 1e20	P-Region	2
Si	0	250	0	500	NType 1e24	N-Region	3
Si	500	750	0	500	NType 1e24	N-Region	4

Similarly, user needs to add the metal and insulator for selecting device boundary conditions in over the device structure.

Following the step, user may add several Metal contacts at any edges or part of edges as below,

Metal	0	200	500	500	NType	1e24	Ohmic_UP	5
Metal	550	750	500	500	NType	6e23	Ohmic_UP	6
Metal	250	500	500	500	0	0	Schottky_UP	7

Select Metal from the Select Material drop down list and select NType doping for defining each and every contact on the device structure. To make reservoir of carrier, the doping concentration of metal region must be equal to the maximum doping concentration of semiconductor region. With Metal selection two types of contacts can be defined i.e. Ohmic and Schottky.

Here four edges up, down, left and right are in the MESFET structure. The source, drain and gate contacts are taken at upper edge of the device with varying x-dimensions whereas y-dimensions are constant.

User need to take care to define the contacts at different edges over semiconductor material i.e. Left, Right, Up, Down, as these will work as dirichlet boundary condition for the device.



Similarly user must add remaining device edges with insulator for setting the Neumann boundary conditions following the steps defined.

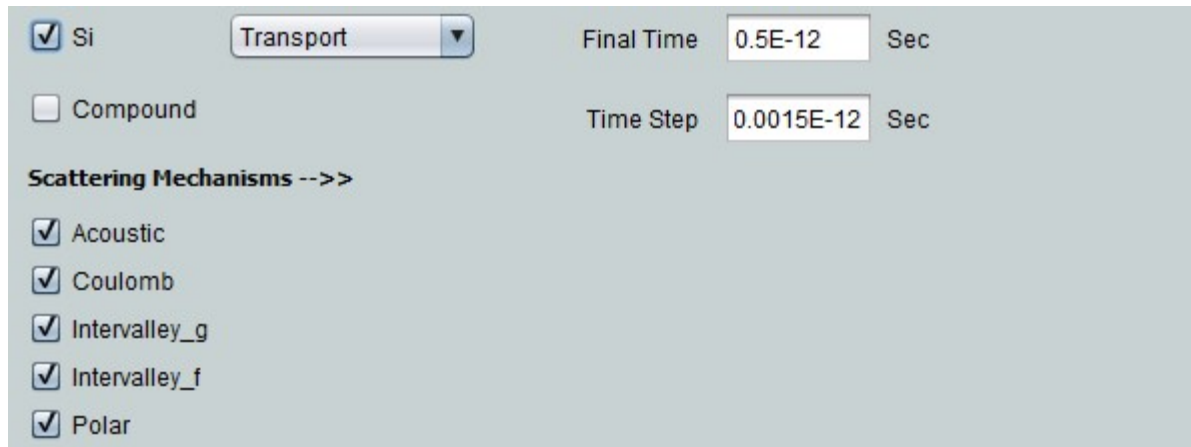
```
Insulator 0 0 0 500 0 0 Insulator_LEFT 8
Insulator 750 750 0 500 0 0 Insulator_RIGHT 9
Insulator 0 750 0 0 0 0 Insulator_DOWN 10
```

At the left, right and down edges the insulator material satisfies the Neumann boundary condition.

In Mesh tab, user will add the meshes over the device structure. User will fill step size  $x=10\text{nm}$  and step size  $y = 10\text{nm}$ . The GUI feature will automatically calculate the total number of meshes in x- and y-dimensions. E.g. in MESFET structure the meshes are

```
Total_Number_X_Mesh 75.0
Total_Number_Y_Mesh 25.0
```

In Physics tab, User will select the material so that appropriate material specific scatterings can be chosen. For MESFET, Si specific scatterings are acoustic, intervally and coulomb, it will be automatically selected.



Defining the total simulation time and time step as  $0.5\text{E-}12$  and  $0.0015\text{E-}12$  sec.

```
Final_Time 1.0E-12
Time_Steps 2.0E-15
```

Select KANE band structure for initiate nonparabolicity in band structure.

```
Band_Structure KANE
```

Select

```
statistical weight = 500 and Media = 500
```

In Material parameters tab, select Si and load and add.

Under Biasing tab, select each and every metal and insulator contact for defining the applied biasing as shown below;

Ohmic_UP	Step	Voltage	0.0	1.0	5.0	1
Ohmic_UP	Constant	Voltage	0.0	0.0	0.0	2
Schottky_UP	Constant	Voltage	-0.8	-0.8	-0.8	3
Insulator_LEFT	Constant	Voltage	0.0	0.0	0.0	4
Insulator_RIGHT	Constant	Voltage	0.0	0.0	0.0	5
Insulator_DOWN	Constant	Voltage	0.0	0.0	0.0	6

Click load and run the simulation, it will ask for the location to save the output data in the computer. The user may check input file which will be save at location provided by user.

User have flexibility to ramp drain voltage under constant gate voltage, it vice-versa is false. i.e. the voltages can only be varied for the current extracting terminal in two contact terminals and three contact terminals device.

The output data will be saved

#### 4.1.2 PN Junction example with Optical Characterization

Following the MESFET example user may add semiconductor, metal and insulator regions and define the appropriate biasing at desired semiconductor edges.

Let us consider an example of n-Si and p-NiO diode. After selection of workspace, the device geometries can be added as

Select N-type Si with back ground doping concentration 5E21 with

Material	Xmin	Xmax	Ymin	Ymax	Doping_type	Conc	Region
Si	0	500	0	300	NType	5e21	N-Region

Similarly select NiO from database with P-type doping concentration 8eE22,

Material	Xmin	Xmax	Ymin	Ymax	Doping_type	Conc	Region
NiO	500	950	0	300	PType	8e22	P-Region

Now semiconductor regions are ready to add metal and insulator. Let us consider ohmic contacts at left and right edges of device structure whereas up and down edges are considered as insulating contacts.

Add Metal from select material drop down box for defining left edge contact to set dirichlet boundary condition. Similarly add Metal at right edge. The ohmic contact doping must be equal to the maximum doping of any of semiconductor region to absorb and emit equal number of electron, i.e. making charge reservoir.

The biasing syntax is,

```
Metal      0      0      0      300  NType      5e21  Ohmic_LEFT
Metal      950    950    0      300  NType      5e21  Ohmic_RIGHT
```

For setting Neumann boundary condition, we will add Insulator at up and down edges. At insulating contacts the reflection boundary is by default active in the simulation program. The syntax after addition of Insulating contact is

```
Insulator   0      950    300    300    0      0      Insulator_UP
Insulator   0      950    0      0      0      0      Insulator_DOWN
```

The device structure at GUI viewer looks as

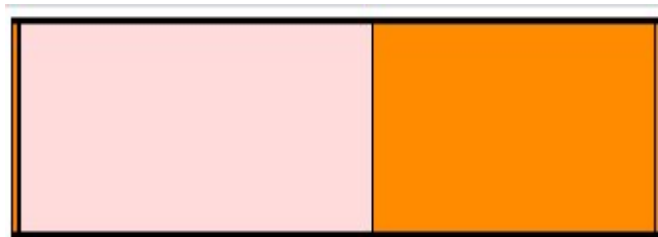
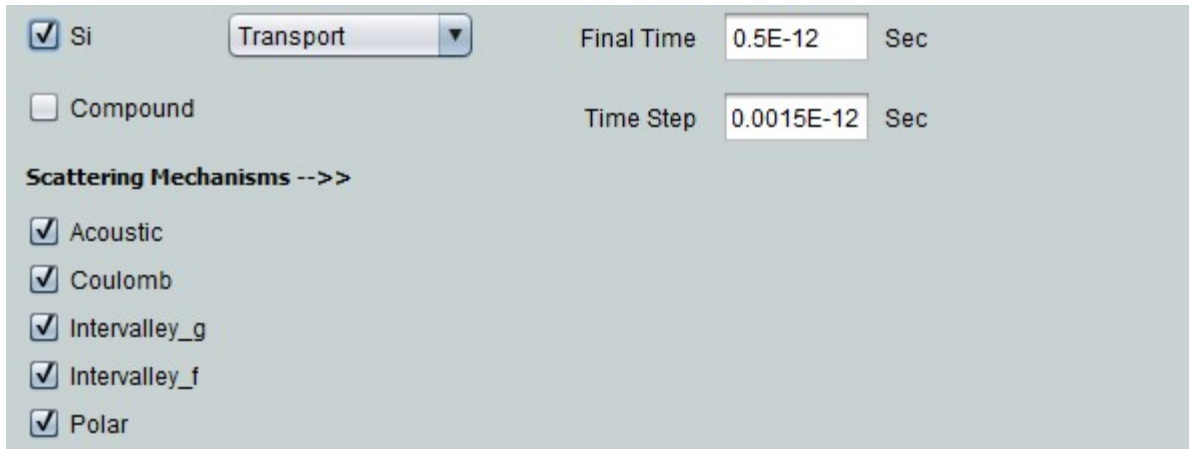


Fig. PN Junction device

In Mesh tab, user will add the meshes over the device structure. User will fill step size  $x=10\text{nm}$  and step size  $y = 10\text{nm}$ . The GUI feature will automatically calculate the total number of meshes in x- and y-dimensions. E.g. in MESFET structure the meshes are

```
Total_Number_X_Mesh  100.0
Total_Number_Y_Mesh   50.0
```

In Physics tab, User will select the material so that appropriate material specific scatterings can be chosen. For MESFET, Si specific scatterings are acoustic, optical and impurity, it will be automatically selected.



Defining the total simulation time and time step as 0.5E-12 and 0.0015E-12 sec.

```
Final_Time 1.0E-12
```

```
Time_Steps 2.0E-15
```

Select FULL band structure for initiate nonparabolicity in band structure drop down box.

```
Band_Structure FULL
```

Select

```
statistical weight = 500 and Media = 500
```

Statistical Weight basically used here to normalize the (initial) number of super-particles in a cell containing the maximum doping concentration of the device. The cells that have a lower doping density will be filled consequently.

Media term is used for fixing the (integer) number of final steps over which the observables are averaged over in order to smooth out the natural spurious oscillations intrinsic to the Monte Carlo method.

In Material parameters tab, select Si material and load material parameters from inbuilt database and add. Similarly do it for NiO material.

Under Biasing tab, select each and every metal and insulator contact for defining the applied biasing as shown below;

Ohmic_LEFT	Step	Voltage	0.0	1.0	5.0
Ohmic_Right	Constant	Voltage	0.0	0.0	0.0
Insulator_LEFT	Constant	Voltage	0.0	0.0	0.0
Insulator_RIGHT	Constant	Voltage	0.0	0.0	0.0

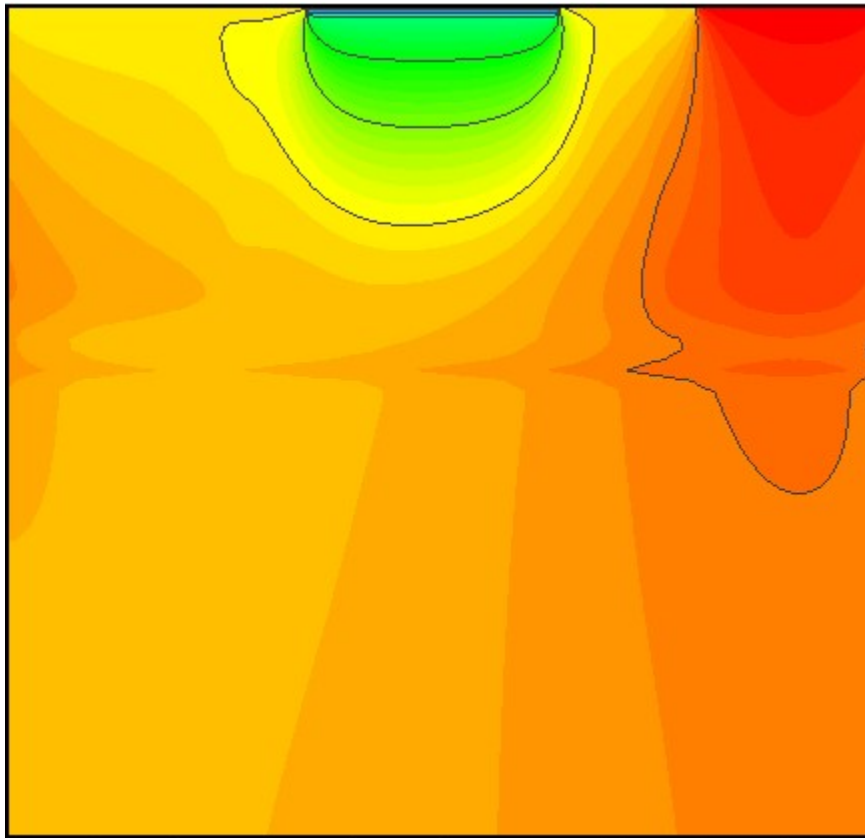
In case of diode simulation, user must remember that on left ohmic contact is on the n-Si semiconductor material while the right ohmic contact is on the p-NiO semiconductor material, it that diode is in reverse biasing. For applying forward bias to the diode, user needs to specify ramping +ve voltages at right ohmic contact or p-type region.

User may simulate electronic transport under forward and reverse bias condition.

In this example, the dark current under produce by diode is characterized.

# Chapter 5

## UNIPOLAR Devices



TNL-PD (UNIPOLAR) simulator is user friendly GUI enabled simulation tool with very convenient way to describe a device geometries and structure that need to be simulated. The user may define a device geometry, material parameters, biasing etc by simply using mouse click in GUI interfaced frame.

For new user to get familiar with MC Particle device simulator, user may follow step by step the given tutorial. In current tutorial the Simulation of 20 nm channel length SOI MOSFET is described exploiting the Monte Carlo Particle Device Simulator.

### 5.1 Technology and Workspace setting

- Set Technology to UNIPOLAR.
- Set workspace as per requirement.
- In present case our device dimension is in nanometer (nm)
- Set X Scale 100nm.
- Set Y Scale 100nm.
- By-default all scale in nm
- Click “GO” button.
- Information about all the above things will get displayed on below blank text area.

### 5.2 Add Region

#### Adding Source Region:

Mater...	Xmin	Xmax	Ymin	Ymax	Doping	Dose	Name	Regio...
Si	0	20	0	10	NType	1e25	Source	1

- Choose Source as a First region. For source region choose material Si (Silicon) using mouse or up/down key in keyboard.
- Doping type, N Type, Dose 1E25.
- Select region Source.
- Set X and Y Dimensions as  
X Min: 0, X Max: 20nm.Y Min: 0, Y Max: 10nm.
- Click Add Button.

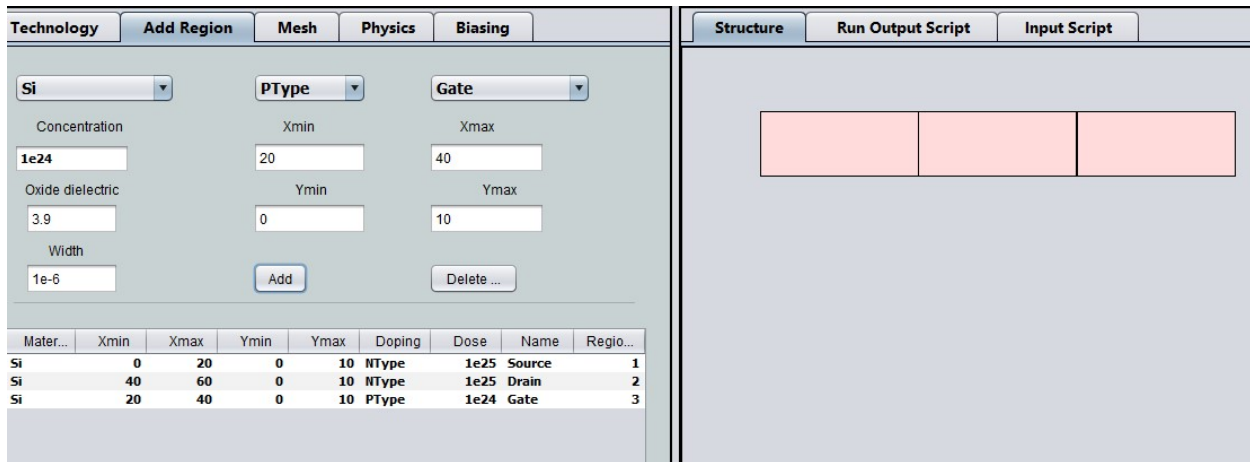
### Adding Drain Region:

Mater...	Xmin	Xmax	Ymin	Ymax	Doping	Dose	Name	Regio...
Si	0	20	0	10	NType	1e25	Source	1
Si	40	60	0	10	NType	1e25	Drain	2

- For Drain Region choose material Si (Silicon) using.
- Doping type N Type, Dose 1E25.
- Select region Drain.
- Set X and Y Dimensions as  
X Min: 40, X Max: 60nm.Y Min: 0, Y Max: 10nm.
- Click Add Button.

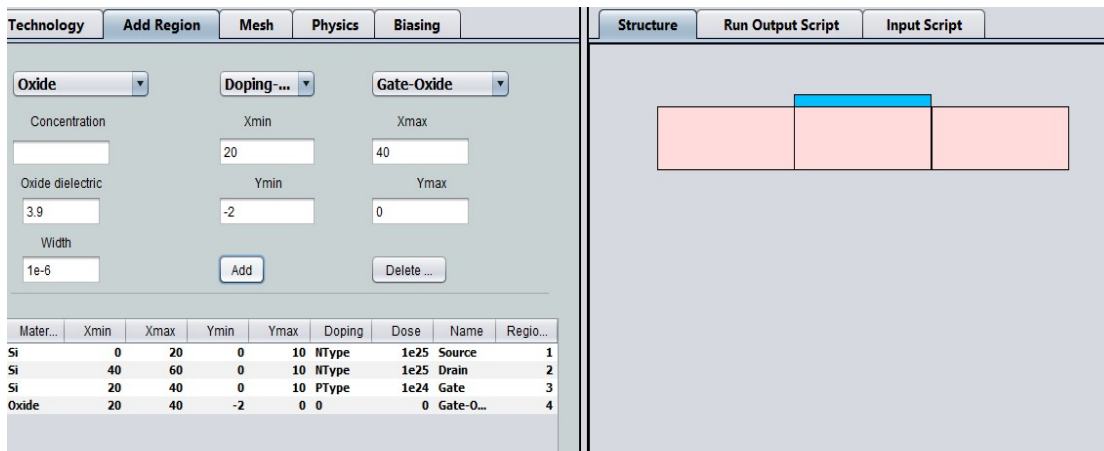


## Adding Gate Region:



- For Gate Region choose material Si (Silicon).
- Doping type P Type, Dose 1E24.
- Select region Gate.
- Set X and Y Dimensions as  
X Min: 20, X Max: 40nm.Y Min: 0, Y Max: 10nm.
- Click Add Button.

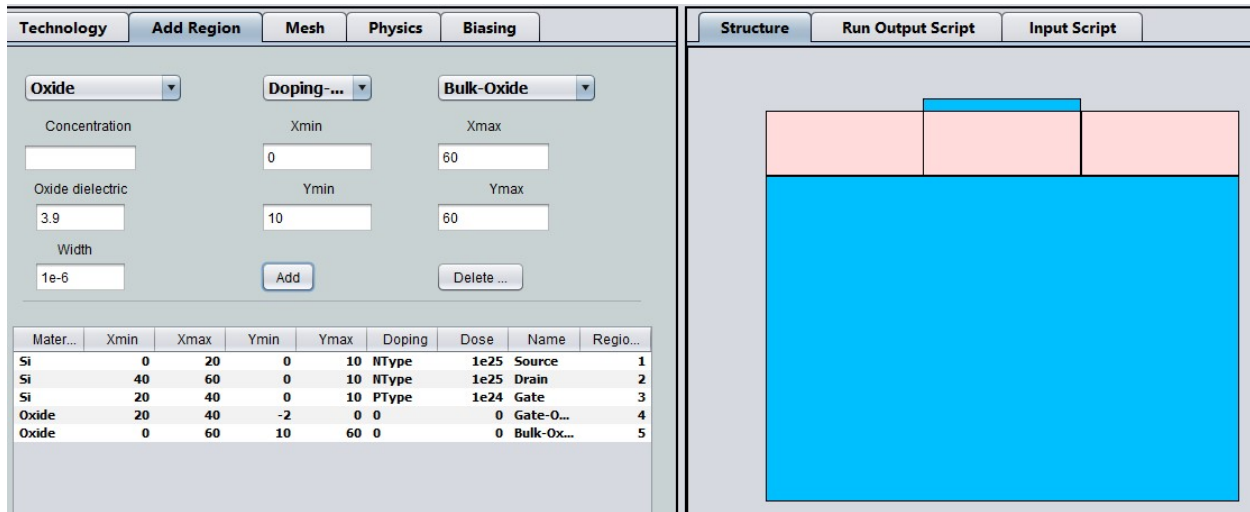
## Adding Gate Oxide Region:



- For Gate Oxide Region choose material Oxide.
- Set Doping type as Doping type, Dose 0.
- Select region Gate-Oxide.
- Set X and Y Dimensions as  
X Min: 20, X Max: 40nm.Y Min: -2, Y Max: 0nm.

- Click Add Button.

### Adding Bulk Oxide Region:



- For Bulk Oxide Region choose material Oxide.
- Set Doping type as Doping type, Dose 0.
- Select region Bulk-Oxide.
- Set X and Y Dimensions as  
X Min: 0, X Max: 60nm. Y Min: 10, Y Max: 60nm.
- Click Add Button.

### Adding Contact1 (Ohmic):

- Ohmic contact over **Gate** region.
- For Contacts choose material Al (Aluminium).
- Set Doping type as Doping type, Dose 0.
- Select region Ohmic.
- Set X and Y Dimensions as  
X Min: 20, X Max: 40nm. Y Min: -2, Y Max: -2nm.
- Click Add Button.

### Adding Contact2 (Ohmic):

- Ohmic contact under **Source** region.
- For Contacts choose material Al (Aluminium).
- Set Doping type as Doping type, Dose 0.

- Select region Ohmic.
- Set X and Y Dimensions as  
X Min: 0, X Max: 20nm.Y Min: 0, Y Max: 0nm.
- Click Add Button.

#### Adding Contact3 (Ohmic):

- Ohmic contact under **Drain** region.
- For Contacts choose material Al (Aluminium).
- Set Doping type as Doping type, Dose 0.
- Select region Ohmic.
- Set X and Y Dimensions as  
X Min: 40, X Max: 60nm. Y Min: 0, Y Max: 0nm.
- Click Add Button.

#### Adding Contact4 (Ohmic):

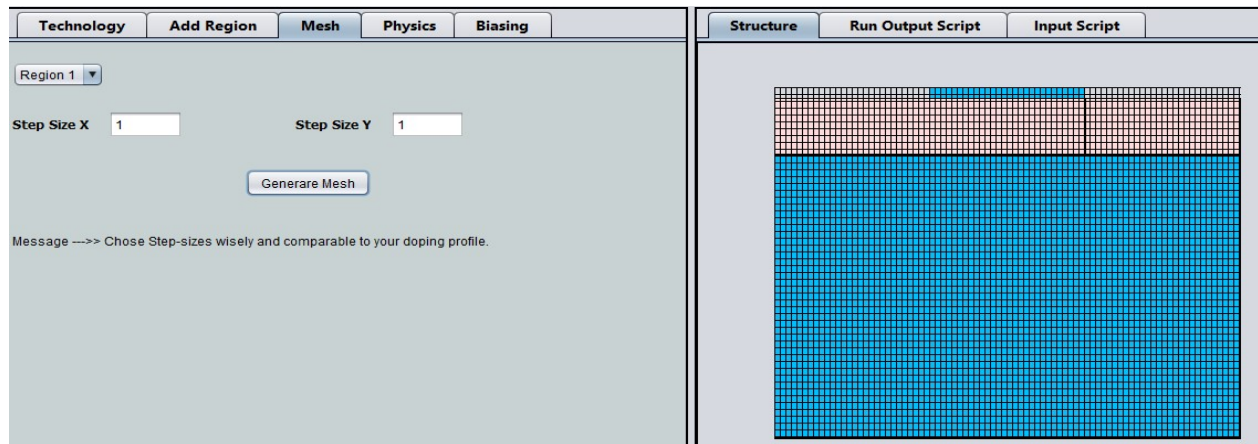
- Ohmic contact under **Substrate** region.
- For Contacts choose material Al (Aluminium).
- Set Doping type as Doping type, Dose 0.
- Select region Ohmic.
- Set X and Y Dimensions as  
X Min: 0, X Max: 60nm.Y Min: 60, Y Max: 60nm.
- Click Add Button.

The screenshot displays the 'Add Region' dialog box in a software application. The dialog is configured for an Ohmic contact with material Al, doping type Ohmic, concentration 0, oxide dielectric 3.9, width 1e-6, and dimensions Xmin: 0, Xmax: 60, Ymin: 60, Ymax: 60. The 'Add' button is highlighted. Below the dialog is a table showing the region configuration:

Mater...	Xmin	Xmax	Ymin	Ymax	Doping	Dose	Name	Regio...
Si	0	20	0	10	NType	1e25	Source	1
Si	40	60	0	10	NType	1e25	Drain	2
Si	20	40	0	10	PType	1e24	Gate	3
Oxide	20	40	-2	0	0	0	Gate-O...	4
Oxide	0	60	10	60	0	0	Bulk-Ox	5
Al	20	40	-2	-2	0	0	Ohmic	6
Al	0	20	0	0	0	0	Ohmic	7
Al	40	60	0	0	0	0	Ohmic	8
Al	0	60	60	60	0	0	Ohmic	9

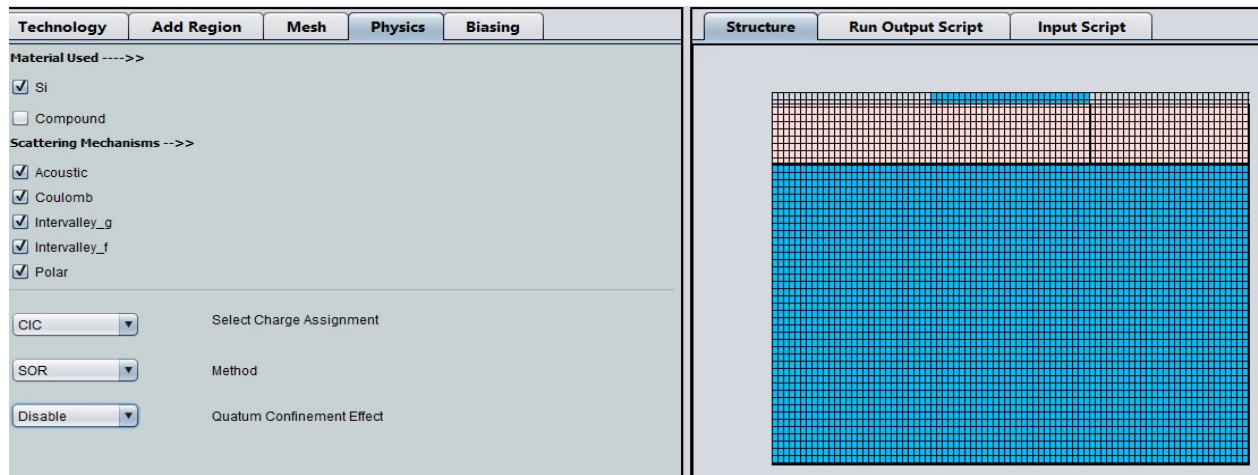
The right side of the screenshot shows a 2D layout view with a blue substrate, a red gate region, and a yellow drain region. The 'Add Region' dialog box is overlaid on the left side of the layout.

### 5.3 Mesh



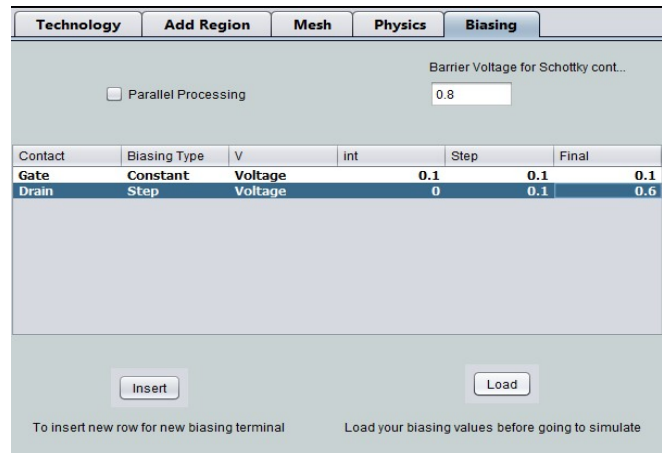
- Select Mesh tab
- In Step-size X write 1.
- In Step-size Y write 1. It means you are working on 1nm X 1nm mesh.
- Click on Generate Mesh
- Mesh graphics will be seen in Structure tab.

### 5.4 Physics



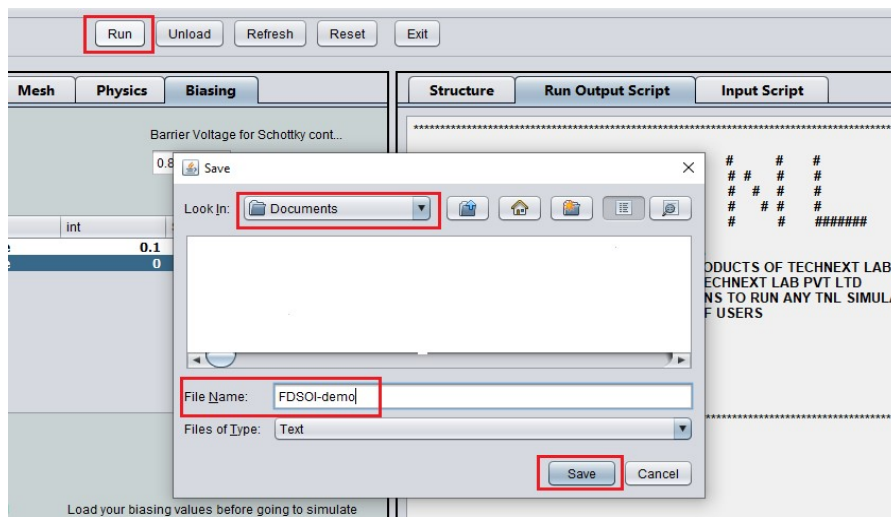
- Select Si check-box in Material Used options
- In Scattering Mechanism all five mechanism are auto-selected
- In Select Charge Assignment select option CIC.
- In Quantum Confinement Effect choose Disable option.

## 5.5 Biasing



- For biasing click below Contact in the table,
- Choose Gate, chose Constant bias, Voltage in next field.
- Gate initial voltage 0.1, step size 0.1, final 0.1 V.
- Click insert choose Drain as contact,
- Chose step bias, provide initial voltage 0.0, step size 0.1, final 0.6 V.
- Click Load Button.

## 5.6 Start Simulation

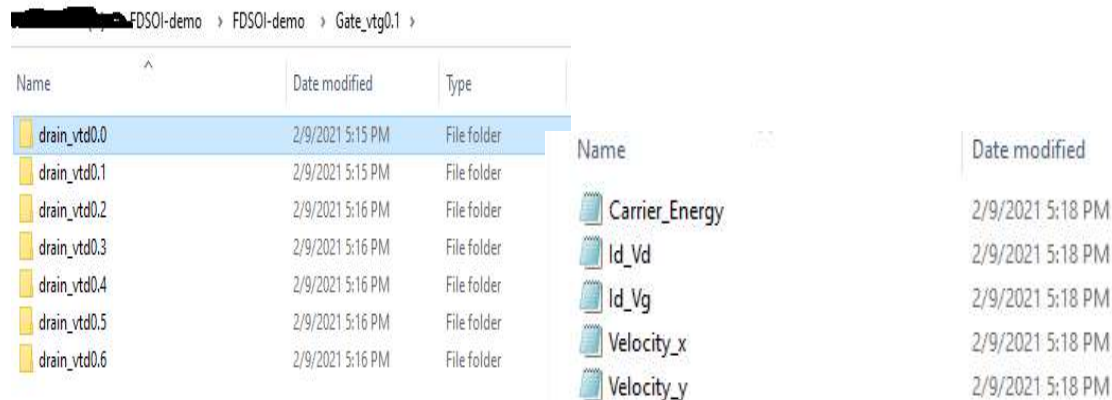


- Click on Run button, a Save pop-up window opened as shown in above figure.
- In save window default directory is 'Documents'. Go to field named File name and write name of your file name (FDSOI-demo for this example) to create a folder in the 'Documents' path of your system.

- Now click Save button. With this step your FDSOI device simulation starts and you can see the information about this in Run Output Script.
- Output script column shows the working directory “C:\Users\...\Documents\FDSOI-demo\FDSOI-demo\...”. It also shows calculation points, no. of particle initialized at a bias point and no. of particles used in every steps.
- When simulation gets completed ‘Simulation Successful message will be displayed

## 5.7 Output Files

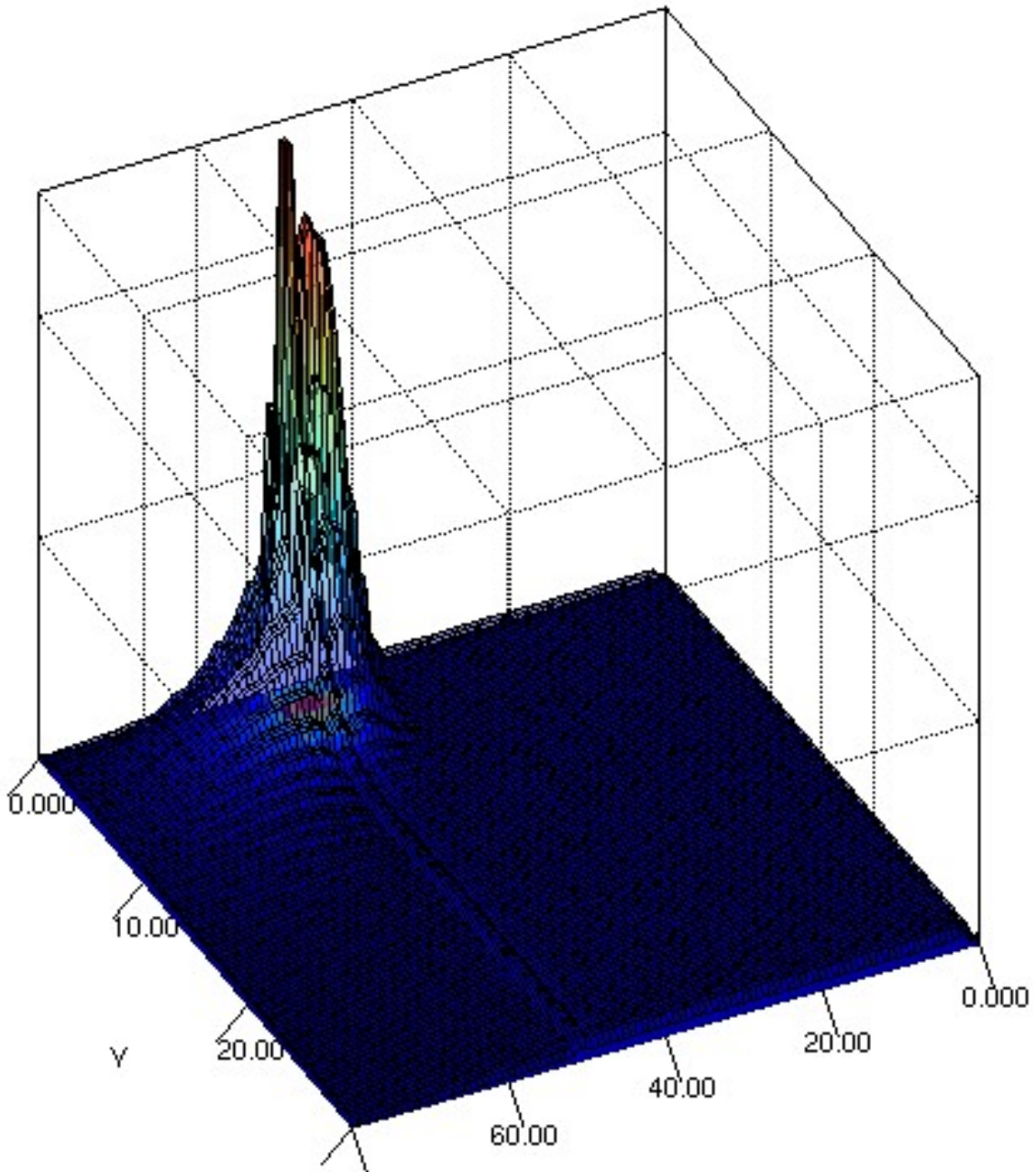
- After the completion of simulation, go to the directory you selected there is a folder named FDSOI-demo.



- Open this folder, you get several folder and text file like FDSOI-demo, plot and FDSOI-demo.txt
- FDSOI-demo folder will contain data folder for drain voltage steps at every gate voltage steps. (drain\_vtd\_y within Gate\_vtg\_x ). Open these folders which contains various file related to the simulation.
- Plot folder contains i-v curves data, velocity-energy-average and carrier energy data files.
- The text file contains all the input information of the device given to simulator.
- User can plot this data on TNL-PLOT by importing the data file.

# Chapter 6

## Optical Characterization



## 6.1 Optical Characterization

Optical device characterization can be simulated through propagation and absorption program integrated into the TNL PDS framework. The monochromatic and polychromatic sources with optical intensity profiles can be defined by using TNL Optical Source frame. The selected light illuminates the semiconductor device either from top or bottom edges. The intensity profiles are then converted into photo generation rates, which are directly integrated into the generation terms in the carrier distribution function in Boltzmann transport equation. The unique coupling of tools allows user to simulate electronic responses to optical signals for a broad range of optical detectors applications.

The physics of carrier generation due to light absorption in to particle device simulation is considered at each DC bias point or transient time step. Absorption coefficient is dependent upon the imaginary component of refractive index and is

$$\alpha(\lambda) = \frac{4\pi}{\lambda} k \quad (6.1)$$

Here  $k$  is the imaginary part of refractive index of the material and  $\lambda$  is the wavelength of the incident light.

User can check and choose the complex refractive index data dependent on wavelength during defining filling information in the TNL Optical Source frame. The wavelength dependent refractive index data is imported from the SOPRA database. With selection of material in the refractive index data can be loaded into frame and after defining the type of source and incident wavelength values, the selected wavelength appropriate real and imaginary refractive index data will be displayed. SOPRA, a thin film metrology company located worldwide ([www.sopra-sa.com](http://www.sopra-sa.com)). The unit consions will automatically handle by TNL Optical Source frame.

## 6.2 Photo Generation due to Light Absorption

The effects of the reflection coefficients with absorption over the ray path are saved for each ray in case of monochromatic and polychromatic optical source. The carrier generation at each mesh point is calculated by integration of the carrier Generation Rate equation over the entire area of the interaction between the light ray and with the grid points. The carrier generation rate is

$$G_n = \eta_0(1 - R) \frac{I_{op}\lambda}{hc} \alpha(\lambda) \exp[-\alpha(\lambda)y] \quad (6.2)$$



Here  $G_n$  is the per unit volume per sec carrier generation rate,  $\eta_0$  is the photon to electron hole pair conversion efficiency,  $R$  is the Fresnel coefficient of reflection,  $I_{op}$  is the optical intensity of the beam,  $y$  is a relative distance of light penetration inside the device either from top or bottom.  $h$  is Planck's constant and  $c$  is the speed of light.

For more details user may refer to various reputed published books on optical characterization. The implement of the Chu's and other reported mechanisms where spectral response is dependent on the bandgap is in progress and will be available in next version.

### 6.3 Tutorial for Device Optical Characterization

As described in chapter 4, user may notice that under *Physics* tab a button for Optical Characterization as shown in Fig. 6.1 is inbuilt.

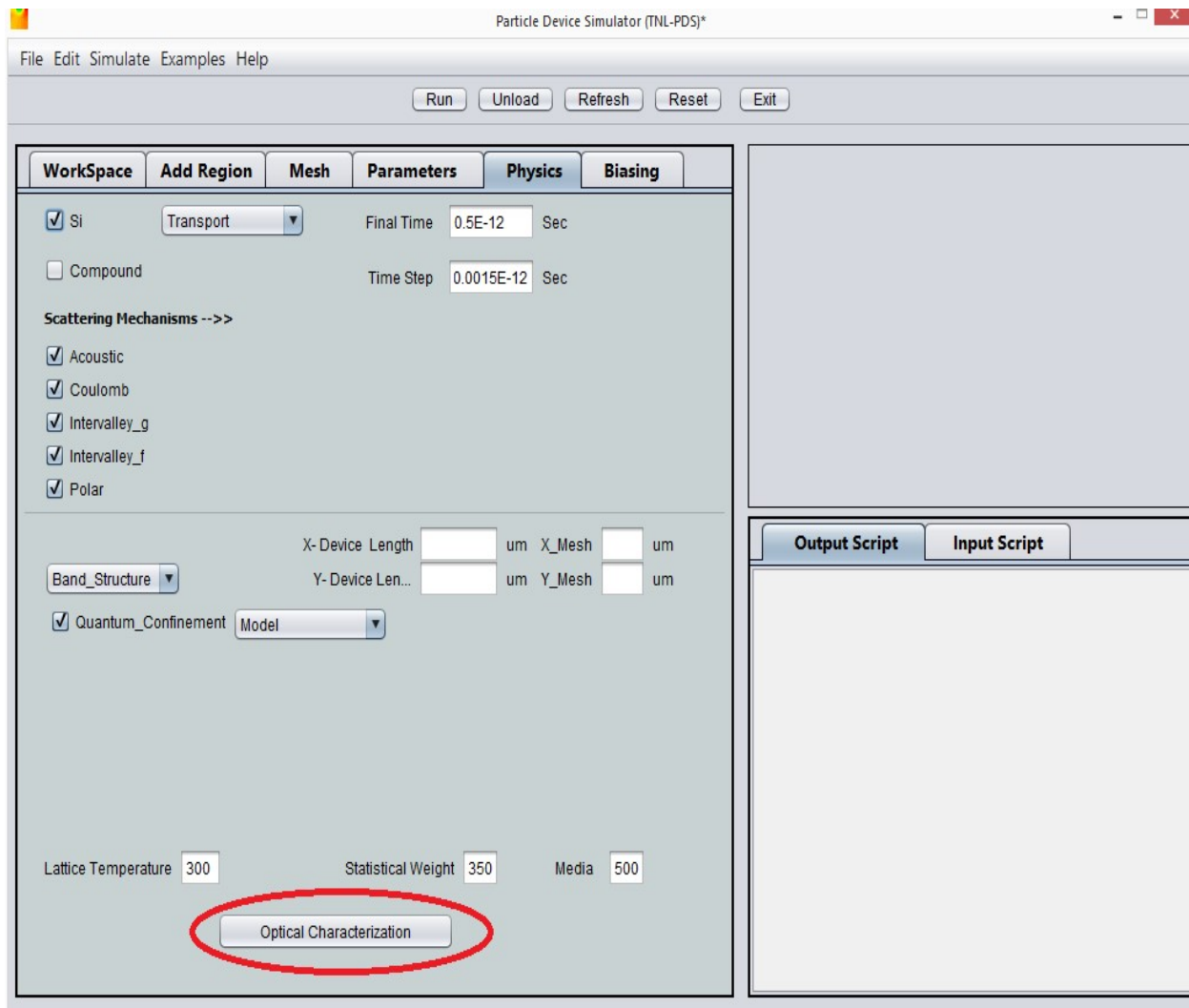


Fig. 6.1 Optical Characterization

The optical characterization of Bipolar devices can be carried out by clicking over this button. A new GUI based form for filling input optical source information will be appeared as shown in Fig. 6.2.

Fig. 6.2 GUI TNL Optical Source Frame

Here user can see that Beam ON is in TNL Optical Source frame. Under Material tab the semiconductor materials initiated during add region for defining the device structure will be automatically shown at the box.

User need to select same material from Material drop down list and click over load button. The Sopra wavelength dependent refractive index data will be loaded in the right panel of the frame as in the Fig. 6.3.

The right panel of frame contains four columns, the first column containing the optical wavelength, second and third columns showing the real part of refractive index data and imaginary part of refractive index data respectively. The fourth column contains the wavelength specific absorpction coefficient data automatically calculated from equation 6.1.

In case the device contain various material like in case of hetero-structure device, repeating above mentioned steps for every materials.

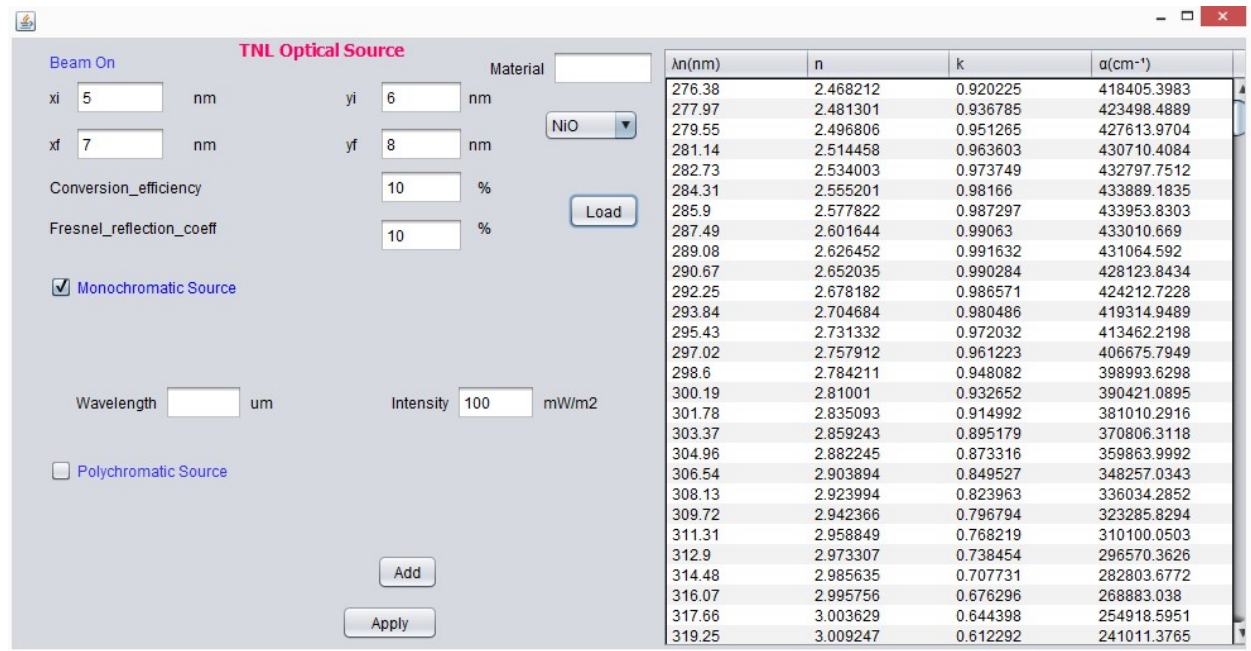


Fig. 6.3 Refractive Index data from Sopra

User need to define the point of contact of beam on the device, which can be defined through filling initial x and final x positions. The illumination can be carried out either from top or bottom so be careful in filling the y-initial and y-final positions. In case of top illumination user will fill maximum device height i.e. Ymax in both yi and yf. For bottom illumination, user will fill zero or Ymin value in both yi and yf.

After defining the beam interaction locations on the device, user need to fill photon to electron hole pair (EHP) conversion efficiency along with the value of Fresnel reflection coefficient at the boxes.

The two types of optical sources can be defined for optical characterization, i.e.

- User may check the Monochromatic Source box by selecting single wavelength with constant intensity.
- User may choose Polychromatic Source, by defining the multispectral wavelengths through filling initial and final wavelengths with constant intensity.

At a time user may select either Monochromatic Source or Polychromatic Source. After filling the above values user need to click add button the right panel will display only selected wavelength specific data in the refractive index table. User need to add same optical data for each and every material of the device.

Click Apply button, all the information will be saved in input file for optical simulation.

### 6.5 Optical Output data

The user may check the optical carrier generation by running two experiments one without invoking optical characterization and other with optical characterization. The number of electrons will be observed different during each iteration in TNL run output window. Also the difference between both experiments will be displayed by the currents obtain.

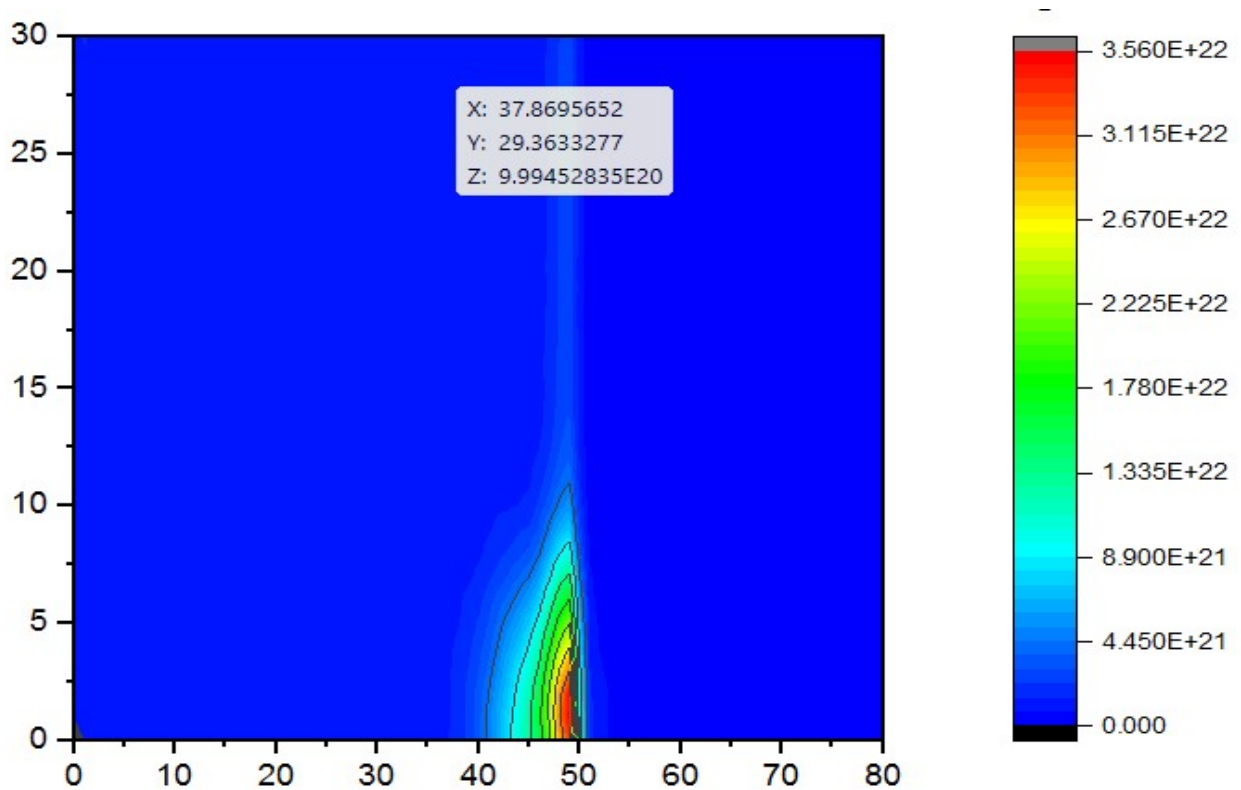


Fig. 6.4 Optical Carrier generation within the Device

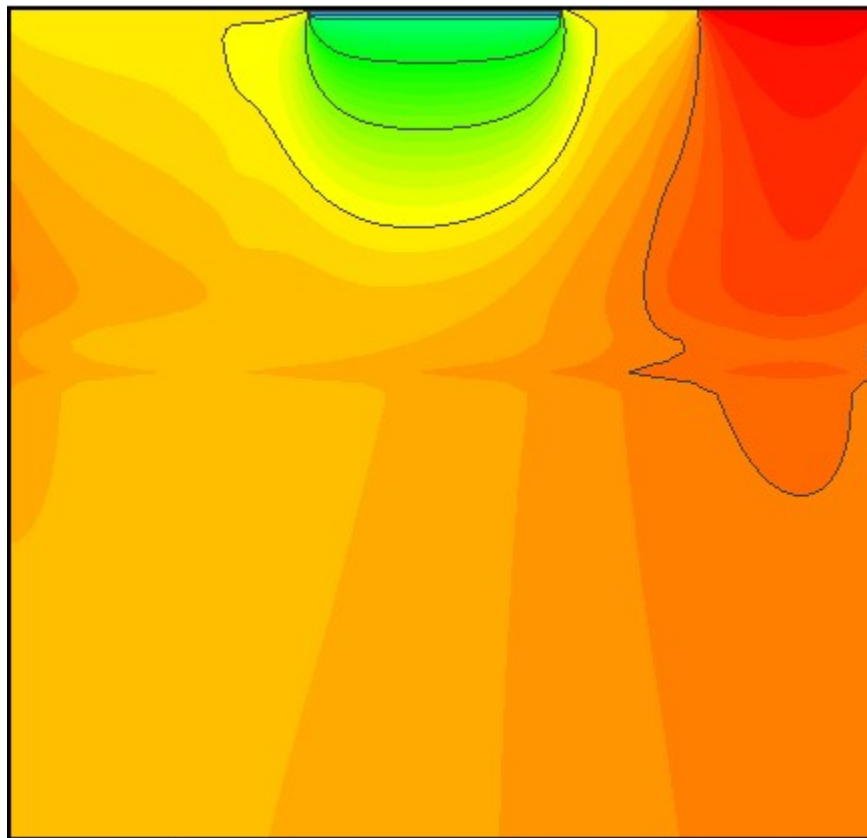
In Fig. 6.4 the carrier density contour is shown, the light is illuminated from the bottom at near hetero junction, the optically generated carriers are displayed through color contour. Similarly other contours e.g. electric field, carrier drift velocity etc will show the carrier generation within the device structure.

The optically generated carrier will contribute in the current conduction process and difference can be observed in the dark current and photo currents comparison under same biasing conditions. The contribution due to optically generated holes in current conduction process is ignored in current version.

# Chapter 7

## TNLPlot

### Visualize Output data



TNLPlot is a powerful graphical and contour visualization tool. It is very easy to load simulation output data from location in the computer. It is user friendly tool with all the robustness require to analyze the output data.

### 7.1. Viewing and Analyzing Output data

In output folder three folders will be generated as the output of simulation of MESFET structure.

#### (i) *PLOT*

In PLOT folder are the out data physical variable is saved against x-axis and y-axis data. User may use third party plotters e.g. Origin to access the contour plot of the physical variables e.g. density, energy, potential, electric field, carrier velocity etc.

#### (ii) *PLOT 2d*

PLOT-2d folder same physical variable data is extracted from PLOT data during saving output data saved ONLY along device length to check the graphical representation. The suffix 2d represents that only physical variable data along device length is saved.

#### (iii) *Contour*

In contour folder we normalize the axis data save in PLOT folder to visualize the contour profile over the TNLPlot contour as;

$$\begin{aligned}x\text{-axis} & - \textit{Original } x \textit{ values} * 1000 \\y\text{-axis} & - \textit{Original } y \textit{ values} * 1000\end{aligned}$$

The physical variable data remains same as it is in PLOT folder.

User need to open TNLPlot from TNLframe.



Fig.7.1. TNLPlot

Here it clearly seen over TNLPlot viewer, the two options for loading the output data file.

*Clicking over File menu, it will ask for location in the computer where user has saved the output data. User may load 2d data for each physical variable to analyze the output data.*

*Clicking over Contour menu, it will also ask for location in the computer where user has saved the output data. User may load contour data for each physical variable to analyze the output data.*

User may use both option simultaneously to visualize graphical representation along with 2D and 3D contour profile as shown below;

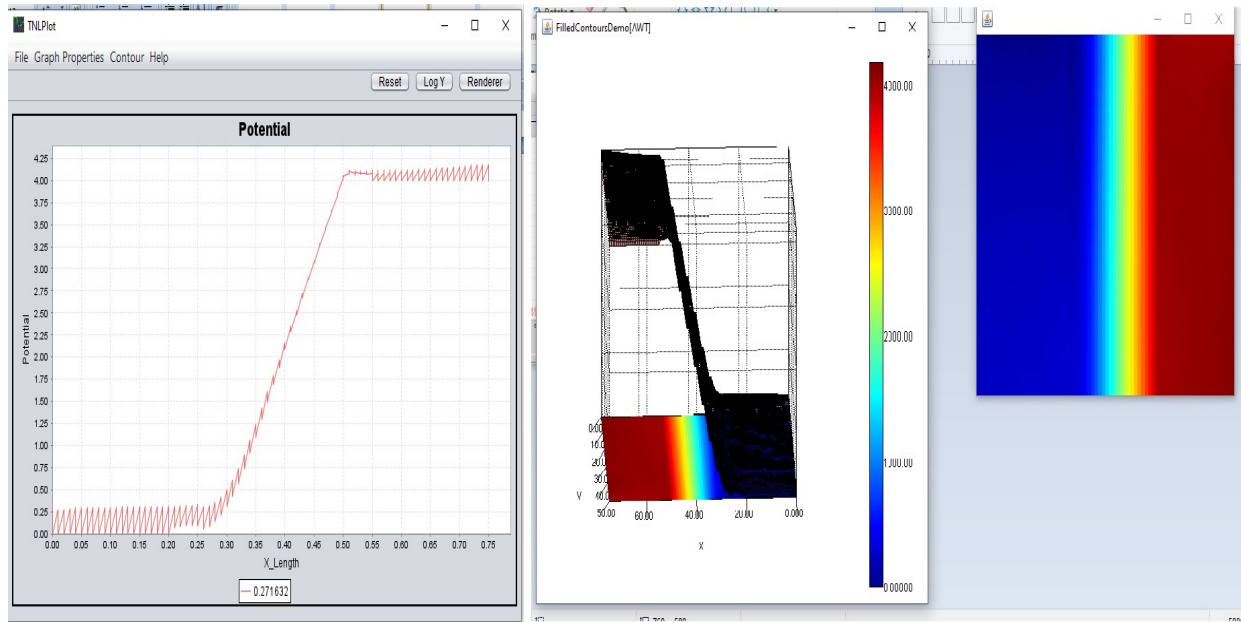


Fig.7.2. Potential distribution along the MESFET device

For example to use TNLPlot effectively, the demonstration of MESFET output data is used to demonstrate the TNLPlot.

TNLPlot is dependent on the output data, visualization and analysis purpose it is independent from any UNIPOLAR or BIPOLAR simulators.



### 7.2 Electric Field Profile of MESFET

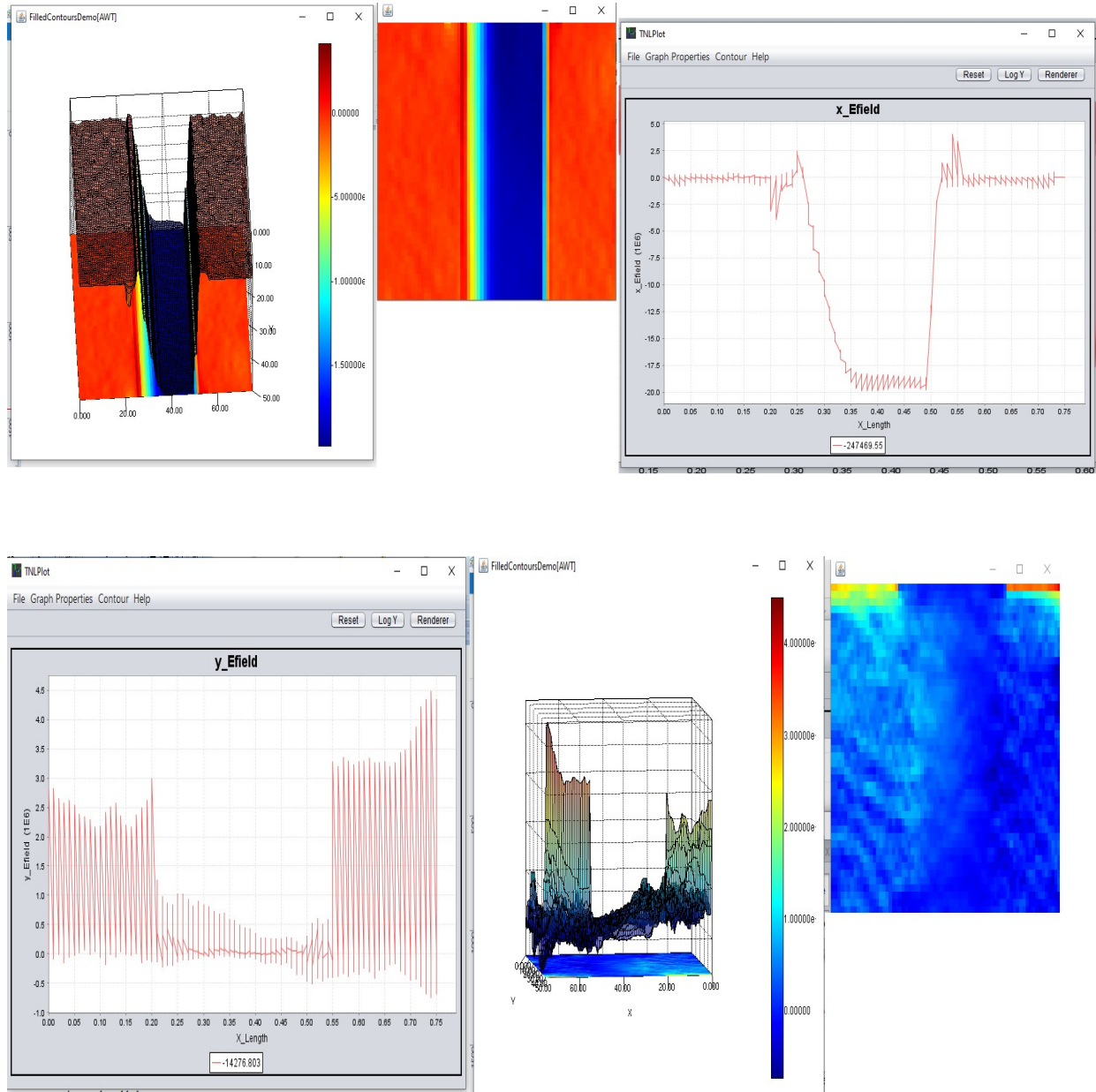
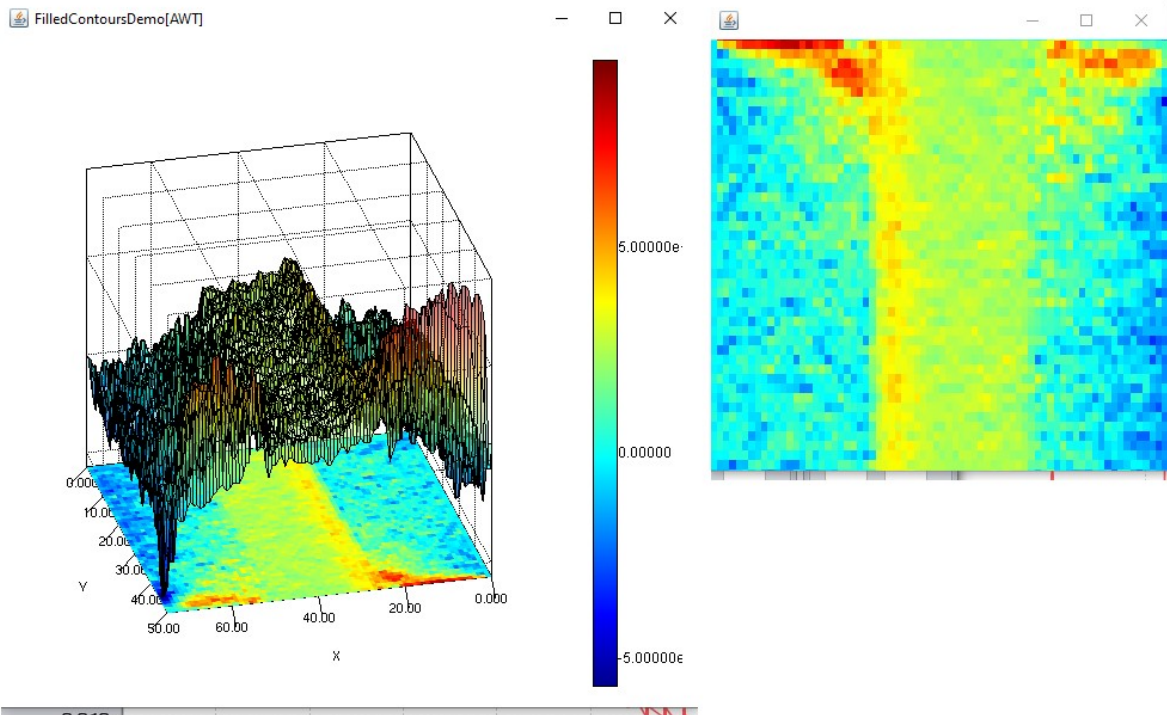
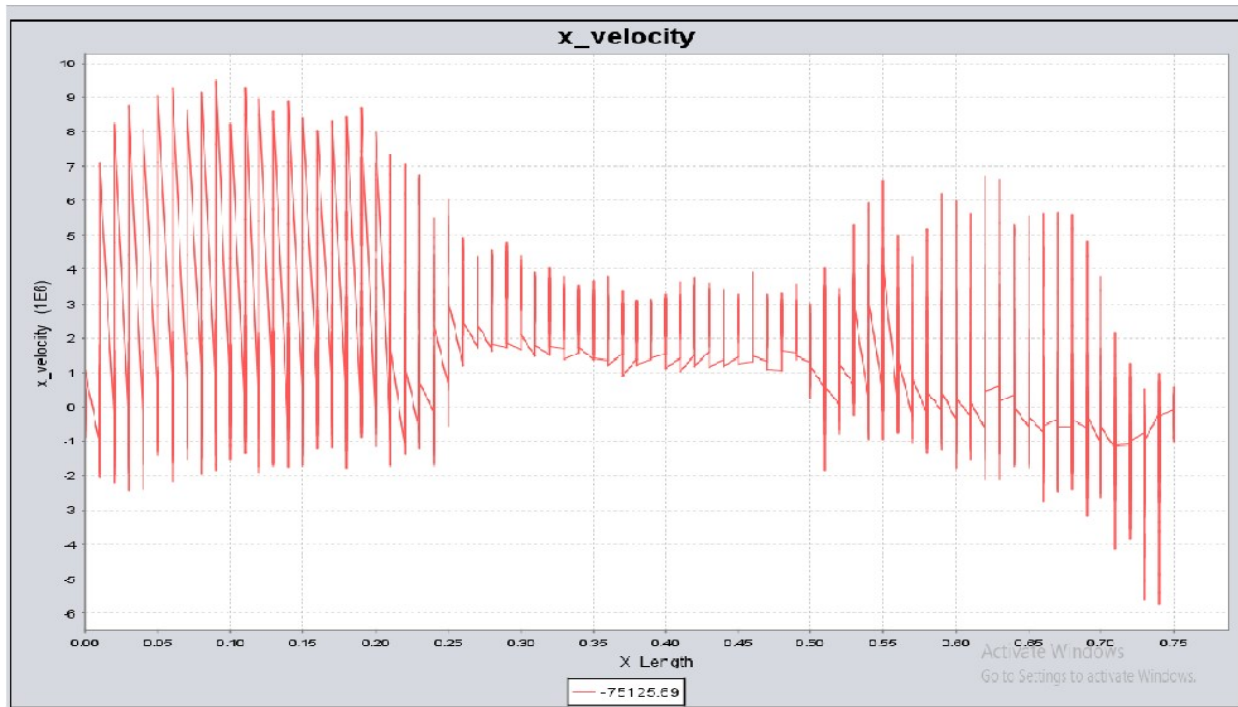


Fig. 7.3 Electric Field distribution along the MESFET device in x- and y-direction respectively.

### 7.3 Carrier velocity along device length



Similarly other variable output physical parameters can be visualized and analyzed.

#### ***7.4 Current Analysis***

TNL Particle Device (PD) simulator is based on atomistic technique with capabilities to track and trace each and every electron in cloud under the influence of applied electric potential at the edges covering the semiconductor regions in terms of Dirichlet and Neumann boundary conditions. During particle based simulations the carriers reach at any of edge defined over semiconductor region is counted and in turn generate the current.

In the output data, whatever Metal and Insulator defined over semiconductor region, the current file will be generated based contact edges defined by user. User may analyze current on each edge of the device.

## References

1. Hockney, R. W., Eastwood, I. W.: Computer Simulation Using Particles. New York: McGraw-Hill. 1981.
2. C. Jacoboni and P. Lugli, The Monte Carlo Method for Semiconductor Device Simulation (Springer-Verlag, Vienna, Austria, 1989).
3. K. Hess, Monte Carlo Device Simulation: Full Band and Beyond (Kluwer Academic Publishing, Boston, MA, 1991).
4. D.Vasileska, S.M.Goodnick, G.Klimeck, Computational Electronics- Semiclassical and Quantum Device Modeling and Simulation (CRC Press © 2010 by Taylor and Francis Group, LLC).
5. Fischetti, M. V., Laux, S. E.: Phys. Rev. *B38*, 9721 (1988).
6. S. E. Laux, IEEE Trans. Comput.-Aided Des. Int. Circ. Sys., 15, 1266 (1996).
7. Ravaioli, u., Ferry, D. K.: Superlattices and Microst. 2, 75 (1986).
8. J Ravaioli, u., Ferry, D. K.: Superlattices and Microst. 2, 377 (1986).
9. Fawcett, W., Boardmann, A. D., Swain, S.: J. Phys. Chem. Solids 31,1963 (1970).
10. Ferry, D. K, Superlattices and Microstructures, Vol. 28, No. 5/6, (2000).
11. Ramey,S.M, Ferry,D.K, Physica B, 314, 350–353, (2002).
12. Xinchun Guo, Algebraic Multigrid Poisson Equation Solver, Master of Science thesis submitted ARIZONA STATE UNIVERSITY (2015).
13. G.E. Moore, “Cramming more components onto integrated circuits,” Electronics, vol. 38 (1965).
14. R.H. Dennard, F.H. Gaensslen, H.N. Yu, V.L. Rideout, E. Bassous, and A.R. LeBlanc, “Design of ion-implanted MOSFET’s with very physical dimensions,” IEEE J. Solid-State Circuits, vol. SC-9 (1974): pp. 256-268.
15. J.R. Brews, W. Fichtner, E.H. Nicollian, and S.M. Sze, “Generalized guide for MOSFET miniaturization.” IEEE Electron Dev. Lett., vol. 1 (1980): pp. 2-4.
16. G. Baccarani, M.R. Wordeman, and R. H. Dennard, “Generalized theory and its application to 114 micron MOSFET design,” IEEE Trans. Electron Devices, vol. 31 (1984): pp. 452-462.
17. K.K. Ng, S.A. Eshraghi, and T.D. Stanik, “An improved generalized guide for MOSFET scaling,” IEEE Trans. Electron Devices, vol. 40 (1993): pp. 1895-1897.
18. K.J. Kuhn. “Moore's Law past 32nm: Future Challenges in Device Scaling.” [download.intel.com/pressroom/pdf/kkuhn/Kuhn\\_IWCE\\_invited\\_text.pdf](http://download.intel.com/pressroom/pdf/kkuhn/Kuhn_IWCE_invited_text.pdf).
19. G.D. Wilk, R.M. Wallace, and J.M. Anthony, “High- $\kappa$  gate dielectrics: Current status and materials properties considerations,” J. Appl. Phys., vol. 89 (2001): pp. 5243-5725.
20. S-W Sun, P.G.Y. Tsui, “Limitation of CMOS Supply-Voltage Scaling by MOSFET Threshold-Voltage Variation,” IEEE J. Solid-State Circuits, vol. 30, No. 8 (1995): pp.947-949.
21. B. Razavi, Design of Analog CMOS Integrated Circuits (Boston, MA: McGraw Hill, 2001), pp. 579-600.

22. D.A. Tichenor, G.D. Kubiak, S.J. Haney, R.P. Nissen, K.W. Berger, R.W. Arling, A.K. Ray-Chaudhuri, K.B. Nguyen, R.H. Stulen, J.B. Wronosky, J.D. Jordan, T.G. Smith, J.R. Darnold, P.M. Kahle, A.A. Jojola, S.M. Kohler, R.S. Urenda, D.R. Wheeler, J.E. Bjorkholm, O.R. Wood II, G.N. Taylor, and R.S. Hutton, "Recent results in the development of an integrated EUVL laboratory tool," *Proc. SPIE Int. Soc. Opt. Eng.*, vol. 2437 (1995): pp. 292-307.
23. G.D. Wilk, R.M. Wallace, and J.M. Anthony, "High- $\kappa$  gate dielectrics: Current status and materials properties considerations," *J. Appl. Phys.*, vol. 89 (2001): pp. 5243-5725.
24. T. Mimura, S. Hiyamizu, T. Fujii, and K. Nanbu, "A New Field-Effect Transistor with Selectively Doped GaAs/n-AlxGa1-xAs Heterojunctions," *Jpn. J. Appl. Phys.*, vol. 19 (1980): pp. L225-L227.
25. H. Daemkes, *Modulation-Doped Field Effect Transistors: Principles, Design and Techniques*, (New York: IEEE Press, 1991).
26. P. Price, "Low-temperature, two-dimensional mobility of a GaAs heterolayer," *Surf. Sci.*, Vol. 143, No. 1 (1984): pp. 145-156.
27. W. Walukiewicz, H.E. Ruda, J. Lagowski, and H.C. Gatos, "Electron mobility in modulation doped heterostructures," *Phys. Rev. B, Condens. Matter*, Vol. 30, No. 8 (1984): pp. 4571-4582.
28. D. Dawson, L. Samoska, A.K. Fung, K. Lee, R. Lai, R. Grundbacher, P.-H. Liu, and R. Raja, "Beyond G-band: A 235 GHz InP MMIC amplifier," *IEEE Microw. Wireless Compon. Lett.*, vol. 15, no. 12 (2005): pp. 874-876.
29. G. Dewey, R. Kotlyar, R. Pillarisetty, M. Radosavljevic, T. Rakshit, H. Then, and R. Chau. "Logic Performance Evaluation and Transport Physics of Schottky Gate III-V Compound Semiconductor Quantum Well Field Effect Transistors for Power Supply Voltages ( $V_{cc}$ ) Ranging from 0.5V to 1.0V," *IEDM, IEEE International*, pp. 1-4, Dec. 7-9, 2009.
30. P.M. Smith, "Status of InP HEMT technology for microwave receiver applications," *Microwave and Millimeter-Wave Monolithic Circuits Symposium, Digest of Papers, IEEE* 1996.
31. S. Takagi et al., *Intl. Symposium on VLSI Technology, Systems and Applications, Solid-State Electronic.*, 51 (2007) 526; 55 (2008) 21; *VLSI symp.* (2010) 147.
32. C. Jacoboni and P. Lugli, *The Monte Carlo Method for Semiconductor Device Simulation*, (Berlin, Germany: Springer-Verlag, 1989).
33. S. Datta and B. Das, "Electronic analog of the electro-optical modulator," *Appl. Phys. Lett.*, vol. 56 (1990): pp. 665-667.
34. D.C. Marinescu, G.M. Marinescu, *Approaching Quantum Computing*, (Pearson Prentice Hall, 2005).
35. P.K. Saxena, & P. Chakrabarti, *Computer modeling of MWIR single heterojunction photodetector based on mercury cadmium telluride. Infrared Physics & Technology*, 2009, 52, 196-203. doi: 10.1016/j.infrared.2009.07.009

36. P.K. Saxena, Modeling and simulation of LWIR photodetector based on mercury cadmium telluride. *Infrared Phys. Technol.*, 2011, 54, 25-33. doi: 10.1016/j.infrared.2010.10.005.
37. P.K. Saxena, Numerical Study of Dual band (MW/LW) IR Detector for Performance Improvement, *Defence Science Journal*, Vol. 67, No. 2, March 2017, pp. 141-148, DOI : 10.14429/dsj.67.11177.